Development of a design cycle for an additively manufactured aircraft rudder bracket

N Britz

orcid.org/0000-0002-7886-8083

Dissertation accepted in fulfilment of the requirements for the degree *Magister in Mechanical Engineering* at the North-West University

Supervisor:	Mr CP Kloppers
Co-Supervisor:	Dr JJ Janse van Rensburg

Graduation:	August 2021
Student number:	22807780

ACKNOWLEDGEMENTS

I would like to express my deepest and sincere gratitude to the following people and institutions, in no particular order, for their contribution and support during the course of this project:

- Aerosud Aviation
- CPAM (Collaborative Program on Additive Manufacturing)
- Jean-Pierre Serfontein
- CP Kloppers
- Wouter Gerber
- Piet Britz
- Jane Nortje

"It had long since come to my attention that people of accomplishment rarely sat back and let things happen to them. They went and happened to things." – Leonardo DaVinci

TRUST IN THE LORD WITH ALL YOUR HEART AND LEAN NOT ON YOUR OWN UNDERSTANDING; IN ALL YOUR WAYS, SUBMIT TO HIM, AND HE WILL MAKE YOUR PATHS STRAIGHT. DO NOT BE WISE IN YOUR OWN EYES; FEAR THE LORD AND SHUN EVIL. THIS WILL BRING HEALTH TO YOUR BODY AND NOURISHMENT TO YOUR BONES.
Proverbs 3:5-8

GENERAL NOTE

1. For this paper, please download a Quick Response (QR) scanner on any mobile device. The QR codes will display videos relative to the section or image. The following applications are recommended:

   QR-code scanners for Android and IOS:

   https://play.google.com/store/apps/details?id=tw.mobileapp.qrcode.banner&hl=en for Android

   https://play.google.com/store/apps/details?id=com.gamma.scan&hl=en_ZA for Android

   https://apps.apple.com/us/app/qr-reader-for-iphone/id368494609 for IOS

   Camera (the iPhone and iPad built-in app) for IOS

2. The table below are links referred to in the appendices for the supporting documentation.

Document name	Title	Description/Type	Share link
X0100000BU001	SIMUFACT CALIBRATION FOR ADDITIVE MANUFACTURED COMPONENTS	ENGINEERING TEST PLAN	https://figshare.com/s/a7f496a5b90de2bbf79c
X0100000BU002	STATIC TEST PLAN OF THE CPAM BOTTOM BRACKET	ENGINEERING TEST PLAN	https://figshare.com/s/ff7934133570b34d72dc
X0100000RA001	CPAM PROCESS REPORT – CAD	PROCESS MANUAL	https://figshare.com/s/785e47acadf10effaa13
X0100000RA002	CPAM PROCESS REPORT – OPTIMISATION	PROCESS MANUAL	https://figshare.com/s/1ec610cf338120bd61b7
X0100000RA003	CPAM PROCESS REPORT – INTERNAL AND EXTERNAL FEATURING	PROCESS MANUAL	https://figshare.com/s/2e76ff9d7b2d3a5b3e33
X0100000RA004	CPAM PROCESS REPORT - MANUFACTURABILITY	PROCESS MANUAL	https://figshare.com/s/c08687d918c53dbd30d6
X0100000RA005	CPAM PROCESS REPORT - QUALIFICATION AND CERTIFICATION	PROCESS MANUAL	https://figshare.com/s/4ec8895fdcd982d41d31
X0100000RU001	SIMUFACT CALIBRATION FOR ADDITIVE MANUFACTURED COMPONENTS	ENGINEERING TEST REPORT	https://figshare.com/s/ee116e1c1bb485943f55
X0100000RU002	STATIC TEST OF THE CFRTP CURRENT BIOMIMETIC BOTTOM BRACKET	ENGINEERING TEST REPORT	https://figshare.com/s/eca5e73257538cd1e94c
X0100000RV001	CFRTP BOTTOM RUDDER BRACKETS FOR THE CPAM PROJECT	STRESS ANALYSIS REPORT	https://figshare.com/s/42fc68a7a5baa0ddd3a5

ABSTRACT

Key terms: Additive Manufacturing (AM), Topology Optimisation, Design Cycle, Aerospace components.

For traditional manufacturing processes, the variation of component quality and mechanical properties exists but these can be minimised by the implementation of process controls. Hence, it becomes key to define the full process for developing and manufacturing components. These processes have been developed and successfully implemented for many years in the aerospace industry and can subsequently be manipulated and shaped to accommodate AM. Given the close link between process conditions and the development of material structures and quality during the AM build, it becomes crucial to define a process that will ensure acceptance of AM components for aerospace.

The purpose of this study was to develop a robust process to design, manufacture and ensure specific quality attributes when manufacturing a component with AM for the aerospace industry. The main objectives of this study were to undertake a literature review identifying the importance of the development of AM in aerospace and the process for the qualification thereof. Given the novelty of the technology, each phase of the possible design cycle and the AM process were investigated individually to develop the process. Another objective was to execute a case study that illustrated the design cycle's capabilities and process validation. Further, to develop competence and integrate the design cycle into an aerospace company's current design capabilities. Process documentation for each phase of the design cycle was developed to ensure the integration into a company's design capabilities for AM.

Through in-depth investigation and development of the design cycle process, the study's objectives were achieved, as each of the phases of the design cycle was identified, developed, and tested using the boundaries set out by the case study. These results substantiate that the design cycle process was effective. Thus, the validation of the design cycle was completed as it produced certifiable components by conforming to the original equipment manufacturer (OEM) requirements and the Federal Aviation Administration (FAA) regulations. However, this is possible after the correct procedures and specifications have been implemented to manufacture consistent components, and the process has been proven by the said OEM. Thus, the study was successfully concluded.

TABLE OF CONTENTS

LIST OF TABLES

LIST OF FIGURES

CHAPTER 1: INTRODUCTION

1.1 Background

Additive manufacturing (AM), commonly known as three-dimensional (3D) printing, is defined by the American Society for Testing and Materials (ASTM) as the process of joining materials layer upon layer to create a 3D model or component. The data used to generate these physical components are created using computer-aided design (CAD) software or 3D-scanning objects [1]. There are several varieties of AM processes in which material is deposited, solidified, or joined under computer control, each having its own benefits and limitations. These processes can produce components from different materials [2]. One of the key attributes of AM is that almost any geometry can be produced regardless of constraints specific to the AM process [3] [4]. This opens up new prospects when it comes to design and manufacturing constraints, including greater design freedom in contrast to the more prismatic, parameter-driven approach of traditional manufacturing methods. These traditional methods impede design freedom as a result of the need for fixtures, diverse tooling, and the possibility of collisions [5]. These limitations of traditional manufacturing make recreating the complex architecture of nature far from possible, which in effect hinders the process of creating biomimetic structures [6].

According to du Plessis et al. [7], biomimicry in engineering involves the study of biological systems, in particular, to solve engineering problems by using information gathered from nature. In nature, there are numerous structural features that define the properties and functions of objects. Integrating biomimicry with modern-day engineering techniques used for design has made it possible to alter structural features and properties while maintaining functionality or to apply simulations to find a design for a specific set of requirements. AM makes possible the convergence of nature and modern-day engineering and can thus be used to transform biomimetic designs into physical objects. These structures are advantageous for many different industrial applications, such as medical, automotive, and aerospace applications.

The aerospace industry is constantly in demand for lightweight aircraft components with a high strength-to-weight ratio to improve fuel efficiency attributes [8]. Hence, aerospace designers and engineers are continually striving to reduce the mass of a design which, in effect, will increase the complexity of the structure, function, and properties [9]. These structurally complex designs are characterised by non-traditional (biomimetic) external shapes that provide the required mechanical properties to attain a reduction in mass. AM allows for the fabrication of complex shapes, such as frame designs that are created using topology optimisation.

A topology optimisation process provides multiphysics simulation and multiscale design methods to find the best-compromised solution among multiple objectives. With the use of these software

tools, aerospace engineers are able to reduce material usage while making designs suitable for AM. These tools also allow for the ability to manipulate mechanical performance and reduce manufacturing cost. Lightweight components can ensure substantial cost reduction from the fabrication process all the way to the end of the aircraft's life [10]. Other advantages of using AM for the aerospace industry include the reduction in waste material, part consolidation, and the use of the finest engineering materials that are usually difficult to process with traditional methods.

To realise these advantages and fully exploit the potential of AM, robust quality control and qualification procedures along with a clear understanding of the certification requirements are needed [11]. While several AM standards have been released recently, a large amount of research must still be done in order to qualify AM components for aerospace [12]. The idea of using AM for aerospace components is far from novel, but the process of developing standards is slow and, more often than not, lacks consensus [10].

The current standards cover a range of areas for AM, such as feedstock details, defect types, and inspection methods; however, there are many areas still to be investigated and researched. Despite the lack of qualification and certification of procedures for AM, some of the larger aerospace companies have either begun or are planning to install AM components in aircrafts. To progress toward this purpose, some of these companies have started developing and deploying qualification and quality control processes. One commercial company, General Electric (GE), has received FAA approval to fly a metal AM component in one of its jet engines for the GE90. They also have duel certification with FAA and the European Aviation Safety Agency (EASA) for metal AM fuel nozzles for their Leading Edge Aviation Propulsion (LEAP) engine [11]. These examples show that it is essential to have the full process developed from design and manufacturability assessment all the way through to the qualification and certification of an aircraft component.

1.2 Problem statement

AM is increasingly being used in the development of new products for the aerospace sector. While there is a universal understanding of the contributions and control methodologies for design high surface roughness values, manufacturability, and residual stress and their potential effect on the component acceptability are still developing. These factors are not fully understood for the AM process and materials, which puts the optimal performance of components at risk. The lack of engineering experience in AM technology in these avenues often causes designs and applications to be over-conservative, which in effect reduces performance.

For traditional manufacturing processes, the variation of component quality and mechanical properties exists but these can be minimised by implementing process controls. Hence, it becomes key to define the full process for developing and manufacturing components. These processes have been developed and successfully implemented for many years in the aerospace industry and can subsequently be manipulated and shaped to accommodate AM. Given the close link between process conditions and the development of material structures and quality during the AM build, it becomes crucial to define a process that will ensure acceptance of AM components for aerospace.

The purpose of this study is to develop a robust process to design, manufacture and ensure specific quality attributes when manufacturing a component with AM for the aerospace industry.

1.3 Project objectives

The main objectives of this study are to:

- Undertake a literature review to identify the importance of the development of AM in aerospace and the process for its qualification. Given the novelty of the technology, each phase of the possible design cycle and the AM process will be investigated individually to develop the process.
- execute a case study to illustrate the design cycle’s capabilities and process validation.
- develop competence and integrate the design cycle into the current design capabilities of an aerospace company. Process documentation for each phase of the design cycle will be developed to ensure its integration into a company’s design capabilities for AM.

1.4 Importance of the research problem

This design cycle will aid and advance AM technology's adoption in the aerospace industry, given the many benefits that can be realised from using the technology. This study anticipates that by using metal AM, aerospace companies will be able to produce simple components in days rather than months once the process and part qualification have been completed. It further anticipates a significant reduction in the design, development, testing and evaluation time for more complex aerospace components [13]. Other benefits anticipated are a reduction in part weight, lower assembly component count, smaller inventory, increased level of component complexity, and improved performance. These anticipations substantiate the importance of the research of this study. The full development of the design cycle process will have a positive outcome for any adopters.

CHAPTER 2: LITERATURE STUDY

This chapter will investigate the relevant literature required for the development of the design cycle that will enable the manufacturing of aerospace AM components. A clear view of what should be considered during the development will be established, which will build on chapter one. This chapter aims to inform the reader of the fundamentals of AM in meeting aerospace requirements coupled with its development.

2.1 Aerospace materials and requirements

Aerospace materials are usually metal alloys, although the industry also focuses on polymer-based materials that have been developed or have become popular in the aerospace industry. The uses of these materials often have specific requirements, for example, strength, heat resistance, and high strength-to-weight ratios [14]. These unique materials often come at a high price when used in conventional manufacturing [3]. Other materials are also often used for their reliability in the safety-critical field of aerospace, especially for their resistance to fatigue loading. The work that metallurgical engineers do is significant to aerospace engineering. There are international standard bodies that maintain standards for the materials and processes involved. These standards include the ASTM, Aerospace Materials Specifications (AMS), and OEM specifications. Usually, the OEM specifications do not contain a lot of information due to the protection of proprietary information. These specifications are generally only shared with the provider, who must always adhere to these specifications during the process of manufacturing components for the customer. Recent developments in AM technology have made it possible to use these specialised materials to manufacture near-net shapes, which in effect makes it more cost-effective to use these materials for the aerospace industry. Thus, the development of AM materials has become a popular topic for research and development over the last several years, including the development of standards.

2.2 Additive manufacturing (AM)

To elaborate on the introduction of AM and its definition that were introduced in Chapter 1, this chapter will expand on the topic of AM. AM is an advanced manufacturing method that produces near-net 3D structures directly from CAD models by adding material layer by layer [15] [16]. This process stands in contrast with the traditional method of subtractive manufacturing [17]. The first use of AM was known as rapid prototyping, founded in the late 1980s. This technique was used to create a scaled model of a physical component in order to reduce mistakes. The scaled models were referred to as prototypes, and they shortened the time to generate components without having to manufacture multiple iterations due to errors [18]. With the advancement of technology

over the years, this method developed into the process that is now known as AM. After a considerable amount of research and development, the process has reached a point where it can produce components that are ready to be used.

Many different processes are classified as AM technology, as shown in Section 7.1, Appendix A. The feedstock for AM can be classified under two categories – powder and wire-based. Two different technologies are applicable when the powder-based feedstock is used, namely, laser powder bed fusion (LPBF) and direct energy deposition (DED) [14]. LPBF allows for the manufacturing of components with complex features and requires high precision and single material builds. These key assets, together with the correct rare material, make AM technology very applicable to the aerospace industry. For the purpose of the study scope and to guide the research, the LPBF process and Selective laser melting (SLM) technology will be the only methods investigated in detail due to their advantages and applicability in the aerospace industry [10] [12] [13] [19] [20] [21].

2.2.1 Laser powder bed fusion (LPBF)

LPBF is an AM technology with the capability to produce functional components from a variety of engineering alloy powders [17] [22] [23]. According to ASTM, laser powder bed fusion is the process in which thermal energy selectively fuses regions of a powder bed" [24]. This is a brief description of the technology. According to Wang et al. [25], selective laser sintering (SLS) was the first commercialised LPBF process. Figure 2-1 is a basic illustration of the process known as SLS. All the other PBF processes are modified variations of SLS adapted for different materials and enhancing machine capability. SLM and SLS are remarkably similar processes – in principle, exactly the same; however, SLM can go one step further than sintering and fully melt the powder. These processes all share a general set of characteristics – a heat source to fuse the powder particles, a way to control the powder fusion at a designated area for each layer, and a mechanism to add powder and smooth it across the build area [25]. The method used in this study is known as SLM, which will be discussed in the next section.

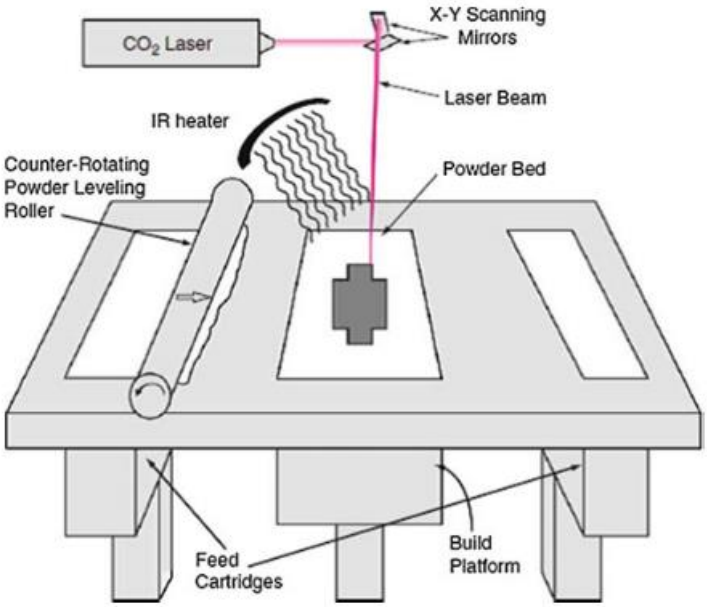

Figure 2-1: The basic layout of LPBF technology – selective laser sintering [25]

2.2.2 Selective laser melting (SLM)

According to Redwood et al. [2], SLM is a process that uses a laser to melt the powder completely to form a homogenous component. With this process, the component has a single melt temperature. The high processing temperature puts the components at risk of distortion due to the residual stresses. Thus, the process requires structural support, unlike its predecessor, SLS [2]. Given its popularity in the aerospace and biomedical industry, LPBF has been used to manufacture a broad variety of materials, such as aluminium-, titanium- and nickel-based alloys. TI-6AL-4V was used in this study for its ductility and fracture resistance at slightly elevated room temperatures [23]. An example of the application of this process is the study done by Salmi et al., which used LPBF to print a component with Ti64, as seen in Figure 2-2 [26]. The QR code shows a video of the process.

Figure 2-2: Ti64 component printed with the LBPF process

2.2.3 Additive Manufacturing of Ti64 (Titanium)

Ti6AL4V alloy, also commonly known as Ti64, is a mixture of alpha- and beta-titanium alloys with high strength, low density, high fracture toughness, and corrosion resistance. Ti64 was originally developed in the 1950s for structural components used in aircraft. Its high strength-to-weight ratio makes Ti64 suitable for many applications in the aerospace industry, for example, jet engines, gas turbines, and many airframe components [15]. For instance, GE Aviation is producing low-pressure turbine blades using AM [27]. However, titanium alloys are limited by their relatively high cost compared to other materials [21] as well as their poor machinability [28]. As mentioned previously, AM technology makes it possible to manufacture these premium materials [10].

2.3 Design for AM in aerospace

The aerospace industry is constantly in demand for lightweight components with high strength-to-weight ratios to improve fuel efficiency, reduce emissions and respond to safety and reliability requirements [8]. Taking this into consideration, aerospace designers strive to minimise the amount of material used in every component; this, in effect, increases the design complexity with respect to the structure, function, and properties. Due to the free-form fabrication capabilities of AM, it is possible to manufacture any shape or any form of component [10].

Kamal et al. have a holistic approach when describing design for AM with a method for developing components that consider the design as well as the means of manufacture. There is a strong link between the process and design when considering AM as a manufacturing method. It is key to

understand the flexibility and limitations of the process in order to capitalise on the advantages of AM fully. In this view, the following sections will focus on design and process considerations for AM and their correlation with the manufacturing of aerospace components [29]. Thus, the key considerations when deciding to produce an aerospace component using AM will be discussed in the section to follow.

2.3.1 Structural design

There are several definitions for structural design. Braga et al. [8] mention an extract from the Concise Encyclopaedia of Engineering that states: “Structural design is the science of selecting material and member type, size and configuration to carry loads in a safe and functional way”. The structural design normally includes at least five distinct phases:

- Project requirements
- Materials
- Structural scheme
- Analysis
- Design

Although, some structures may still require an extra phase, which is testing, and more complex structures which require the use of state-of-the-art materials or concepts, proof of concepts, and capabilities. To summarise, structural design is the combination of several principles of engineering in the process of new product development [8]. The design principles used to develop aerospace structures explore all properties and failure modes of the materials in order to produce optimum structures which tolerate inherent inadequacies. As mentioned in the previous sections, AM allows for the manufacturing of complex structures with some constraints depending on the limitations of the technology [10].

2.3.2 Part consolidations

Part consolidation is a process applied to multiple component assemblies and structures. The definition is the use of fabrication to reduce multiple component assembly into one redesigned component with the same operational functionality [30] [31]. The benefits of part consolidation in AM is the simplification of components, potential performance improvement, and the reduction in fabrication time [29]. From a manufacturer’s point of view, this includes a smaller amount of components to manufacture and a significant cost reduction associated with labour, tooling, part traceability, and items in stock [10]. From an operator’s point of view, it usually means the components are easier to use and maintain. Given these factors, part consolidation is a direct driver for the reduction in cost for both supplier and customer [9].

2.3.3 Computer-aided design (CAD)

The primary use for CAD in a design process is to design a component, prepare the existing geometry for optimisation, or consolidate parts as mentioned in the previous sections.

For the preparation of the optimisation geometry, it is advantageous to re-evaluate the geometry and ensure that the maximum design space is used for the assembly or application of the component. The design space is the area in which the topology optimisation is carried out [32]. In Figure 2-3, the design space is shown in blue and the fixed space in green. The fixed space is the area of the component that will not be removed during the optimisation process.

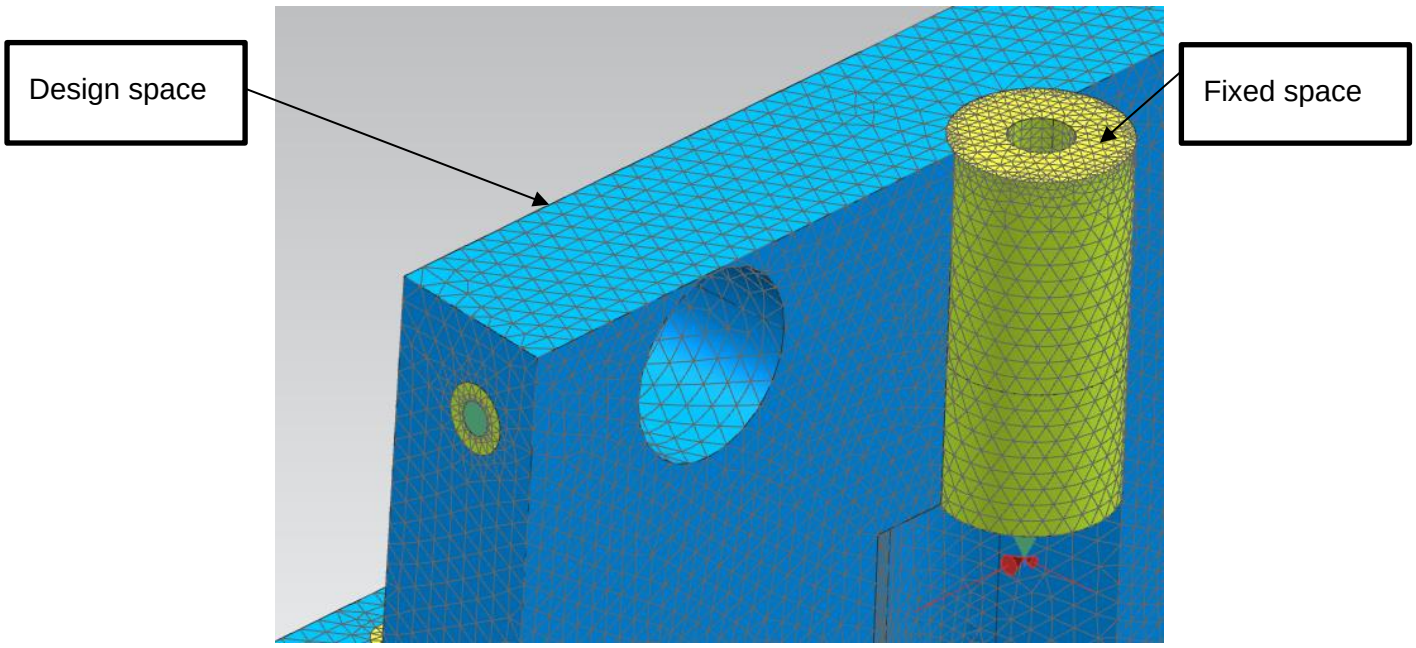

Figure 2-3: Design space

When there is no need for optimisation, the geometry can be prepared or designed for manufacturing. This is done by taking into consideration all the constraints of the manufacturing process and checking that the component adheres to the constraints, such as the overhang angle shown in Figure 2-4. The overhang angle will be discussed in the next section.

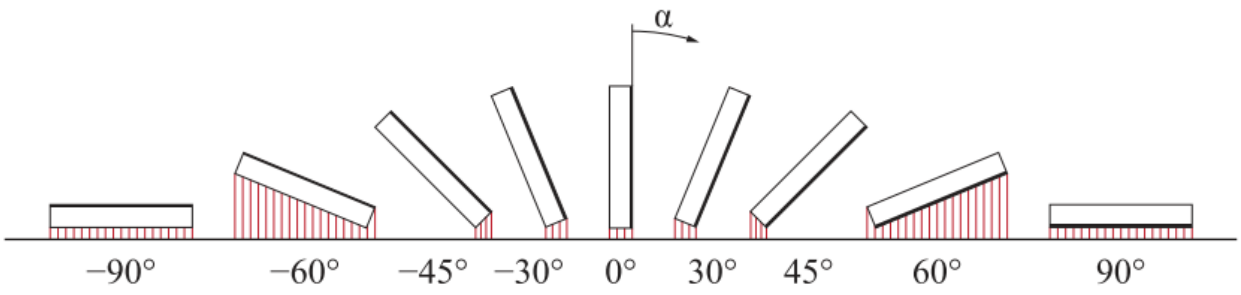

Figure 2-4: Overhang angle example [18]

Design for certification ensures that the designer conforms to all the requirements and specifications that are set by the OEM. This design stream will form part of the qualification and certification phase of the study.

The CAD phase will be used in conjunction with several of the phases to perform changes to the geometry. In conceptualising components, it is key to generate the initial shape for the application, which entails defining interface planes and points. This will ensure that the maximum design space is used in the operation or working space of the component [33]. In some cases, the topology optimisation software requires certain file types, which are exported from CAD. It is not necessary to export the data when using one platform. A platform refers to a software package that has more than one function. For example, the finite element method (FEM) has the capability to do topology optimisation and finite element analysis (FEA). Any CAD software can be used for the exportation of the following file formats:

- STEP
- IGES
- STL

In addition, existing components that will be optimised require the geometry to be re-evaluated. This refers to removing features such as fillets and chamfers and consolidating components, if possible. This process is defined as the volumetric re-evaluation of the component in preparation for FEA [9].

2.3.4 Topology optimisation

Topology optimisation is one of the structural optimisation methods [34]. The distribution of the material is optimised based on a set of loading and boundary conditions while adhering to the structural requirements of the component [35]. Topology optimisation techniques are conducted using a combination of engineering knowledge with CAD and FEA concepts while considering the manufacturing technique. The volumetrically re-evaluated data is then used in the FEA software to calculate the stress and displacement throughout the component. The primary objective in topology optimisation investigations is the removal of material not subjected to load; however, structural integrity must be maintained [36].

Bendsoe and Kikuchi's study [6] has triggered renewed interest in topology optimisation, and the popularity of using the methods has increased tremendously. Topology optimisation has developed rapidly with an increase in the number of tools and the evolution of the theory, which have become a notable addition to design methodology [1]. With reference to Section 1.1, specifically prismatic and biomimetic structures, it is pertinent to note the limitations and requirements of the component for optimisation. This will determine the manufacturing constraints, design objectives, and design constraints.

2.3.4.1 Prismatic structure

Prismatic refers to a parametric shape with geometrical features that are defined by parameters and the manufacturing process. Topology optimisation for traditional manufacturing (TM) methods have many stumbling blocks. Complex geometries created are either manufactured at uneconomical rates or are not manufacturable using TM. According to Chen et al., to conceptualise components that conform to TM, efforts have been made to integrate manufacturing constraints into the optimisation process [37]. The following factors are denoted as the main aspects that must be considered for effective outputs to be achieved from a topology optimisation process:

1. Minimum feature size and geometric symmetry as manufacturing constraints:

Topology optimisation is a concept design method; thus, it is essential to keep in mind that there are limitations in the manufacturing process. Zuo et al. state that minimal hole size for machining tools is generally not taken into consideration in the topology optimisation process. Still, minimal hole size is seen as a characteristic that affects casting and the symmetry property of the component's function [33]. The minimum feature size should thus be taken into consideration as a manufacturing constraint during the topology optimisation process to avoid non-manufacturable geometry. With the latest software, manufacturing constraints are now a general part of setting up the optimisation.

2. Cost of manufacturing in the optimisation process:

According to Chang et al. [38], engineers in the automotive and aerospace industries are challenged to create and design components that take certain load cases that are strong enough to sustain substantial impact. The geometry of said load-bearing components is usually complicated due to efficiency requirements, where efficiency refers mainly to strength and weight. These requirements typically come at a high price because the more complex a component, the more time it takes to manufacture, and this increases the cost of the component [38].

2.3.4.2 Biomimetic

Since the development of the AM industry, the ability to design components with the extent of manufacturing freedom has made topology optimisation a lot more relevant [10]. The general meaning of biomimicry is “innovation inspired by nature”; in other words, it entails using nature as the inspiration for any natural or organic shape in a design [7]. Biomimetic structural components are a result of the geometry generated by the topology optimisation that eliminates the material that is not situated on the load path. The shapes generated emulate the growth of tree branches, but this is only inherent to the path based on the loading and boundary conditions. In an ideal world, AM would be able to satisfy any design, but the current state of the technology still has limitations, for instance:

1. Surface quality

An excellent surface finish generally requires post-processing, and these processes come at a high cost. Surface finish will influence the fatigue life of a component, as the inferior surface condition most likely will induce cracks due to defects such as porosity [2].

2. Overhang angle

Overhang angle is a well know constraint in the AM industry. The typical overhang angle for metal AM is 45 degrees and lower. If this angle is exceeded, support structures are required [2].

3. Support structures

As mentioned in the previous section, the support structure is not ideal for surface finish. These structures are often large and require additional post-processing to remove. Reduction in support structures would significantly reduce manufacturing cost and finishing effort [39].

2.3.5 Internal features

This section will focus on features that affect the internal structure of an AM component and the surface clean-up of the topology optimisation facet geometry.

2.3.5.1 Lattice structures

The basic description for “Lattice” is a framework or structure of crossed woods or metal strips. It can be implemented in a geometrical arrangement of points or objects over a designated design space [40].

For this study, a peripheral view of lattice structures will be investigated for additively manufactured aerospace components. A way of qualifying and certifying the components as flight airworthy is yet to be determined due to the variability of the lattice beams and the multitude of load paths that would exist within a lattice.

Hussein et al. completed a study that investigated new steps for the design and manufacture of a more effective support structure using a lattice structure with minimum volume [41]. Support structures will only be investigated in the manufacturability phase of the design cycle.

2.3.5.2 Bamboo structures

This is still a very new concept, as there is little to no literature describing where it has been used for AM in tube-like structures. Figure 2-5 is an example of the bamboo structure generated by Kranz et al. [42].

Figure 2-5: Bamboo structure to save weight [42]

2.3.6 Surfacing

Surfacing is not to be mistaken as the surface roughness of an actual manufactured component. Rather, it refers to the surface clean-up of the faceted geometry created by the optimisation process. An example of this can be seen in Figure 2-6. A shape generated from the topology optimisation process is facet geometry, alternatively termed a “dumb solid”. Facet geometry is not directly compatible with subsequent CAD tools. Non-uniform rational B-splines (NURBS) are preferred in this conversion method because they represent the geometry more efficiently and accurately. However, converting third-order meshes to NURBS is difficult and time-consuming [43].

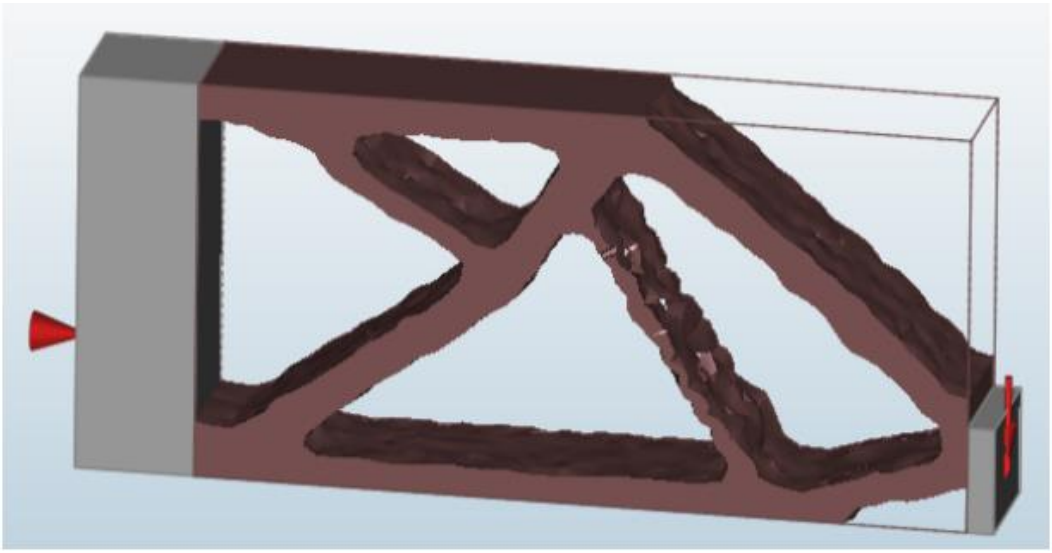

Figure 2-6: Facet geometry created from the TOP process [43] [44]

In 2016, SolidThinking addressed this problem by developing a solution called PolyNURBS [43]. According to SolidThinking [43], this new modelling method allows the user to easily trace over the facet results from the topology optimisation process to create a smoother, watertight NURBS version of the facet geometry. An example from the help file can be seen in Figure 2-7. This PolyNURB model can be exported to other CAD systems and be prepared for the next phases of the design cycle.

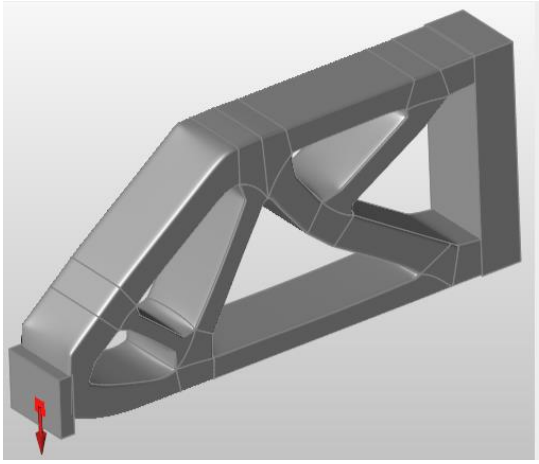

Figure 2-7: PolyNURB geometry [43] [44]

2.4 Process characteristics of design

Design opportunities with AM, as discussed in the previous sections, continue to be one of the most popular aspects of AM. Regardless of the manufacturing process, all components still have some form of functional requirement, and this is where the process characteristics of design become crucial.

2.4.1 Manufacturability

Residual stress and distortion are major technical challenges for LPBF, as excessive diction can cause build failure, cracks, and loss of structural integrity. As mentioned previously, LPBF is a very popular topic in the aerospace, automotive and medical industries. However, the inadvertent presence of residual stress and distortion hinders wider application. The main cause of residual dictions is the rapid heating and cooling inherent to the AM process [45]. The complexity of the process means that there are many contributing factors to residual diction, of which one key aspect is the build parameters. Some of the parameters are listed below [46]:

- Beam width
- Laser power
- Laser velocity
- Hatching strategy
- Material type
- Layer thickness
- Powder size and morphology

Bugatti et al. [46] refer to the manufacturability phase as “process optimisation”. The process relies on the results of expensive experimental campaigns. This approach is advantageous because it offers the most accurate solution since the results come directly from the machine. However, this is an iterative process that is time-consuming and can be overly expensive because it relies on quality measurements of the components [46]. Due to the high cost of this process, utilising a new process that is driven by simulation and minimal experiments will lower the cost. This will invoke the thought process of “first time right” by identifying or supervising during the simulation for any problems with the build. Using simulation software to predict the build process accurately and the inherent residual stresses will effectively ensure manufacturability and component quality.

Simufact Engineering has developed Simufact Additive for the simulation of metal AM. This software simulates all the critical process steps in the AM process. These process steps are:

- A component build
- heat treatment
- cutting from the build plate
- removal of support structures
- hot isostatic pressing (HIP).

Simufact Additive predicts the final distortion and residual stresses of the metal components. The inherent strains are determined through several iterative calculations using an experimental calibration process. The inherent strains associated with the calibrated machine are then used in simulating a component. The software can then accurately determine where the distortion and stress will accrue during the build after it has been cut from the build platform, and all the support structures have been removed.

2.4.2 Qualification and certification

As mentioned in the previous section, the potential application of AM technology to manufacture components in the aerospace industry has grown tremendously of late. However, to realise the advances and exploit the full potential of AM, robust quality control and qualification procedures along with a clear interpretation of the certification requirements are necessary. Despite the proprietary qualification and certification procedures due to the OEMs not being publicly available, some aerospace companies have begun or are planning to install AM components in aircrafts. Some organisations have already started to develop internal proprietary processes for qualification and certification [11]. For example, Airbus has created the process specification AIPS

01-04-020 for LPBF. Based on the special process qualified list (SPQL), currently, only one company is certified for manufacturing components with LPBF from metallic materials.

The highlighted advantages throughout the literature study are a good indication that AM can benefit the aerospace industry tremendously. However, the aerospace industry has strict regulations set by the European Aviation Safety Agency (EASA) and Federal Aviation Administration (FAA). The regulatory bodies prescribe the Certification Specification (CS) and Federal Aviation Regulation (FAR), respectively. The regulations are detailed and extensive [47] and require manufacturers to conform by implementing various specifications. The regulation used for this study is the FAR/CS – 23: Normal and utility category aircraft. The sections most relevant in the context of AM are FAR 23.305 Strength and deformation, FAR 23.307 Proof of structures, FAR23.603 Material and workmanship, and FAR 23.607 Fabrication methods [48].

2.4.2.1 FAR 23.305 Strength and deformation

a. The structure must be able to support the limit loads without permeant deformation or failure.

b. Deformation may not interfere with safe operation with any load up to the limit load.

c. The structure must be able to survive the ultimate load for at least three seconds before failure occurs.

d. Local failures or structural instability (buckling) between the limit and ultimate loads are acceptable if the structure can sustain the ultimate load for at least three seconds.

e. The three-second limit does not apply when proof of strength is done by dynamic testing that simulates actual load conditions.

2.4.2.2 FAR 23.307 Proof of structures

a. The structure must comply with the strength and deformation requirements mentioned in the previous section for each of the critical load conditions.

b. Structural analysis may be used only if the structure conforms to those for which experience has shown this method to be reliable. Structural analysis may be used if the structure conforms to a proven method. On the other hand, load tests must be done to substantiate the method.

c. If the design load conditions are simulated, dynamic test and structural flight tests are acceptable.

d. Certain parts of the structure must be tested as specified in section D of the FAR 23 document.

2.4.2.3 FAR23.603 Material and workmanship

The suitability and durability of the material to be used for components that may affect safety must:

a. Be established by experience or tests

b. meet approved specifications that ensure that they have the strength and other properties assumed in the design data

c. take into count the effects of the environmental conditions, such as temperature and humidity, expected in service

d. have workmanship of a high standard.

2.4.2.4 FAR 23.607 Fabrication methods

a. The methods of fabrication used must produce consistently sound structures. If a fabrication process requires close control to reach this objective, the process must be performed under an approved process specification.

b. Every new aircraft fabrication method must be substantiated by a test program.

The regulation creates a clear view that extensive work must be done to qualify the AM process, materials, and methods to ensure that the components meet the requirements. Due to the lack of maturity of AM in terms of the abovementioned requirements, it takes the OEM a tremendous amount of time and resources to develop these specifications and databases for a specific AM alloy [47] [49]. It is a well-known fact that AM alone is not enough to produce airworthy components. However, the aerospace industry is well known for its development of many processes and manufacturing methods, which can fill the gap for the post-processing of AM components.

CHAPTER 3: APPROACH AND METHODOLOGY

There are set processes and phases during the development of traditionally manufactured aerospace components for structural design, as mentioned in Section 2.3.1. These processes are project requirements, materials, structural schemes, analysis, and design. These processes can be altered and shuffled to cater to the design of AM components. There are also process-related aspects that are not covered in structural design, which must be considered to improve the overall quality of the components. Taking all the information into account from the literature study, a process was derived and developed to manufacture components from AM. The process from here on out will be referred to as the design cycle. This design cycle is depicted in Figure 3-1. It consists of five phases that were identified as crucial during the literature study. The chapters that follow will substantiate the importance of each phase and the value-added to the overall progress of the development to industrialise AM in the aerospace industry. The five phases that were investigated are known as:

- Computer-aided design (CAD)
- optimisation
- internal features and surfacing
- manufacturability
- qualification and certification.

Figure 3-1: The design cycle for additively manufactured aerospace components

The thought process behind the design cycle is that it should be iterative, as the solution for a specific design case might not conform to all the requirements in the first iteration. A secondary action for this study was to develop process manuals that would prescribe design rules and a methodology to standardise AM designs for aircraft components. This study comprised quantitative research with various methods to obtain data for each phase of the design cycles. These said methods were computer methods, mathematical methods and procedures, which ensured that each of the phases was investigated and developed thoroughly to achieve the objectives in the next section.

3.1 General issues to be addressed

The following sections describe the general issues, desired outcomes, and limitations for the CAD, optimisation, internal features and surfacing, manufacturability, and qualification and certification.

3.1.1 Computer-aided design (CAD)

The desired outcome for this phase of the design cycle is to consolidate components and create a design space for the optimisation process. It will also be used to conceptualise components traditionally with experience and engineering knowledge. The limitations in this phase will be the knowledge of the designer or the lack thereof to design components and designate design space.

3.1.2 Optimisation

The desired outcome for the optimisation phase of the design cycle is to generate a component with biomimetic features that is structurally sound to sustain ultimate loads during its operational life. The outcome was also to minimise the weight of the component to make it more efficient. The most significant limitations for this section will be time and budget constraints, as it is known that software is costly and to gain competency in the software takes time.

3.1.3 Internal features and surfacing

The desired outcome is to generate usable geometry from the optimisation phase that was generated by the topology optimisation process. This is required, as the facet geometry that is generated by the topology optimisation process cannot be manipulated or used in the rest of the design cycle. Cleaning up the geometry is a time-consuming process, which can become an issue when the complex geometry must be converted.

3.1.4 Manufacturability

The desired outcome for the manufacturability phase of the design cycle is to predict whether the build will fail and to determine how to avoid failure. The components will be manufactured during this phase to verify that the software predicts the correct failure by comparing the actual distortion

with the simulated distortion. The actual distortion will be measured by 3D scanning of the component. Once the component is built correctly, it will be deemed ready to be certified.

3.1.5 Qualification and certification

The outcome of the final phase will be successful when a clear outline is available of what is required for metal AM to be qualified and for the certification of the structural integrity of the component. Traditionally, the level of qualification and certification requirements for aircraft parts has been linked to the level of criticality, which is defined with various degrees of importance. For this study, a case study will be applied to a class 1 component that is deemed as structurally critical for flight.

CHAPTER 4: CASE STUDY

This chapter will give more insight into the application of the design cycle derived from the research that was conducted and explained in the previous chapters. The case study was derived from a previous study done on an aircraft rudder assembly by the Aerosud Aviation Research and Development (R&D) team. Due to the proprietary nature of the technology and application, only limited information on the previous work done can be shared in this chapter. The sections that follow will give the reader insight into the general definition of the case study as well as the boundary conditions that were applied.

4.1 General definition

The general definition of this case study is the design of the bottom bracket that forms part of the continuous fibre-reinforced thermoplastic (CFRTP) rudder assembly. The original rudder was all metallic and made up of machined brackets, ribs, a spar, skins, and cleats as the main components of the assembly. Aerosud Aviation had CFRTP-forming capability and demonstrated a complete CFRTP rudder. The main goal for the previous CFRTP study was to reduce the weight of the full rudder assembly. The original brackets that interfaced with the rest of the aircraft were manufactured from multiple parts. These brackets were intended to consolidate the multiple parts by utilising the capabilities of AM and to reduce the overall weight of the bracket. The complex geometry of the bottom bracket could not be modelled with the software available at the time of the previous study. The bottom bracket was revisited in the present study to investigate the latest developments in optimisation simulation and the inclusion of manufacturing simulation capability.

To evaluate the effectiveness of the proposed design cycle in Chapter 3, the abovementioned bottom bracket was redesigned. The goal of the presented case study was to achieve an AM-manufactured component that conforms to the airworthiness requirements and takes full advantage of the benefits of AM. In Figure 4-1, the bottom bracket is shown in the rudder assembly. The assembly will give the reader insight as to where all the interface planes and points were defined and how the boundary and loading conditions were rederived for the simulations. The interface planes refer to the areas where the bracket comes into contact with the rest of the CFRTP assembly skins. The points refer to the fastener positions as well as the pins that invoke the movement of the entire rudder.

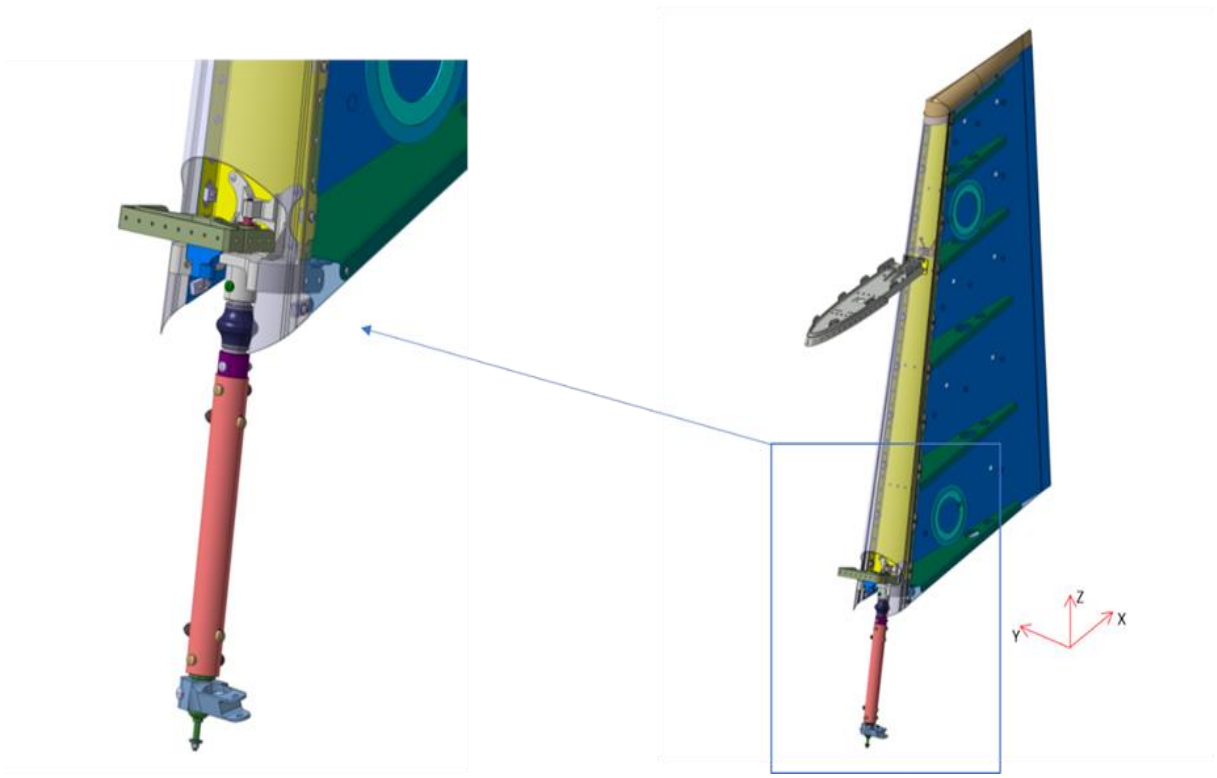

Figure 4-1: The CFRTP rudder assembly depicting the bottom bracket [50]**.**

4.2 Loading conditions

Aircraft are designed to sustain two loading conditions, namely, limit and ultimate loading. Limit loads are the typical operational conditions that an aircraft must sustain in everyday use. Ultimate loads are the extreme cases aircrafts are subjected to during flight. Components cannot permanently deform under limit conditions and cannot fail under ultimate conditions. Ultimate loads are derived by multiplying the limit loads by a factor of 1.5 – refer to FAR 23 section 23.301, paragraph a [48]. The definition of loading conditions was given for clarity on the variants and will aid in the understanding of the decision to subject the bracket to the ultimate loading conditions. The bracket is required to sustain the ultimate loading condition for it to be structurally acceptable. The global load cases in Table 4-1 are defined as the load cases that were applied to the original structural assessment of the CFRTP assembly in the original case study for the development of the composite technology. These load cases were applicable to the present study, as the bracket that was investigated forms part of the assembly.

Table 4-1: Global load case definition

Load Case	Load Case Description
LC001	Inward pressure on RH skin
LC002	Inward pressure on LH skin
LC003	Rudder pressure right
LC004	Rudder pressure left
LC011	Outward pressure on RH skin
LC022	Outward pressure on LH skin
LC301	Inward pressure on RH skin Nz -9g
LC302	Inward pressure on LH skin Nz - 9g
LC303	Rudder pressure right Nz - 9g
LC304	Rudder pressure left Nz -9g
LC311	Outward pressure on RH skin Nz - 9g
LC322	Outward pressure on LH skin Nz - 9g
LC200	9g downward inertia (Nz - 9g)
LC400	Rudder stop load LH
LC401	Rudder stop load RH

The pressure loads from Table 4-1 were applied, as seen in Figure 4-2, to the outer skin of the rudder in the global finite element model (GFEM). These pressure loads simulate the force of the air applied to the rudder during the yawing of the aircraft. A yaw motion is a side-to-side movement of the nose of the aircraft caused by the deflection of the rudder.

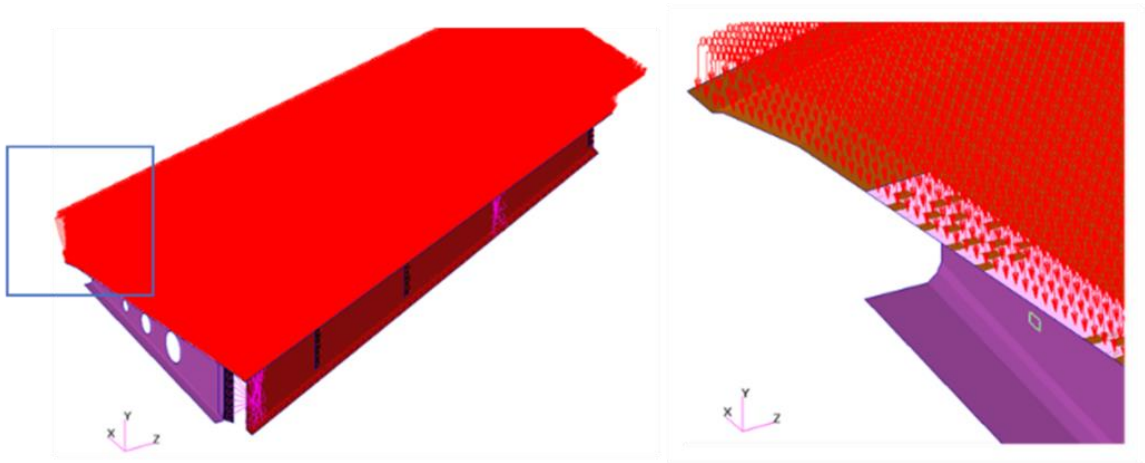

Figure 4-2: Pressure load applied to the skin

The interface points were defined by nodes 11 and 12, as shown in Figure 4-3. These interface pins were the connection points of the rudder to the rest of the aircraft. In the initial study, the full assembly was simulated to assess the failure of any component of the entire assembly. For this study, the interface loads were extracted from the assembly's finite element model (FEM). This made it possible to assesses the brackets in isolation with the same boundary conditions as the full assembly. This would reduce the simulation time, as there were significantly fewer elements for the solver to consider. These interface loads are found in Table 4-2.

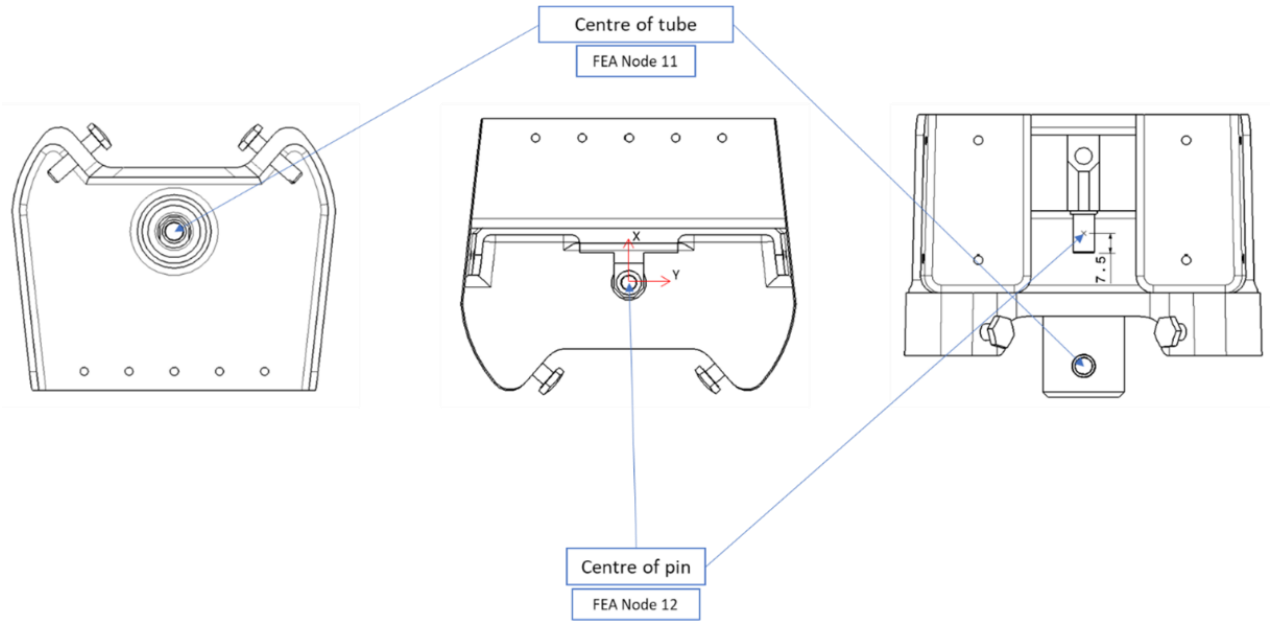

Figure 4-3: Interface loading points

Table 4-2: Load case definition for the bottom bracket

Bottom bracket ultimate loads							
Node 11					Node 12		
	Px(N)	Py(N)	Pz(N)	Mz(Nmm)	Px(N)	Py(N)	Pz(N)
LC001	0	0	69	322,566	-85	-943	0
LC002	0	0	70	-330,563	-94	924	0
LC003	0	0	0	-326,564	-5	933	0
LC004	0	0	0	326,564	5	-933	0
LC011	0	0	-69	-322,566	85	943	0
LC022	0	0	-70	330,563	94	-924	0
LC301	0	0	243	322,617	-103	-943	0
LC302	0	0	244	-330,512	-113	923	0
LC303	0	0	174	-326,514	-23	933	0
LC304	0	0	174	326,615	-14	-933	0
LC311	0	0	105	-322,516	66	943	0
LC322	0	0	104	330,613	76	-924	0
LC200	0	0	174	51	-18	0	0

Table 4-3 shows that there were two additional load cases for the stop location to prevent the rudder from over-rotating. Figure 4-4 depicts the loads applied.

Table 4-3: Stop loads

Load case	**Load**
LC400	9483
LC401	9483

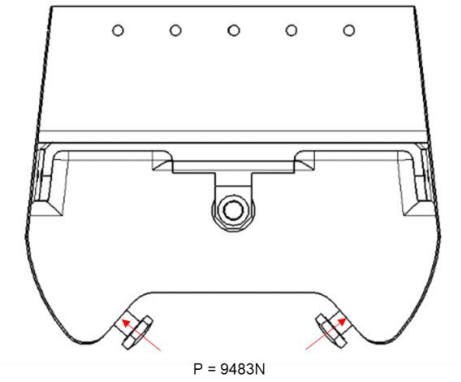

Figure 4-4: Stop loads applied to the bracket

4.3 Fastener definition

As the bracket was assessed in isolation from the GFEM, fastener stiffness was required to ensure that the correct interface loading was still considered. Figure 4-5 depicts the location of each fastener.

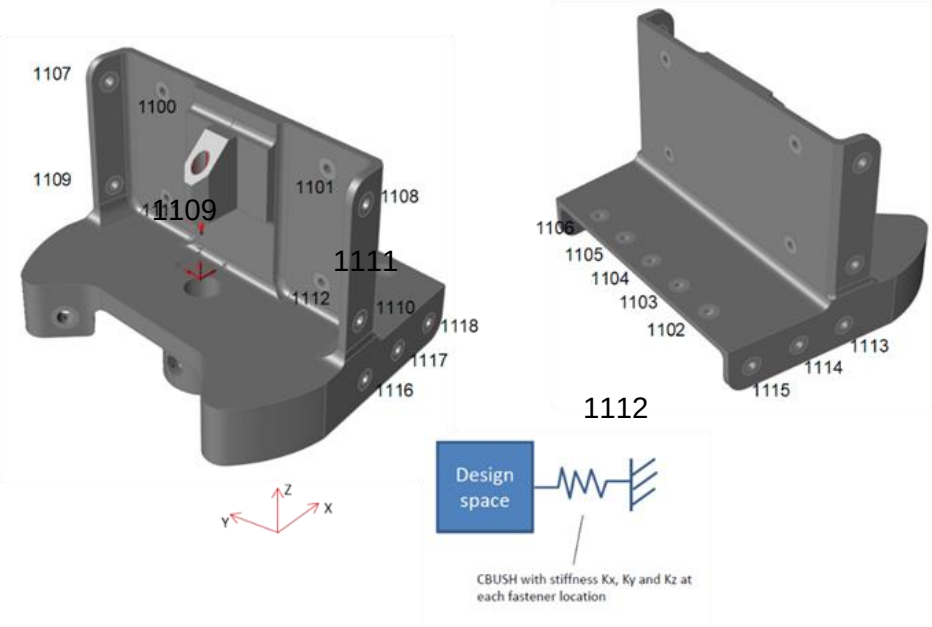

Figure 4-5: Fastener point definition front

Table 4-4 presents the data extracted for the fastener interface stiffness at each defined point. A joint was defined as the two materials that the fasteners joined mechanically. Shear stiffness of the joint was driven by the rivet, whereas the tensile stiffness was a combination of the spar, the skin, the cleat, and the rivet joint assembly.

Table 4-4: Stiffness definition for each fastener

Node Point	Kx(N-mm)	Ky(N-mm)	Kz(N-mm)
1100	49	1893	1893
1101	47	1893	1893
1102	1893	1893	84
1103	1893	1893	87
1104	1893	1893	85
1105	1893	1893	87
1106	1893	1893	84
1107	1893	102	1893
1108	1893	113	1893
1109	1893	259	1893
1110	1893	265	1893
1111	647	1893	1893
1112	642	1893	1893
1113	1893	184.75	1893
1114	1893	184.75	1893
1115	1893	184.75	1893
1116	1893	184.75	1893
1117	1893	184.75	1893
1118	1893	184.75	1893

CHAPTER 5: OUTPUTS AND RESULTS

This chapter details the outputs and results from the case study. The outputs from the design are also the results for the design cycle, which was a benchmark for the developed processes. The proposed design cycle was tested, as mentioned in Chapter 4, using the set boundary conditions for the optimisation and structural analysis.

The design cycle was tested for three different scenarios. Each of the scenarios has a distinct difference:

- In the first scenario, the initial components were consolidated, and the design space was enlarged to improve the outcome of the topology optimisation.
- For the second scenario, the consolidated part was used in the initial stage of the design at the time, without changing the design space.
- The third scenario was a traditional design approach where a prismatic bracket was designed. This scenario was a simpler approach that was done without the component being exposed to the topology optimisation, internal features, and surfacing phases.

The results from each scenario are summarised in the first section of this chapter. Sections 5.2 to 5.6 provide a detailed explanation of the particulars that have been achieved for each phase of the design cycle. The objective of creating process manuals was achieved with each of the process flows detailed in the corresponding phases. Due to the nature of the content in these process manuals, they have been added in Section 7.5, Appendix E; these manuals are a step-by-step guide on how each of the processes was used to obtain the results.

5.1 Results summary

As mentioned earlier in this chapter, three scenarios for the bottom rudder bracket were investigated. Figure 5-1, Figure 5-2, and Figure 5-3 depict visual representations and summarise the results from the case study for each of the phases of the AM design cycle. The three scenarios were chosen because they represented the three most common ways that a design would be approached for an AM component. Due to the unique application area, the design space of the component was limited – even with the free-form manufacturing, the designs were still limited to specific interface points. The results of each scenario are different. For the first two scenarios, the same design cycles where used, but the initial input geometry varied. The third scenario, as mentioned above, was not optimised. Each scenario and outcome can vary since the design cycle is still dependent on the requirements for a specific application of a component. As mentioned in Chapter 2, the advantages of weight reduction while still maintaining structural integrity are

essential to the aerospace industry. This is one of the reasons why the optimisation was an important addition to the design cycle. Table 5-1 presents the percentage of weight save for each of the components compared with the current (initial) design.

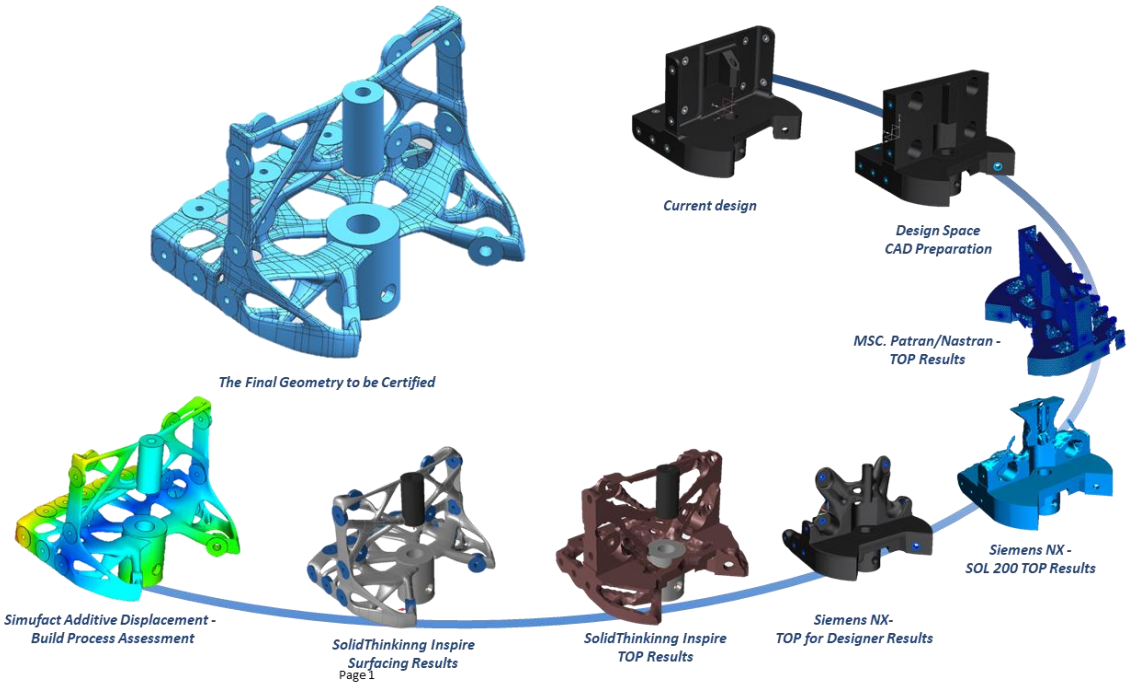

Figure 5-1: Results summary of the design cycle for the biomimetic volumetric bracket

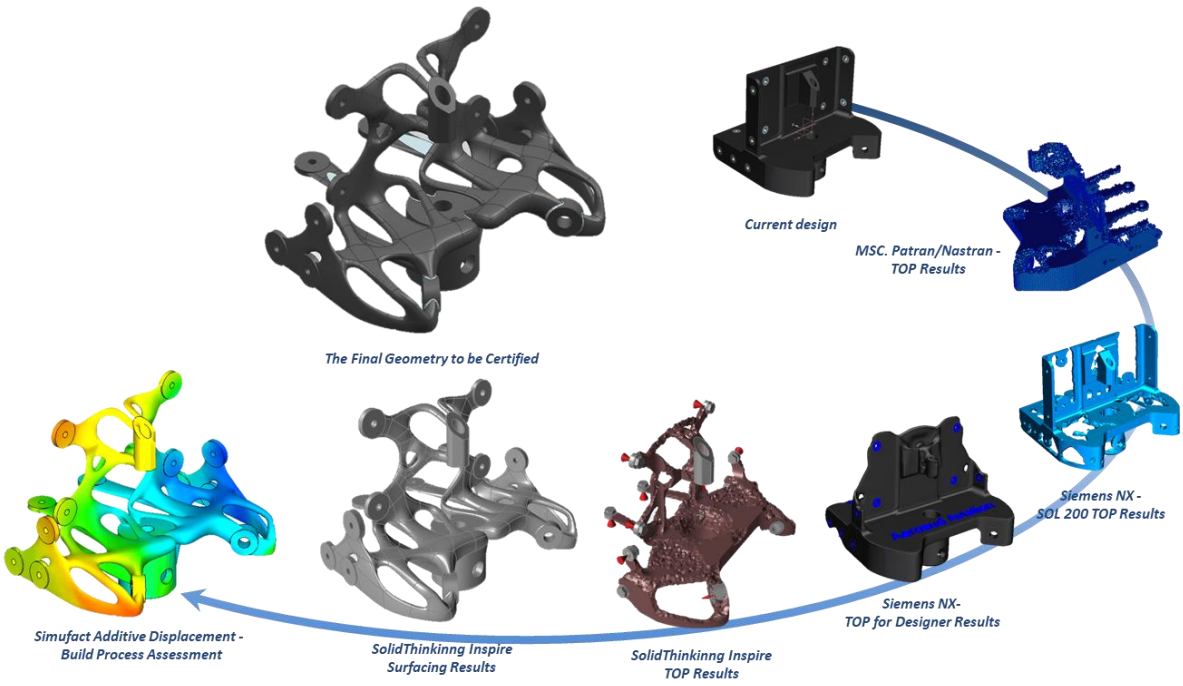

Figure 5-2: Results summary of the design cycle for the biomimetic current bracket

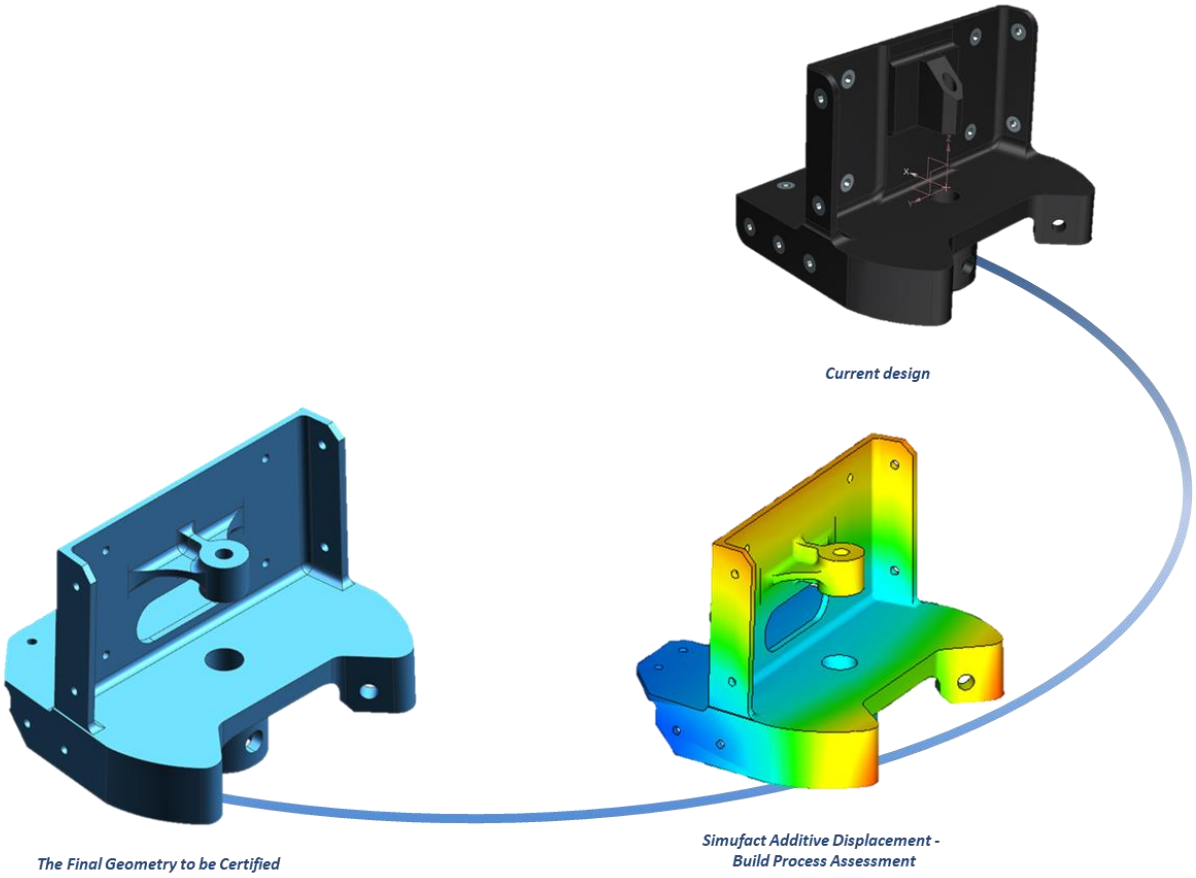

Figure 5-3: Results summary of the design cycle for the prismatic bracket

Table 5-1 Weight comparison results

Part in TI64	CAD Mass Measurement (kg)	Difference(kg)	%	Actual mass measurement (kg)	%	error
Initial design	0.87414	N/A	N/A	N/A	N/A	N/A
Prismatic	0.49608	0.37806	43	N/A	N/A	N/A
Biomimetic volumetric	0.34823	0.52591	60	0.3248	63	6.728
Biomimetic current	0.2628	0.61134	70	0.2385	73	9.246

5.2 CAD results

The initial component design was defined by the case study and previous work done on the CFRTP project, as mentioned in Chapter 4. In this phase, the component is re-evaluated as described in Section 2.3.3 of Chapter 2. Section 7.5, Appendix E shows the process manual for the CAD phase, and the process flow of this phase can be seen in Figure 5-4. The difference between the current geometry and the re-evaluated geometry can be seen in Figure 5-5. The initial design's volume is $1.32 \times 10^5\ mm^3$ compared with the re-evaluated geometry, which has a volume of $3.90 \times 10^5\ mm^3$.

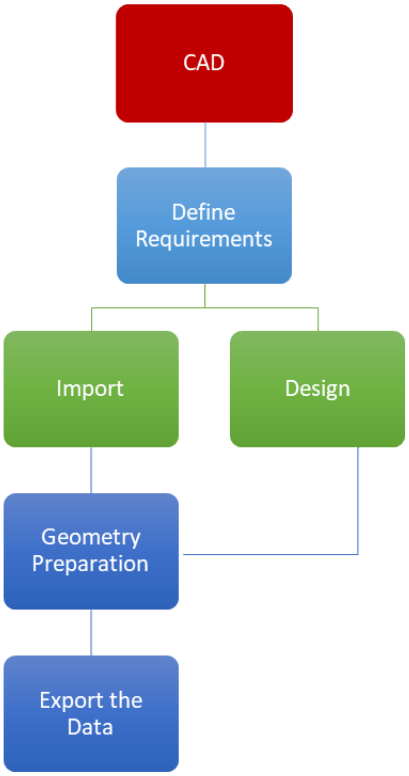

Figure 5-4: CAD process manual flow

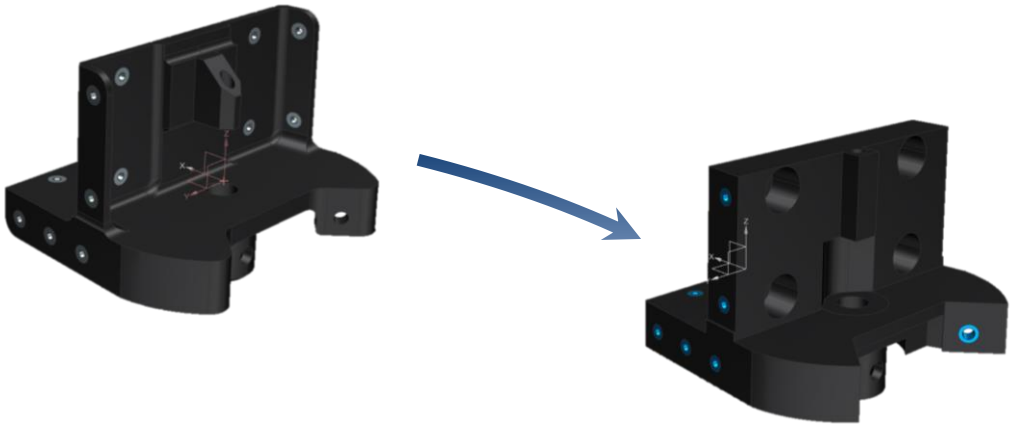

Figure 5-5: Re-evaluation results

For the first and second scenarios, the re-evaluation can be done using any software to edit the geometry. Figure 5-6 and Figure 5-7 show that SolidThinking Inspire and Siemens NX capabilities simplify the geometry by removing fillets, chamfers and partitioning areas that must be kept. The re-evaluated geometry encapsulates the entire design space that the component can utilise without altering the rest of the assembly. The designated design space was used to allow for the most efficient load path to be defined by the topology optimisation simulation without limiting or forcing a defined path. The design space was defined in a way that would take many aspects into account, for instance, the accessibility of fastener holes with the rivet tools, the movement of the rudder and the area constraints around the rest of the assembly.

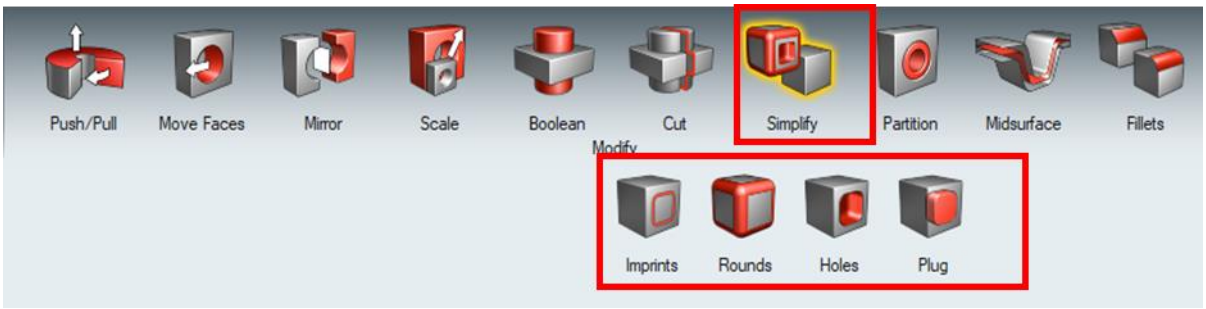

Figure 5-6: SolidThinking Inspire geometry clean-up capabilities

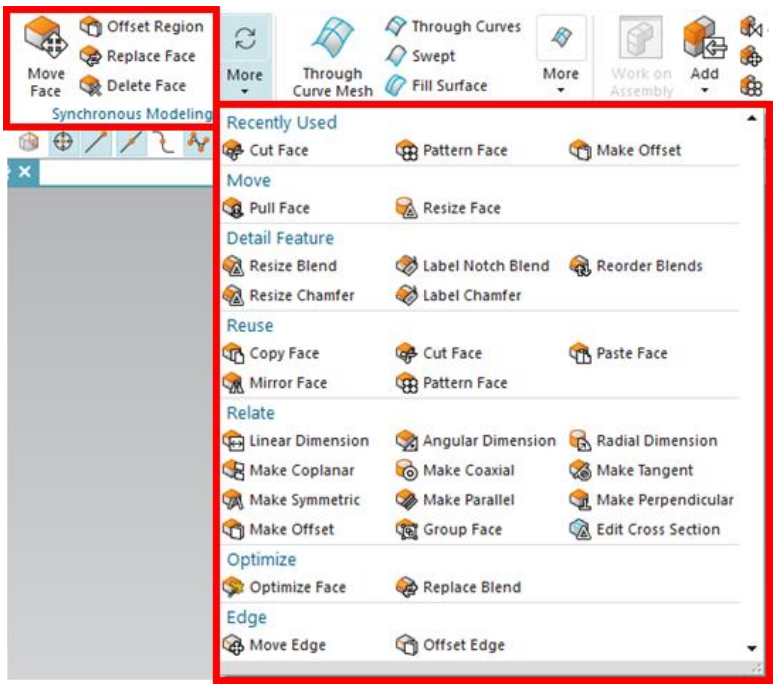

Figure 5-7: Siemens NX geometry clean up capabilities

In this section, the traditional design was used to derive the prismatic component seen in Figure 5-8. This was done with the knowledge and experience of the chief designer at Aerosud, who gave input on where the initial design could be improved. The component was not designed for AM, as there are many aspects to the design that were not ideal for the SLM process, with overhang angles exceeding the maximum allowable angle without adding support structures, large flat areas, and large variation in the thickness of the component.

Figure 5-8: The final prismatic geometry

5.3 Optimisation results

The optimisation phase was an essential part of the design cycle, as it provided insight into the complex structures that were not achieved through traditional hand-calculation assessment and design principles. The goal of the optimisation phase of the design cycle was to achieve geometry with a biomimetic structure where the structure mimics the shapes seen in nature, as described in Section 2. Literature has shown that topology optimisation has become a popular topic since the development of AM. Due to its popularity, many FEA software vendors have begun further development of their topology optimisation capabilities.

The process flow in Figure 5-9 was developed as a generic method that could be applied to any software package. The optimisation process manual presented in Section 7.5, Appendix E, provides a detailed step-by-step method on how to conduct an optimisation irrespective of the simulation software package used. To illustrate the usefulness of the proposed optimisation process, a benchmark investigation using several software packages was conducted. The following software packages were investigated in the present study:

- Patran/Nastran, 2014.1 and 2018 (MSC. Software Corporation)
- NX, 12(Siemens)
    - Sol 200 NX Nastran Topology Optimization
    - Topology Optimisation for Designers
- Inspire, 2018.2 and 2019 (Altair SolidThinking)

In Sections 5.3.1 to 5.3.3, the various results from the respective topology optimisation processes will be discussed in detail, together with the process that was followed for each of these results.

Figure 5-9: Optimisation process flow

5.3.1 MSC. Patran/Nastran optimisation results

This section will describe the method used in obtaining the results for MSC. Patran/Nastran. Occurrences were noted during the optimisation process and setup. The software was used inhouse for structural analysis in Aerosud. There was ample knowledge of the FEM setup, for example, in selecting the mesh type and adding load sets and constraints. However, the exposure was limited to the topology optimisation process and thus required training and further development. An issue arose during the case study, which is highlighted in Figure 5-10, which clearly shows that the mesh of the two different bodies is misaligned. Due to this, it was difficult to achieve a complex and properly stitched mesh. The functionality of mesh stitching is for advanced users, so with the right amount of exposure, the problem would not occur, but for a basic user, this would be a stumbling block. Due to the limitation of time and so as not to wander off the topic of the study, other options were explored to mesh the geometry, such as MSC Apex and Siemens NX 12. Both packages could be used to set up the FEM and then export the model as a data file or an MSC Nastran bulk data file. As mentioned in the previous section, the main

goal of the study was to develop the process and not to develop the software used during the study. This limited the scope, as topology optimisation can be seen as a study on its own.

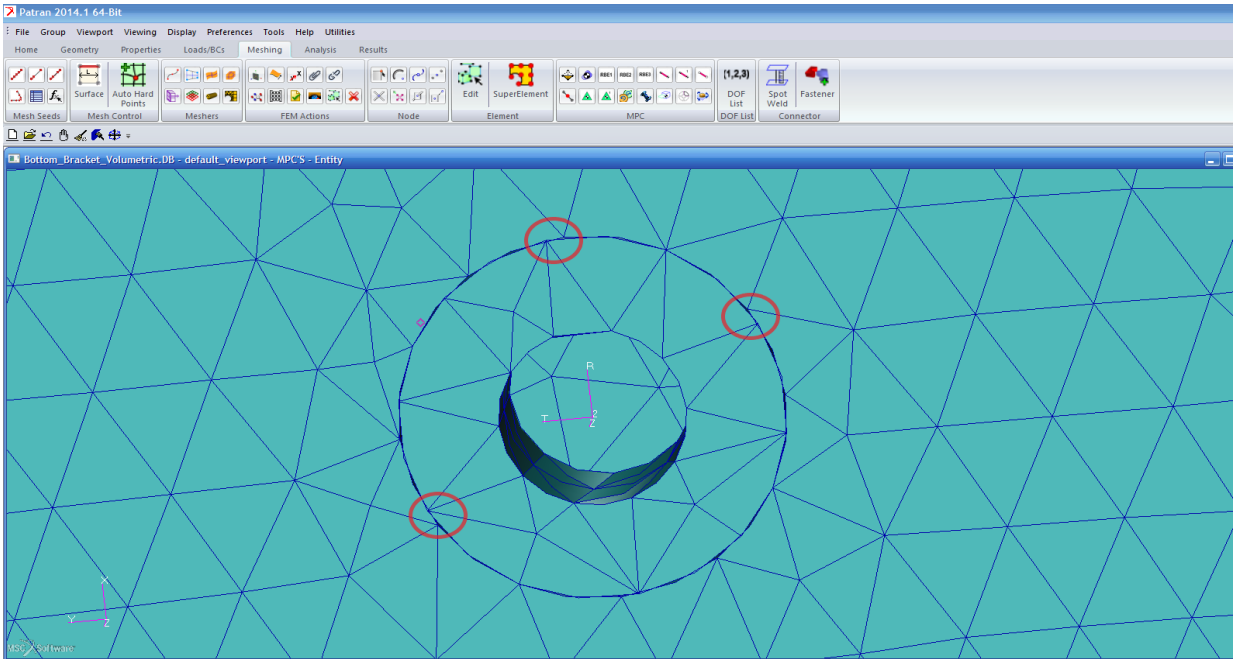

Figure 5-10: Mesh stitch issue

Once the FEM setup was completed and validated, the topology optimisation process was started. Several inputs are required for the optimisation process. The input parameters used for this section are:

- Element type: Tetrahedral – 10
- Optimisation objective: Minimum compliance
- Design constraint: Mass fraction 0.4 (40%)
- Manufacturing constraints: Minimum member size
  Extrusion constraint in the Z-direction
  Symmetric constraint across the ZX-plane

Figure 5-11 depicts the results of the first scenario where the component was re-evaluated during the CAD phase of the design cycle to enhance or improve the design space. The parameter mentioned above was set for optimisation. Several iterations were done to achieve the geometry shown below. MSC is based on the density method and mathematical programming to solve not only classical topology but also multidisciplinary problems similar to this case study. The

component was hollowed out instead of creating the biomimetic structures. The optimisation method retained too many elements for the biomimetic structure to be released. It is highlighted for the reader that this study was done to develop the design cycle process and the functionality of the optimisation process within the design cycle and not to develop the optimisation process itself.

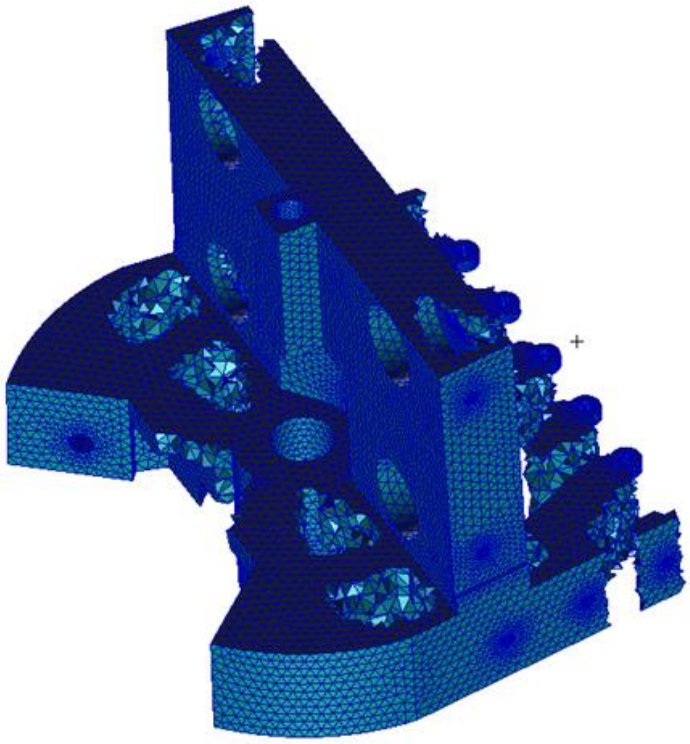

Figure 5-11: Volumetrically re-evaluated design

The same process was applied for the second scenario, as depicted in Figure 5-12. The result has similarities to the results from scenario one, as the same optimisation process was used with the same set of parameters. At first glance, it seems that the optimisation process has eliminated more elements than the previous scenario at the top of the component. Yet, it is still evident that a number of elements were retained in the lower part of the bracket, which is mainly due to the large loads. The results for this scenario represent more of the desired output of the biomimetic structure, but further development is still required from a user perspective to achieve these structures. The Nastran file used to set up the optimisation should be fully understood, and each variable should be investigated during the development to achieve the desired result. As mentioned previously, this is grounds for an entire study on its own.

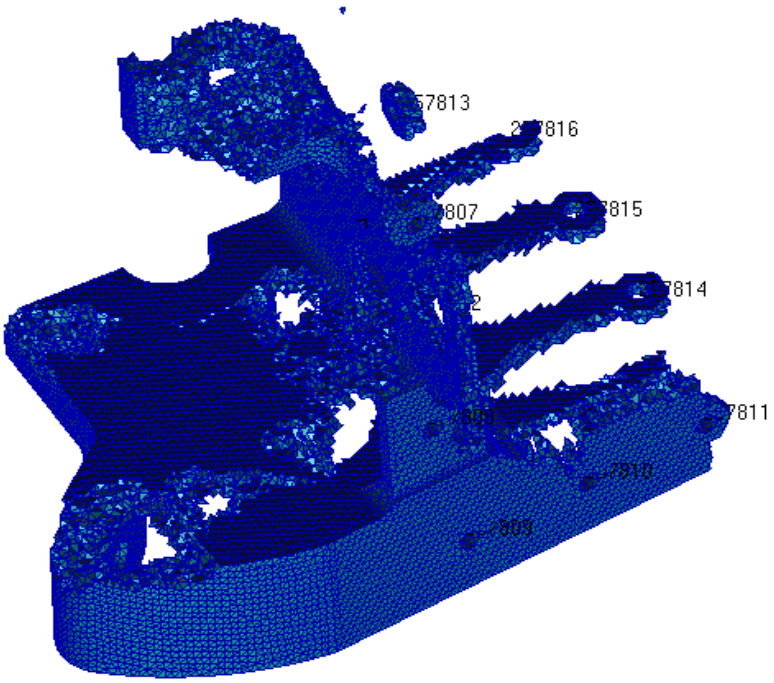

Figure 5-12: Initial design topology optimisation result

Another observation that was made during the optimisation process is that there is no distinct technique to convert the mesh data to an STL without using third-party software. The software used to perform this conversion is part of the MSC suite, Mentat. The mesh data was imported as a Nastran bulk file to complete the conversion of mesh to facet geometry.

5.3.2 Siemens NX 12 optimisation results

This section will describe the process and results for each of the methods offered by Siemens. The optimisation investigation was done using Siemens NX 12 Nastran SOL 200 and Topology optimisation for designers. These two methods use completely different optimisation approaches. Siemens TOP for designers uses the black-box approach, the automated mesh feature, and limited parameters, while with the Nastran SOL 200, it is possible to mesh the component to the operator's desires and set up problems of a multidisciplinary nature. The process is very similar to MSC Patran/Nastran but with additional parameters, for example manufacturing constraints and optimisation objectives.

5.3.2.1 Siemens NX 12 Nastran SOL 200

The process for setting up FEM is similar across all platforms, including setting up the mesh, adding the boundary conditions, and populating material data. The deviations begin to occur during the optimisation process, as there are more parameters to be considered during NX Nastran SOL 200. The consideration of more parameters is possible with other software vendors in the background development. Siemens has added these to the simulation user interface. The input parameters used for this section are defined as:

- Element type: Tetrahedral – 10
- Optimisation objective: Minimum compliance
- Design constraint: Mass fraction, Lower bound 0.3 and Upper bound 0.5
- Manufacturing constraints: Planar Symmetry across the ZX plane
  AM constraint – 45 degrees overhang angle

The result of the optimisation process is depicted in Figure 5-13. The desired result to achieve a biomimetic shape was not fulfilled since no material was removed from the bottom half of the bracket, and there was no construction of thin branch-like beams through the component. The topology optimisation process using NX Nastran as the solver requires extensive development and an understanding of how each of the constraints affects the result, similar to the development that is required in MSC, as both these software vendors use the same type of solver.

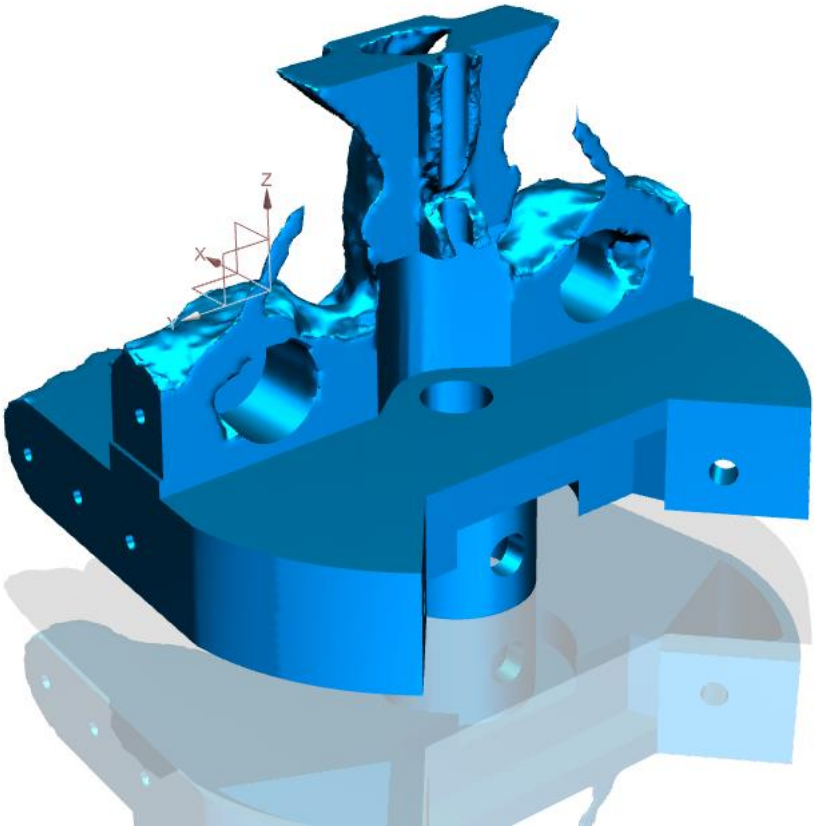

Figure 5-13: Sol 200 NX Nastran topology optimisation result for the re-evaluated design

The same process was applied for the second scenario, as depicted in Figure 5-14. The result has similarities to the results from scenario one since the same optimisation process was used with the same set of parameters. While the biomimetic shape was still not achieved, the results gave a decent indication of where the load paths were and how the design could be optimised. The optimisation method algorithm eliminates redundant material that does not bear any load or has very low stress values.

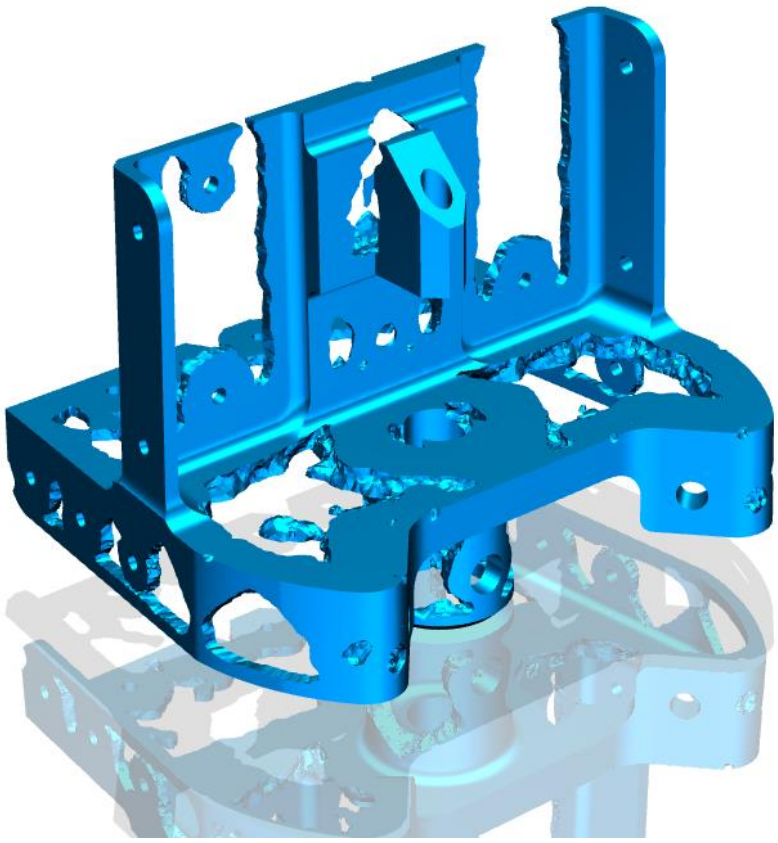

Figure 5-14: Sol 200 NX Nastran topology optimisation result for the initial design

5.3.2.2 Siemens NX 12 Topology Optimisation for Designers

Topology optimisation for designers combines FEA and Frustrum's voxel-based design algorithm to generate multiple iterations of the topology optimisation design. The module allows users to input certain design parameters – such as weight, cost, material, and function. The module generates a mesh that, through Siemens NX, can be incorporated into precise geometry. The output results are watertight, with no intersecting polygons or other errors typically associated with topology optimisation. The black box approach that the module offers was easy to set up; however, it lacked the engineering capabilities to manipulate the FEM. For multiple load cases, the setup became tedious and time-consuming, as the easy-to-use software does not cater for multiple numbers of load cases. The input parameters used for the process are:

- Optimisation objective: Minimum compliance
- Design constraint: Mass fraction, lower bound 0.3
- Manufacturing constraints: Planar symmetry across the ZX plane
  Material spreading of 60%

The results of the optimisation process can be seen in Figure 5-15. The results that were obtained were shaped into the biomimetic structure; however, there was still no effect on the bottom half of the component. In retaining most of the material, as the Frustum caters for AM in its solver, it tried to reduce the overhang angles and make the part more printable.

Figure 5-15: Siemens NX 12 topology optimisation for designers results for the re-evaluated design

The results of the optimisation process can be seen in Figure 5-16. The process did not generate a biomimetic shape and only removed material from the edges of the component. As mentioned previously, Frustrum caters specifically to the AM constraints, and the geometry shows that there are no large variations in thinness or overhang angles except for the bottom base of the component, which bears the biggest load. For an initial idea of where each load will generate load paths, this method presents an adequate geometry for the designer/engineer to interpret. However, for a complex multi-load case problem, the method does not generate biomimetic shapes.

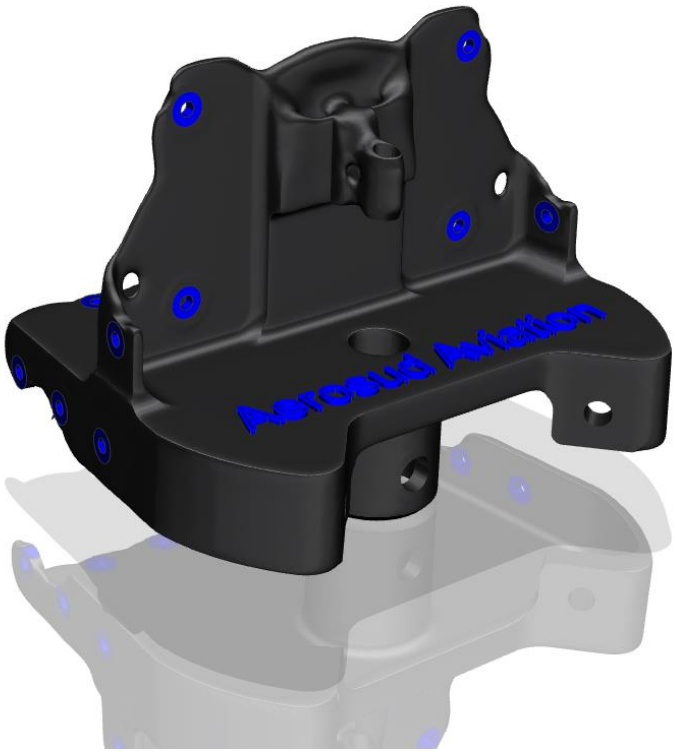

Figure 5-16: Siemens NX 12 topology optimisation for designers results for the initial design

5.3.3 Altair SolidThinking Inspire optimisation results

Since none of the previous topology optimisation processes yielded desirable results, a biomimetic solution was required for further investigation. In 2018, Terry Wohler's and Olaf Diggle presented a course on design for AM, where they used Altair SolidThinking Inspire to showcase topology optimisation possibilities when designing for AM. The process was appealing, and so, the investigation was initiated. This section will describe the methods used and the results achieved during the topology optimisation process. The input parameters for the process are as follows:

- Optimisation objective: Maximise stiffness
- Design constraint: Mass fraction 0.1 - 0.2 (10 - 20%)
- Manufacturing constraints: Minimum member size of 4 mm
  Maximum member size of 7 mm
  Extrusion constraint in the Z-direction
  Symmetric constraint across the ZX-plane

Figure 5-17 depicts the results achieved for the first scenario, where the geometry was re-evaluated to increase the design space. The goal of creating biomimetic shapes with the optimisation process was achieved. The images show the tree-like structures between critical points. These critical points represented the interface points for the rest of the assembly and were designated as fixed spaces during the optimisation process. The easy-to-use user interface made it possible to do multiple iterations of optimisations in one file. The parameters could be altered, and a new solution could be generated. Table 5-2 shows the iterations and the change in objective and how it affects the total mass, the mass of the design space, and the compliance. The results of the multiple iterations are depicted in Section 7.2.1 appendix B.

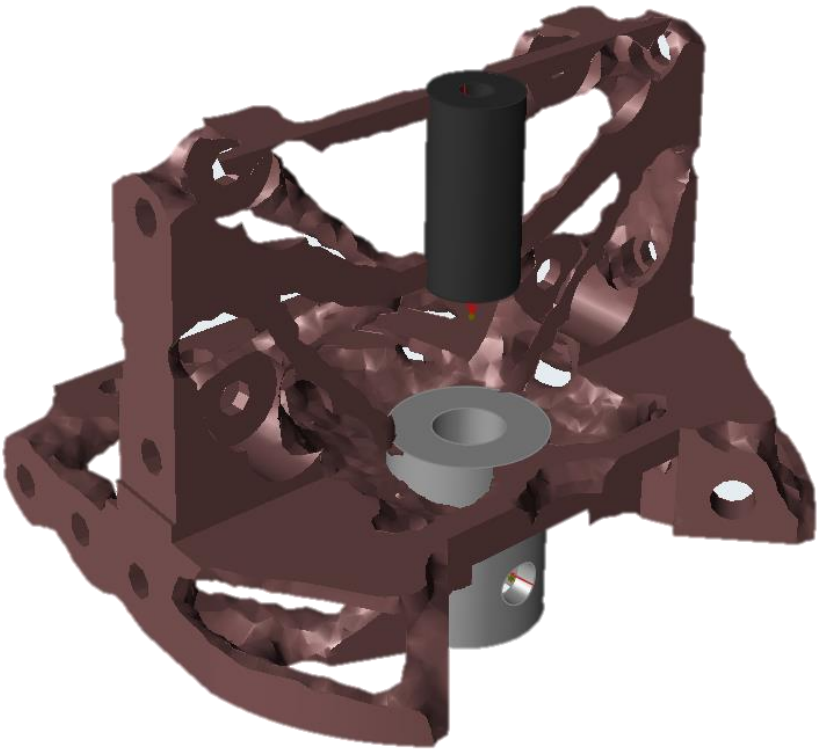

Figure 5-17: Altair SolidThinking Inspire topology optimisation results for the re-evaluated design

Table 5-2: Topology optimisation results for multiple parameter changes for the re-evaluated design

Run	Mass Total (kg)	Mass BODY.32 (kg)	Compliance
Volumetric_Bottom_bracket_Ispire_rev2 Max Stiffness Mass 20% (37)	5.98E-01	4.79E-01	4.94E+01
Volumetric_Bottom_bracket_Ispire_rev2 Max Stiffness Mass 20% (39)	4.21E-01	3.02E-01	4.04E+01
Volumetric_Bottom_bracket_Ispire_rev2 Max Stiffness Mass by Part (BODY.32 14%) (9)	7.67E-01	5.52E-01	9.34E+00
Volumetric_Bottom_bracket_Ispire_rev2 Max Stiffness Mass by Part (BODY.32 25%) (28)	5.12E-01	3.93E-01	3.70E+01
Volumetric_Bottom_bracket_Ispire_rev2 Max Stiffness Mass by Part (BODY.32 25%) (35)	5.08E-01	3.89E-01	3.77E+01
Volumetric_Bottom_bracket_Ispire_rev2 Max Stiffness Mass by Part (BODY.32 31%) (29)	6.10E-01	4.91E-01	4.01E+01
Volumetric_Bottom_bracket_Ispire_rev2 Max Stiffness Mass by Part (BODY.32 31%) (30)	6.20E-01	5.01E-01	3.79E+01

The optimisation process for the second scenario was conducted in the same manner as that for the first scenario. Figure 5-18 depicts the results of the topology optimisation process. Table 5-3 shows the iterations, how the object was changed, and how it affected the total mass, the mass of the design space, and the compliance. The results of the multiple iterations are depicted in Section 7.2.2 appendix B.

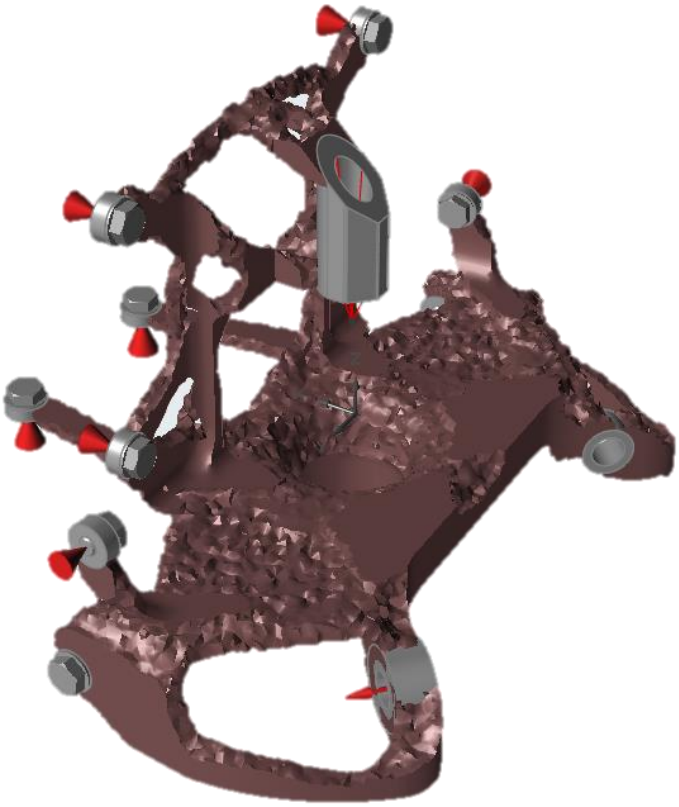

Figure 5-18: Altair SolidThinking Inspire topology optimisation results for the initial design

Table 5-3: Topology Optimisation results for multiple parameter changes for the initial design

Run	Mass Total	Mass PART BODY	Compliance
Parametric_Bottom_Bracket Max Stiffness Mass 20% (6)	3.75E-01	3.39E-01	1.22E+01
Parametric_Bottom_Bracket_rev3 Max Stiffness Mass 15% (7)	1.46E-01	1.26E-01	6.75E+00
Parametric_Bottom_Bracket_rev3 Max Stiffness Mass 15% (8)	1.67E-01	1.48E-01	1.23E+01
Parametric_Bottom_Bracket_rev3 Max Stiffness Mass 15% (9)	1.46E-01	1.26E-01	6.84E+00

The desired outputs of biomimetic structures were not achieved from the MSC. Patran/Nastran and the Siemens NX software packages. The design constraints and manufacturing constraints were set up to achieve the biomimetic structure but yielded prismatic results. Instead of removing all the material that was not associated with the critical load part, many elements were retained. The algorithms for MSC and Siemens are similar for the SOL 200 (Nastran) operation when solving for topology optimisation; thus, there were similarities in results.

It should be noted that the scope of the study was not to investigate software packages but to showcase the methodology of the design cycle and how each process or phase adds value to the overall performance of the component. Taking this into consideration, the final software package, SolidThinking Inspire, was also investigated as an addition after the author had gained exposure to the software during a design for additive manufacturing (DFAM) course. The simplified interface, coupled with automated meshing, reduces Inspire to essentially a “black box” functionality. However, the structures achieved during the optimisation process resulted in biomimetic shapes, which was one of the goals of this phase of the design cycle.

5.4 Internal features and surfacing results

Inspires PolyNURB functions seen in Figure 5-19 were used to clean up the geometry obtained from the optimisation process. This improved the aesthetics of the component and converted the CAE data to usable CAD data. The Wrap function was the most commonly used tool in the process of cleaning up the geometry. The process manual that defines the process can be seen in Section 7.5, Appendix E. This process does not have a defined process flow, as it is an internal step of the optimisation process. It should be noted that any software packages with similar features can be used to clean up the geometry. The fictionality of Inspire was chosen to clean up the biomimetic shapes that were achieved during the optimisation phase of the design cycle.

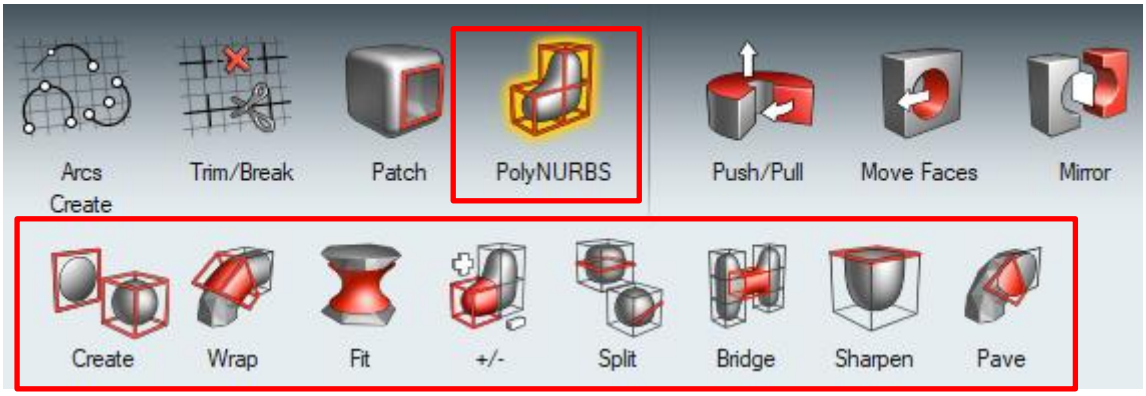

Figure 5-19: PolyNURB functions for Inspire

The final geometry was created by using the results from the topology optimisation from Altair Inspire. As mentioned in Section 5.3.3, the Inspire optimisation process yielded multiple iterations for both the re-evaluated and the initial design. The geometry was derived using each of these iterations to ensure that all the scenarios were covered. This process is effective but time-consuming, as a lot of engineering knowledge and experience in structures is required to understand how the load path will run through the design space. The results can be seen in Figure 5-20 and Figure 5-21 of the cleaned-up topology optimisation results.

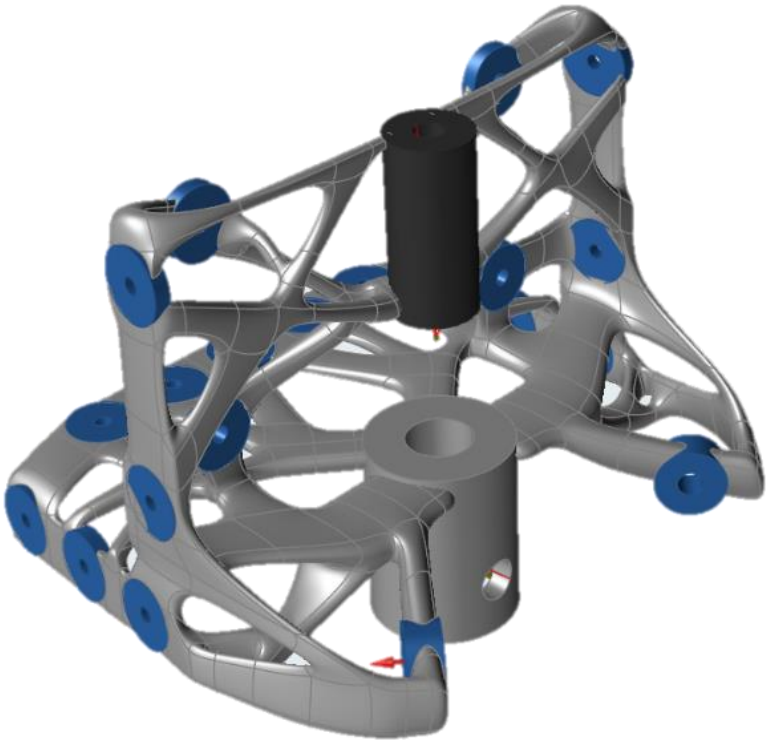

Figure 5-20: Surfacing results for the re-evaluated optimisation process

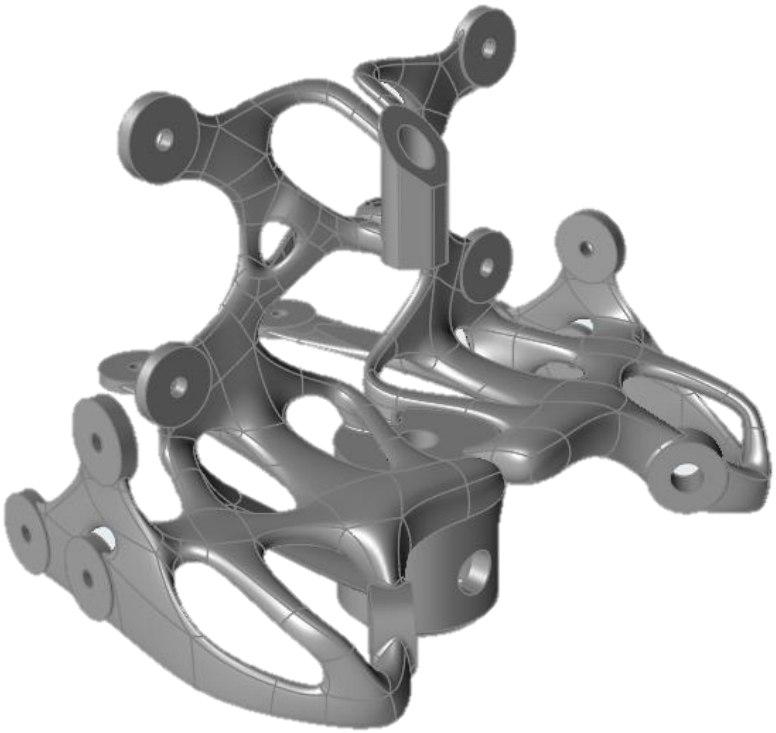

Figure 5-21: Surfacing results for the initial optimisation process

5.5 Manufacturability results

Simufact Additive was used to determine whether the component that was generated during the topology optimisation phase could be manufactured without the risk of build failure or significant distortion. To evaluate an accurate output, a calibration experiment was conducted. The calibration procedure is necessary to capture all the build parameters that were used to print the cantilever test sample. The samples are cut at a defined height, and the deflection in the Z-direction is measured. These values are captured by the software and used to determine the inherent strain values. A machine profile is now defined and will be used for all components manufactured on the specific machine using the defined parameters. The process flow is depicted in Figure 5-22, which was followed to achieve the results in this chapter. The process is defined in the process manual, which can be seen in Section 7.5, Appendix E.

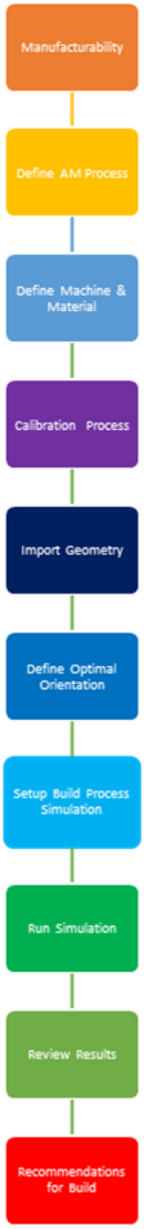

Figure 5-22: Manufacturability process flow

5.5.1 Calibration results

In Figure 5-23, calibration samples have been distributed across the build plate to ensure the whole build plate's inherent strain is calculated. Simufact interpolates from the four data points for the inherent strain value at any given point in the print space. The calibrations samples were manufactured using a Concept laser M2, and the material used for this build was Ti-6Al-4V grade 23. The Engineering Test Plan (ETP) in Section 7.3.1, Appendix C, provides the detailed plan that was followed to conduct the test for the calibration.

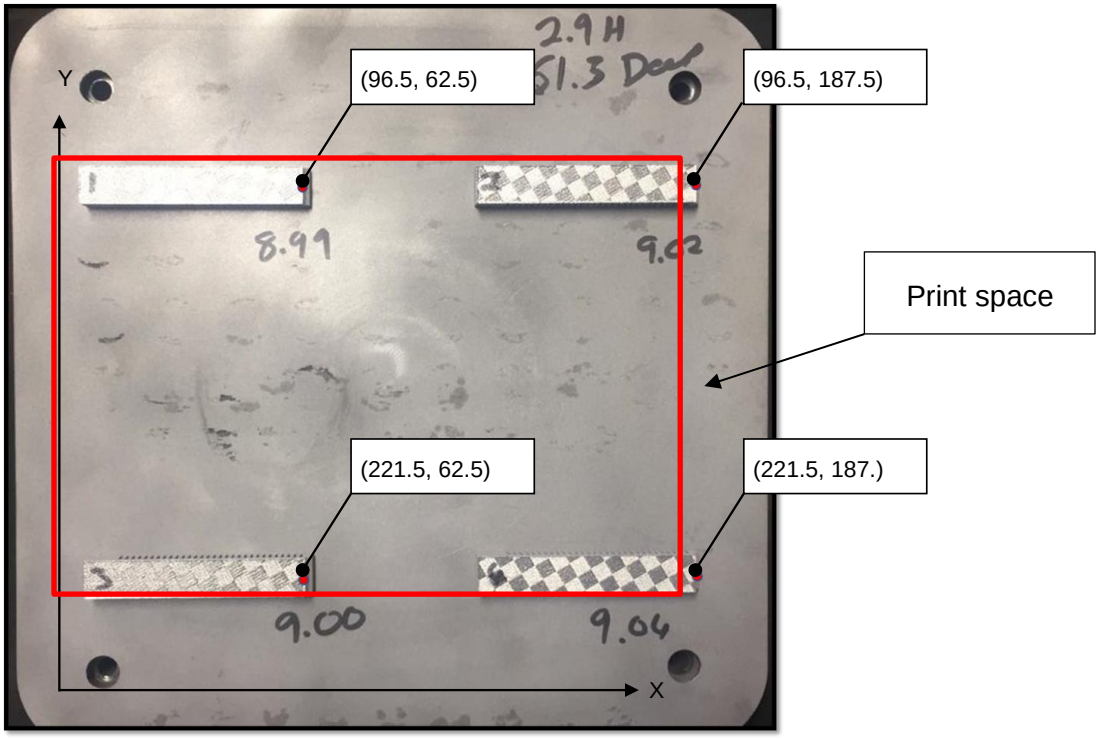

Figure 5-23: Distributed samples across the build plate

In Figure 5-24, the displacements of the cantilever samples are shown after the samples have been cut at 2.9 mm as per the engineering report. The displacement in the Z-direction was measured with a calibrated depth gauge.

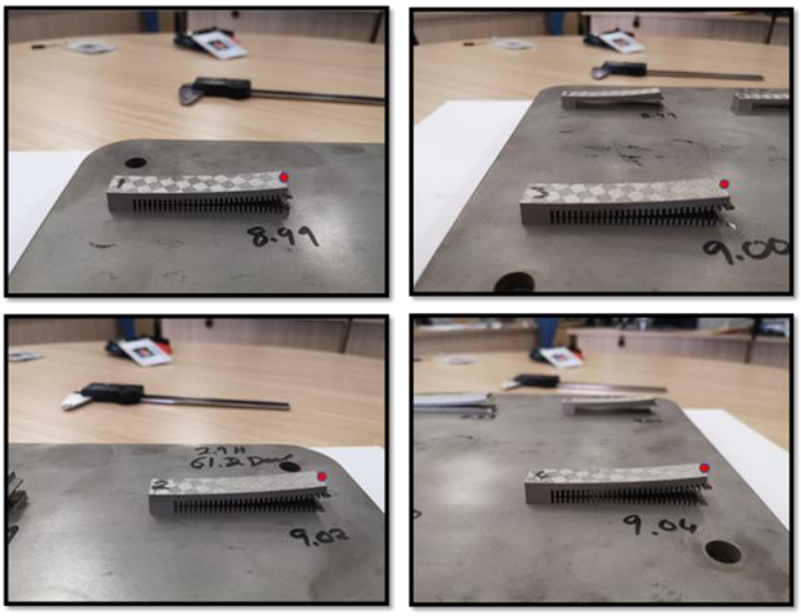

Figure 5-24: Cantilever samples after cutting

Table 5-4 presents the experimental data that was measured compared to the convergent values simulated by the software. In Figure 5-25, the maximum deviation is seen for part 2, with a deviation of 2.94766%. This implies that the simulation outcome of the calibration is accurate to the maximum percentage achieved.

Table 5-4: Output data from Simufact

Part	Δz_max target [mm]	Δz_max simulation [mm]	Δz_max[mm]	Δz_max [%]
1	3.91	3.895	-0.015	0.383632
2	3.63	3.737	0.107	2.94766
3	3.78	3.811	0.031	0.820106
4	3.91	3.903	-0.001	0.179028

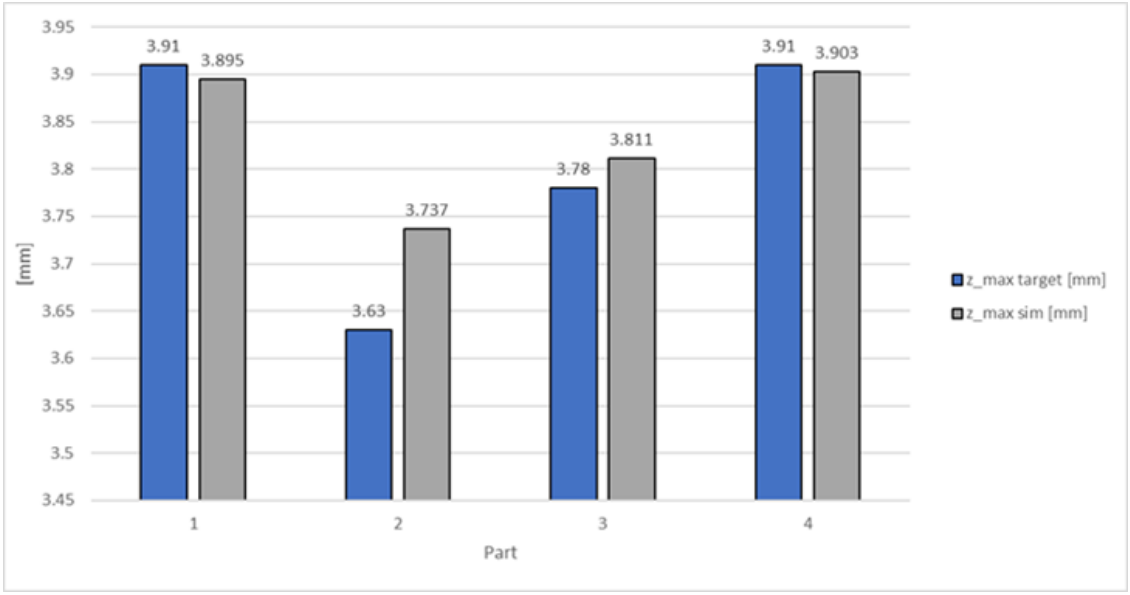

Figure 5-25: Bar graph of the comparison between measured and simulated data

The Engineering Test report can be found in Section 7.3.2, Appendix C, and provides all the results and findings for the calibration process. This report forms part of the process that was followed during the development of the phases of the design cycle and will showcase the setup of the calibration and results achieved.

5.5.2 Component assessment results

The manufacturing assessment was conducted for each of the scenarios and the components that were derived from the previous phases of the design cycle. The assessment was done on Simufact Additive with the strategy of simulating the build as closely as possible. The build process for each assessment will be done in the following order:

- Build
- Unclamp
- Heat treat
- Cutting
- Support removal

For the initial assessment, each component was simulated individually. These results can be seen in Section 7.3.3, Appendix C. Due to budget constraints, the components had to be manufactured by a different company than that of the initial calibration samples. The components were nested in such a way that only two builds were required to save on cost and time. Figure 5-26 shows the nesting strategy that the manufacturer used for the first build.

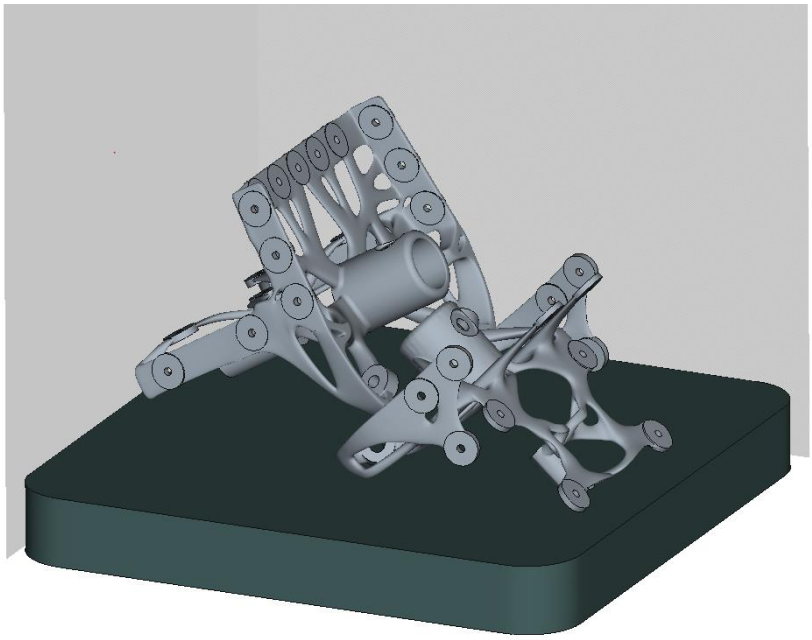

Figure 5-26: Component nesting for the first build

The result of the first build is depicted in Figure 5-27; the witness samples were stopped by the operator during the build process by selecting the specific part and ending the job for that part instead of for the entire build. The witness samples were orientated in accordance with the Airbus requirements, hence the required additional support structures. The witness samples failed due to the distortion pulling the part away from the support material, which could have caused damage to the recoater blade or caused it to fail. Had the recoater blade been damaged or failed, the rest of the build would be likely to fail, as the layers applied would not be evenly spread or smooth.

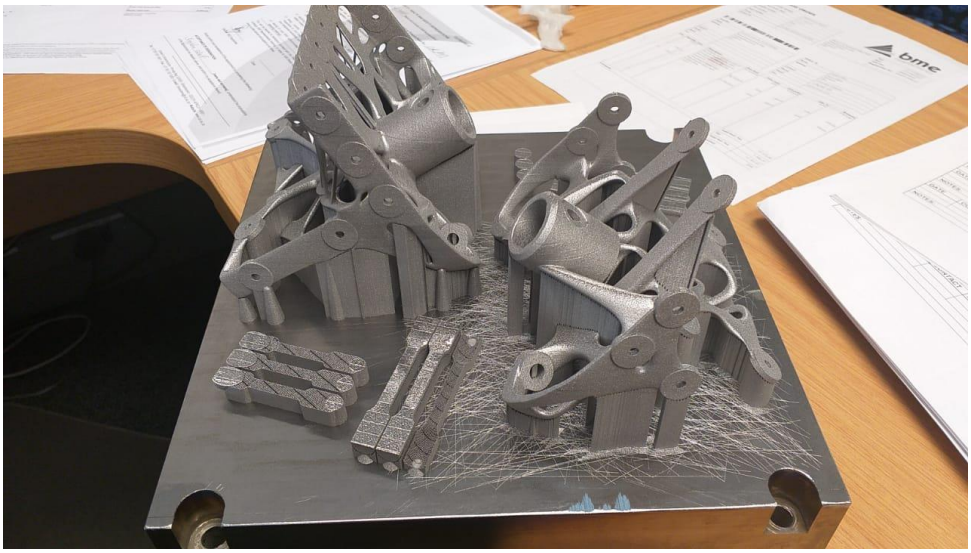

Figure 5-27: The actual result for the first build

After the full inspection, the volumetric biomimetic component failed during the build, as seen in Figure 5-28. The build assessment was done prior to the build and indicated that several areas of the component were at risk of failing. The inherent strain of the component was also very high at the point of failure – higher than that of the ultimate tensile strength of the material. This failure is depicted in Figure 5-29. The QR-code video represents the change in inherent strain during the build.

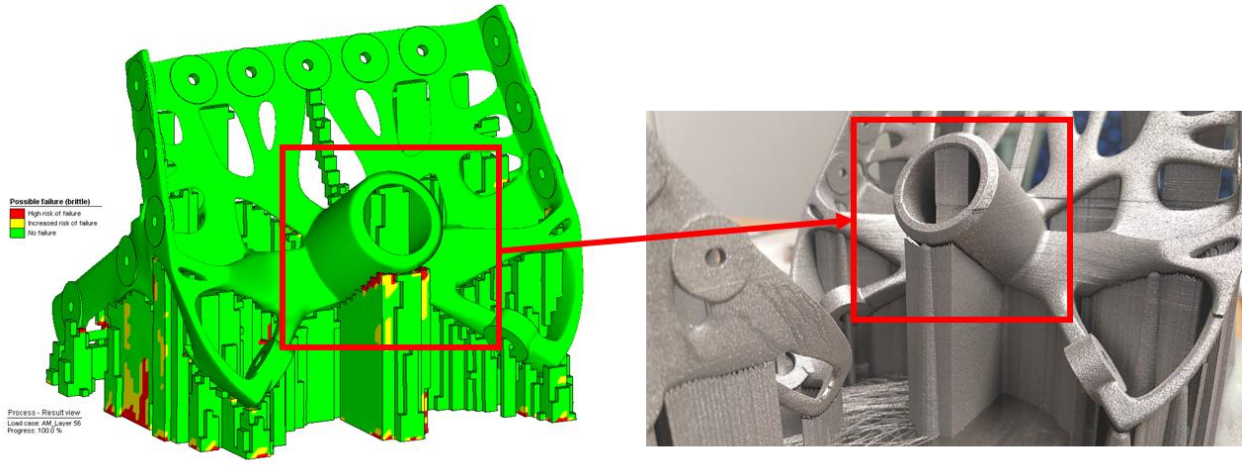

Figure 5-28: Build failure comparison between actual and simulated component

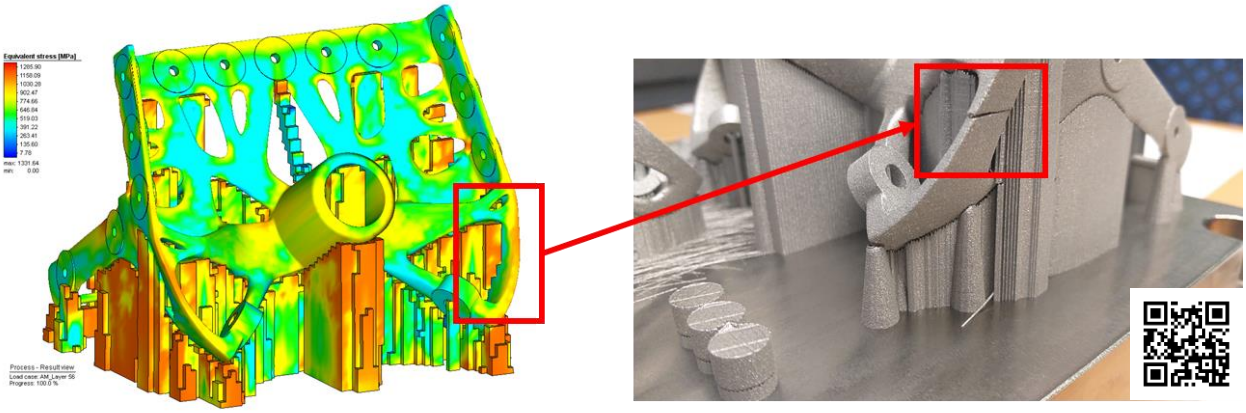

Figure 5-29: Inherent strain build failure comparison between actual and simulated component

After the component was removed from the build plate, it was scanned with a ROMER 3D scanner to compare the distortion between the actual measured component and the predicted simulation value. The 3D scanning report can be found in Section 7.3.4; Appendix C. Figure 5-30 presents the comparison between the 3D-scanned data and the simulated distortion. There was a

maximum deviation of 33% between the scanned and simulated data. The complex geometry made it difficult to scan all the areas of the component. The scanned data was also influenced by the rough surface areas, as the component was not post-processed due to the component failing during the build. The decision was made to not post-process a damaged component and incur unnecessary costs. The scanned data verified the prediction in that the distortion of the software correlates with the actual measured data. This process was only done for one component since it is an expensive process. The scanning process can be seen in the QR code next to the image. No further evaluation was done of the current biomimetic bracket for build one, as the manufacturer broke two of the fastening holes while removing support, which made the part non-conforming and not suitable for use.

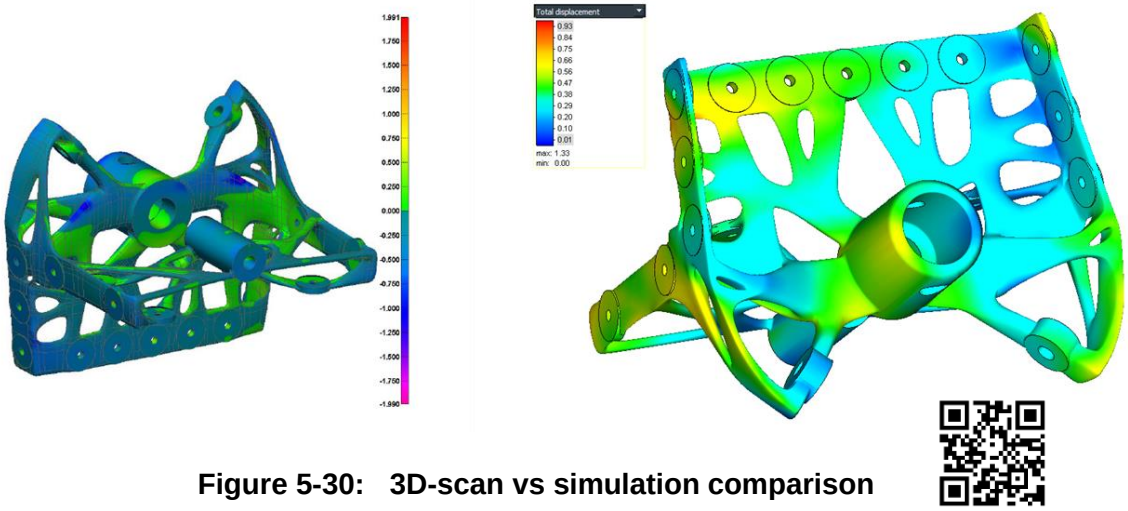

Figure 5-30: 3D-scan vs simulation comparison

For the second build, a different orientation was considered with more support to dissipate the heat better during the build so as to reduce the inherent stresses hereditary to the AM process. Figure 5-31 shows the new orientation nested in the same manner as the previous build.

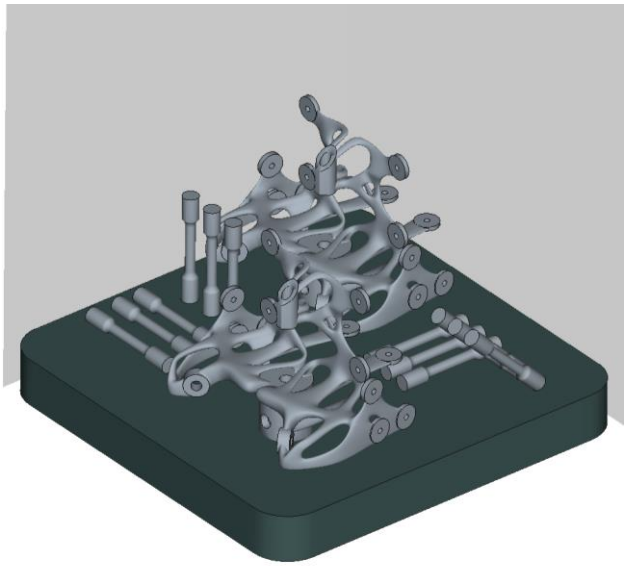

Figure 5-31: Second build strategy

The second build yielded better results than that of the first build, with the surface being the smoother of the components and experiencing no failure during the build. The orientation was changed to the same strategy as mentioned earlier in the section. Figure 5-32 and Figure 5-33 depict the final geometry after all the build stages were completed, and the component was shot-peened to improve the surface finish. More images can be found in Section 7.3.5, Appendix C. Due to the budget constraints and the failure of the first build, the prismatic component could not be manufactured because of the high internal stresses caused by the nature of the geometry, which caused the part to fail continuously after several attempts to manufacture the component.

Figure 5-32: Second build result for the volumetric biomimetic bracket

Figure 5-33: Second build result for the current biomimetic bracket

5.5.3 The final geometry ready to be certified

The components have successfully progressed through the first four phases of the design cycle and are ready for the certification, which is the fifth and final stage of the design cycle. The geometry of the volumetric biomimetic bottom bracket can be seen in Figure 5-34, derived from the first scenario, and the geometry of the current biomimetic bottom bracket derived from the second scenario can be seen in Figure 5-35. The detailed drawings of the three components can be seen in Section 7.3.6, Appendix C, with a detailed view of the dimensions and characteristics of the components in 2D-view.

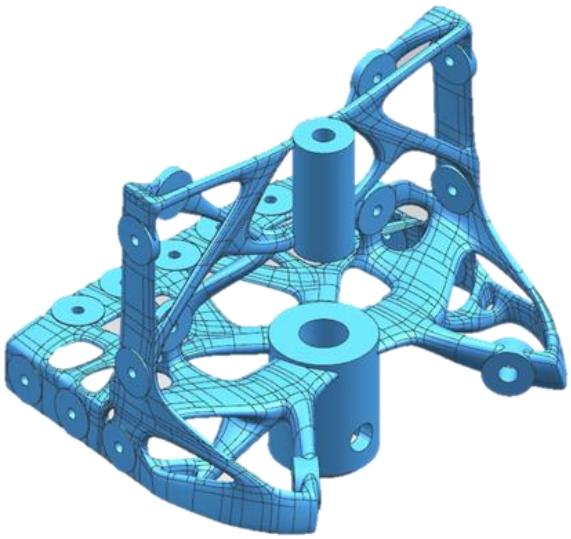

Figure 5-34: Final geometry of the volumetric biomimetic bottom bracket

Figure 5-35: The final geometry of the current biomimetic bottom bracket

5.6 Qualification and certification

This section will discuss the results of the bracket's certification and the development of the manufacturing process' qualification. This is the final phase of the design cycle, where the components are evaluated and deemed structurally sound for their intended use.

5.6.1 Qualification of the build process

In Figure 5-36, the Airworthiness regulations for the FAR 23 and CS 23 are described. It also describes what is essential to consider when designing a component for a normal- and utility category aircraft. The four categories shown in Figure 5-36 are the parts that must be addressed when designing a component that can be deemed airworthy.

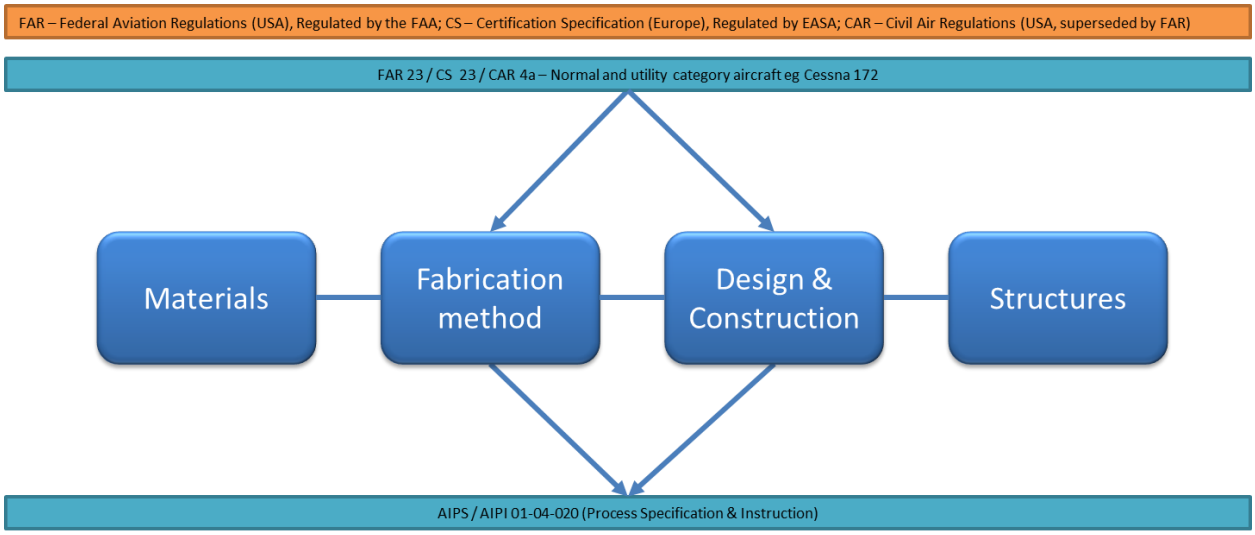

Figure 5-36: Airworthiness regulations for FAR and CS

Figure 5-37 depicts the breakdown of each of the specifications required for the specific part of the manufacturing process. The OEM provides the specifications. In this case, the OEM is Airbus. As mentioned in the literature study, the specifications are developed by the OEM to form part of the manufacturing hub. The specifications must be followed with great precision as there is a tremendous number of tests to do before the process can be qualified. However, the process of qualifying the manufacturing process could only be developed theoretically, as there was no machine or funds available to do each test associated with the OEM requirements physically.

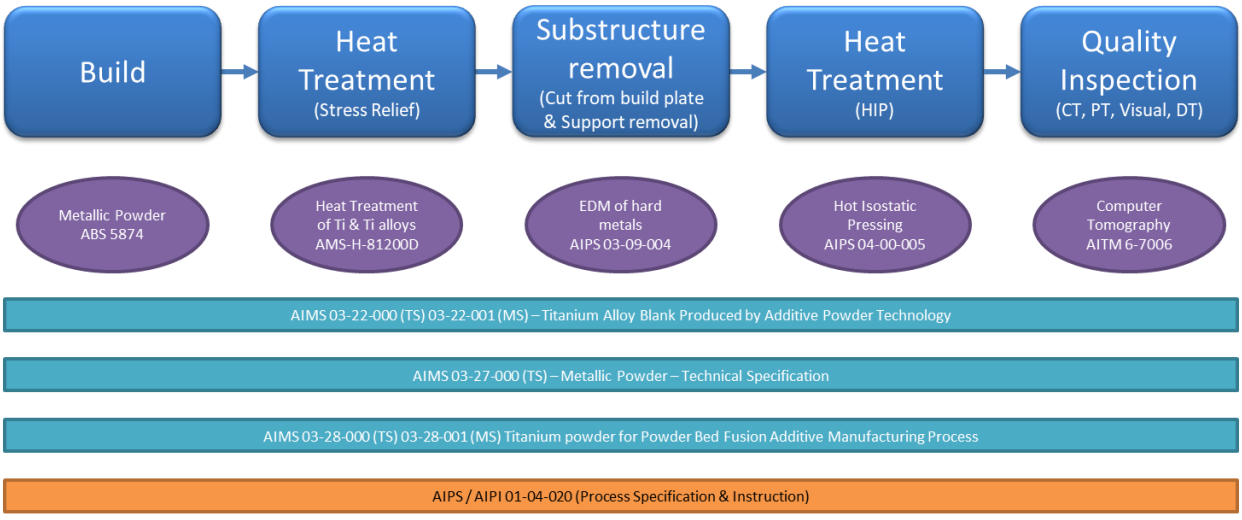

Figure 5-37: Manufacturing process and specification breakdown

5.6.2 Certification of the components

The certification process of the components was conducted to validate whether the components would sustain the unlimited loads induced by the flight envelope. The stress analysis was conducted for all three brackets. The brackets were analysed for Von Mises stress, stability, and the strength of the fasteners. Table 5-5 presents a summary of the reserve factors for all three brackets. Section 7.4.1, Appendix C presents the full stress report that was conducted to evaluate the simulation and the analysis for each of the brackets. The report describes all the details and methods used during the analysis and is a supporting document of the process manual seen in Section7.5 Appendix E. Figure 5-38 depicts the process flow that was followed to achieve the results portrayed in the rest of the section. The stress report also describes the mesh type, element size, loading conditions, and constraints used to set up the FEM. The Neuber method was used to plastically correct the extracted data from the FEM to check the RF.

Figure 5-38: Qualification and certification process flow

Table 5-5: RF Summary for all three brackets

PART NUMBER	DESCRIPTION	MATERIAL	LOAD CASE	APPLIED VALUE	ALLOWABLE VALUE	RF	REMARKS
X0100000 E001001	Volumetric Biomimetic Bottom Bracket - Static	Titanium 64	LC401	806	845	1.049	Neuber Method applied
X0100000 E001002	Current Biomimetic Bottom Bracket – Static	Titanium 64	LC322	824	845	1.025	Neuber Method applied
X0100000 E001003	Prismatic Bottom Bracket - Static	Titanium 64	LC401	816	845	1.035	Neuber Method applied
X0100000 E001001	Volumetric Biomimetic Bottom Bracket - Stability	Titanium 64	LC400			>2	Eigenvalue extraction
X0100000 E001002	Current Biomimetic Bottom Bracket – Stability	Titanium 64	LC401			>2	Eigenvalue extraction
X0100000 E001003	Prismatic Bottom Bracket – Stability	Titanium 64	LC401			>2	Eigenvalue extraction
Rivets	Volumetric Biomimetic Bottom Bracket - Stability	Monel	LC401		Pt – 1501 Ps - 2269	1.17	
Rivets	Current Biomimetic Bottom Bracket – Stability	Monel	LC401		Pt – 1501 Ps - 2269	>2	
Rivets	Prismatic Bottom Bracket – Stability	Monel	LC401		Pt – 1501 Ps - 2269	0.94	Failure in shear due to loading

A static test was required to verify the FEA data and stress analysis. The engineering test plan for the static test can be seen in Section 7.4.2, Appendix D. This test plan describes in detail all the aspects of how the test was conducted, explaining the test jig setup, whiffletree calculations and setup, and the load case definition. For this instance, load case 001 from Table 4-1 was the load case chosen to perform the static test. This load case is defined as the inward pressure on the right-hand skin depicted in Figure 4-2. The design of the whiffletree was calculated based on the chosen load case. The test setup is depicted in Figure 5-39, and more images can be seen in Section 7.4.4, Appendix D. The required load for the rudder assembly must sustain is 304 kg, which calculates to 2 986 N. The detailed loading breakdown can be seen in the engineering test plan in Section 7.4.2, Appendix D.

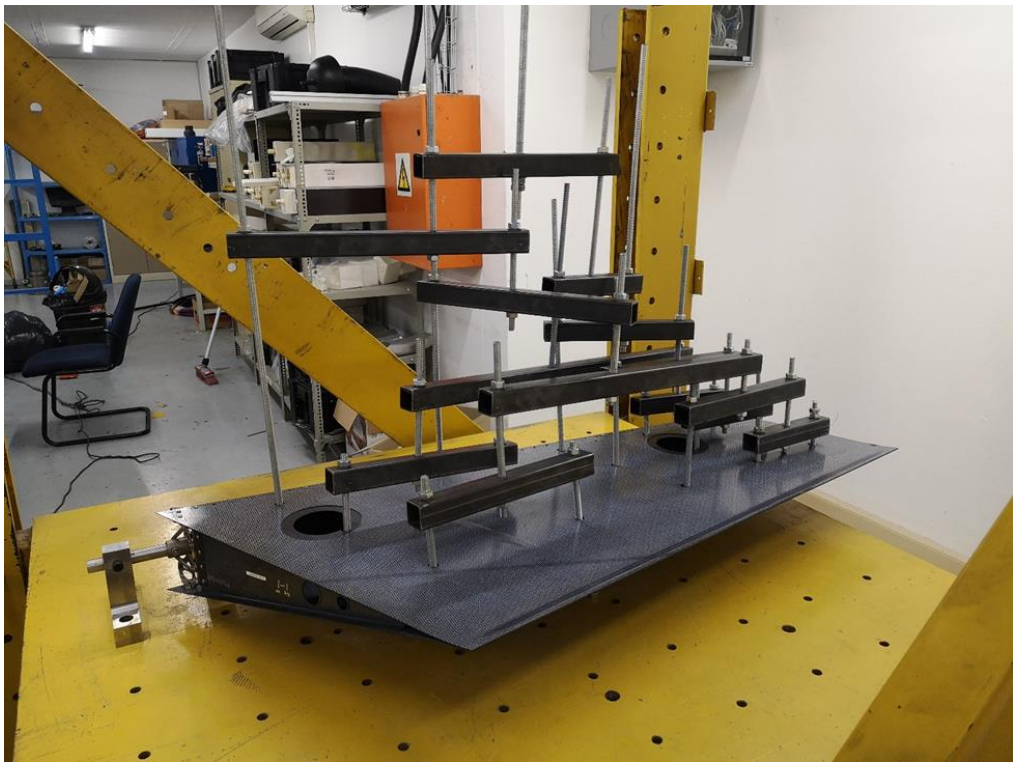

Figure 5-39: Static test setup

The test was only conducted for one component to validate the defined certification process of the design cycle. One full rudder was built using the CFRTP technologies developed from a previous study, as mentioned in the case study. The FAR 23 regulation states that the component should survive the ultimate load for no less than three seconds to be deemed airworthy. Thus, the first part of the test entailed loading the rudder as close to the ultimate load as possible. The rudder was loaded to 331 kg for three seconds and did not fail. The video showing this can be seen with the QR code to the bottom left of Figure 5-40. After the required loads were sustained

by the component, the load was increased to determine at what load the components would fail. However, the whiffletree failed at 970 kg, as seen in Figure 5-40. The whiffletree was developed to sustain the ultimate flight loads and not the load required for the component to break; hence, the failure of the whiffletree was not predicted. The failure of the whiffletree can be seen in Figure 5-41. The video of the failure can be seen with the QR-code at the top right of Figure 5-40. The load is 3.2 times that of the ultimate load required, but none of the components failed. Thus, the verification of the FEM is complete, as the FEM also indicated no failure at ultimate load.

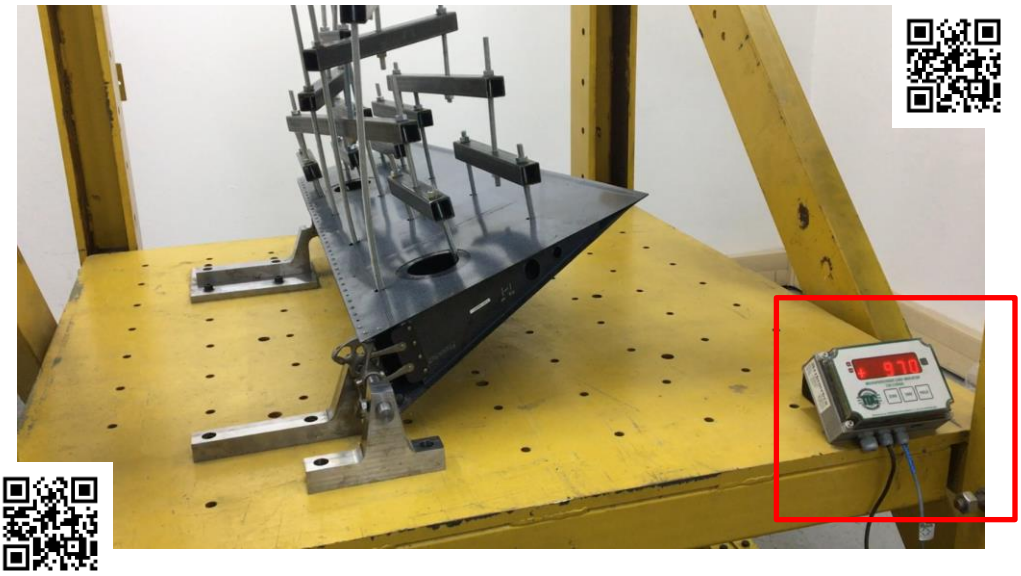

Figure 5-40: Maximum load applied to the rudder assembly

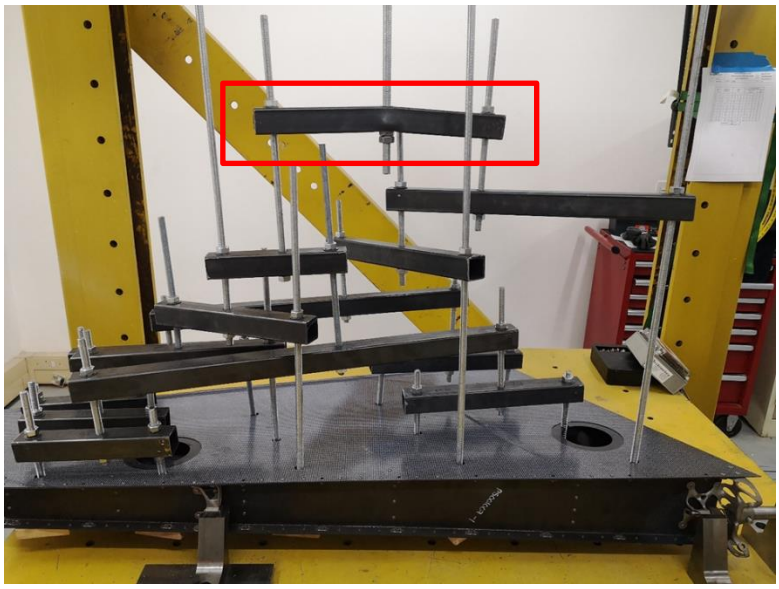

Figure 5-41: Whiffletree failure

CHAPTER 6: CONCLUSION AND RECOMMENDATIONS

6.1 Conclusion

The purpose of this study was to develop a robust process to design, manufacture and ensure specific quality attributes of a component built with AM for the aerospace industry. The objectives of the study were achieved, as each phase of the design cycle was identified, developed, and tested using the boundaries set out by the case study. The process manuals for each phase of the design cycle are referenced throughout the document and can be found in Section 7.5, Appendix E.

The conclusions discussed in this section are made from the results discussed in Chapter 5 and from the practical experiences encountered during the development of the design cycle and related process manuals. The conclusion for each phase will follow:

1. The CAD phase of the design cycle was used to good effect as the geometry of the case study was successfully re-evaluated for the optimisation process. The re-evaluated geometry encapsulates the entire design space that the component utilised during the optimisation process. The designated design space was used to allow for the most efficient load path to be defined by the topology optimisation simulation without limiting or forcing a defined path. The CAD phase and experience in aerospace design was used to derive the final prismatic geometry of the bracket that could be manufactured using AM or TM.

2. The goal of the design cycle's optimisation phase was to achieve geometry with a biomimetic structure, where the structure mimics the shapes seen in nature as described in Chapter 2.3.4.2. The software used for the optimisation phase was investigated as thoroughly as time would allow, and the best result was achieved for each of the methods. It is important to note that MSC and Siemens software with Nastran as a solver requires a vast amount of exposure and knowledge to generate topology from any given geometry. However, SolidThinking Inspire, with its easy-to-use interface, has all the necessary tools to generate the desired geometry with ease. Thus, for the first and second scenario, the desired output of a biomimetic structure was achieved. This illustrates that with the right amount of exposure to any given software package, the optimisation process for the design cycle can be implemented.

3. SolidThinking Inspire also catered for the surface clean-up phase of the design cycle with the PolyNURB wrap function that "wraps" the facet geometry. PolyNURBS was manipulated to a large degree. Thus, it would be possible to generate both prismatic and biomimetic components. Inspire was used as the tool to generate the components that

could be assessed for manufacturability. The functionality of Siemens NX geometry conversion tools was tested but not used to clean up the geometry. The methods used to generate b-splines are not as user friendly and is very time-consuming.

4. The process defined for the manufacturability phase of the design cycle verified that the Simufact Additive's prediction of build failure was correct. The results in Chapter 4 indicates that there were areas with high internal stress values during the build that caused the part to distort and pull away from the support material. These predictions gave insight on how to rectify the build setup to build the components successfully. After the components were manufactured successfully, the qualification and certification phase of the design cycle was set in motion.

5. The qualification and certification phase of the design cycle process entailed doing the theoretical development of the process required to qualify the manufacturing process and the certification of the component. FEA and structural analysis were done to ensure that the components did not fail under the ultimate loading conditions. The stress analysis was summarised in Table 5-5 and showed that none of the components would fail under the loading conditions, but this had to be verified by doing a static test. As mentioned in Section **5.6.2**, due to the budget constraint, only one component could be tested, as the CFRTP material and process to manufacture were too costly. This static test showed that the brackets survived a load of 970 kg, which was 3.2 times stronger than required. This verified the prediction of the FEM, namely that no failure occurred at the ultimate load.

As presented in the results, the weight reduction achieved for scenario one was 60%, scenario two, 70%, and for the third scenario, 40%. These results substantiate that the design cycle process was effective. Thus, the validation of the design cycle is complete, as it produced components that are certifiable by conforming to the OEM requirements and FAA regulations. However, this is possible after the right procedures and specifications have been implemented to manufacture consistent components, and the process has been proven by the said OEM.

Due to this study's magnitude and the cost of AM machines being upward of R10 million, there is still room for improvement to fully develop the manufacturing process as defined by the OEM. Theoretically, the process was defined and understood, but when implementing all the manufacturing requirements of the OEM, it will require a large amount of funding, to procure a machine and set up a facility to ensure that the process is fully defined, developed and documented in accordance with OEM specifications. The funding was limited for this study; thus, to practically test the process for the qualification of the manufacturing process due to the extensive testing to fulfil the requirements was not possible. However, all other processes were

successfully researched and investigated. Thus, the study was successfully concluded with recommendations to follow in the next section.

6.2 Recommendations

This section states the recommended future work to resolve problems and improve processes currently used in the design cycle. The primary recommendation is to split each phase into separate research topics to develop each phase to its full potential and to minimise the overall cost of the study, as this was one of the limitations during this study. Below are key topics recommended for further research:

1. At the time of this study, the most recent commercial finite element software packages were investigated, and their capability to conduct geometric optimisation studies. Topology optimisation phase future research should investigate the constantly evolving and improving principle, methods and software packages that are commercially available.
2. Manufacturability phase future research should investigate in more depth manufacturing simulations in Simufact Additive and conducted a comparison with other software packages. The AM equipment is South Africa lacks senor equipment that monitors the temperature of the surface during the build process. Hence, conducting a thermo-mechanical calibration in this study was not possible. Future research should conduct thermo-mechanical calibration and simulation investigations. In addition, explore and compare the capabilities of other software packages to predict the AM manufacturing process.
3. Facility qualification for the manufacture of aerospace components has yet to be achieved in South Africa. The constantly improving AM machinery is improving confidence in the reliability, and quality output from a metal AM build and thus warrants the economic investment required to qualify a facility. Future research, aligned with other on-going studies, should focus on the value-chain required in South Africa that will support the AM aerospace industry in pursuit of qualified AM facilities nationwide.
4. Future research should investigate the development of A-basis, B-basis and S-basis design allowable from a dedicated AM machine. This recommendation aligns with the facility qualification requirement.
5. Another recommendation is to test the design cycle on other industries with more relaxed requirements, such as the automotive and medical industry

BIBLIOGRAPHY

[1] **ASTM International**, 2013, “F2792-12a - Standard Terminology for Additive Manufacturing Technologies,” *Rapid Manuf. Assoc.*, pp. 10–12.

[2] **B. G. Ben Redwood, Filemon Schoffer**, 2017, *The 3D Printing Handbook*. 2017.

[3] **H. Zhang, J. K. Nagel, A. Al-Qas, E. Gibbons, and J. J. Y. Lee**, 2018, “Additive Manufacturing with Bioinspired Sustainable Product Design: A Conceptual Model,” *Procedia Manuf.*, vol. 26, pp. 880–891.

[4] **W. Gao *et al.***, 2015, “The status, challenges, and future of additive manufacturing in engineering,” *CAD Comput. Aided Des.*, vol. 69, pp. 65–89.

[5] **K. P. Karunakaran, A. Bernard, S. Suryakumar, L. Dembinski, and G. Taillandier**, 2012, “Rapid manufacturing of metallic objects,” *Rapid Prototyp. J.*, vol. 18, no. 4, pp. 264–280.

[6] **Y. Yang *et al.***, 2018, “Recent Progress in Biomimetic Additive Manufacturing Technology: From Materials to Functional Structures,” *Adv. Mater.*, vol. 30, no. 36, pp. 1–34.

[7] **A. du Plessis *et al.***, 2019, “Beautiful and Functional: A Review of Biomimetic Design in Additive Manufacturing,” *Addit. Manuf.*, vol. 27, no. March, pp. 408–427.

[8] **D. F. O. Braga, S. M. O. Tavares, L. F. M. Da Silva, P. M. G. P. Moreira, and P. M. S. T. De Castro**, 2014, “Advanced design for lightweight structures: Review and prospects,” *Prog. Aerosp. Sci.*, vol. 69, pp. 29–39.

[9] **I. Gibson, D. Rosen, and B. Stucker**, 2015, *Directed Energy Deposition Processes. In: Additive Manufacturing Technologies*. 2015.

[10] **S. R. and A. T. Joel C. Najmon and J. GAVIN**, 2019, “Review of additive manufacturing technologies and applications in the aerospace industry,” *Addit. Manuf. Aerosp. Ind.*, pp. 7–31.

[11] **R. Russell *et al.***, 2019, “Qualification and certification of metal additive manufactured hardware for aerospace applications,” in *Additive Manufacturing for the Aerospace Industry*, F. Froes and R. B. T.-A. M. for the A. I. Boyer, Eds. Elsevier, 2019, pp. 33–66.

[12] **H. Krueger**, 2017, “Standardization for Additive Manufacturing in Aerospace,” *Engineering*, vol. 3, no. 5, p. 585.

[13] **M. Seifi *et al.***, 2017, “Progress Towards Metal Additive Manufacturing Standardization to Support Qualification and Certification,” *Jom*, vol. 69, no. 3, pp. 439–455.

[14] **F. Froes, R. Boyer, and B. Dutta**, 2019, “Introduction to aerospace materials requirements and the role of additive manufacturing,” *Addit. Manuf. Aerosp. Ind.*, pp. 1–6.

[15] **S. Liu and Y. C. Shin**, 2019, “Additive manufacturing of Ti6Al4V alloy : A review,” *Mater. Des.*, vol. 164, p. 107552.

[16] **J. C. Withers**, 2019, “Fusion and/or solid state additive manufacturing for aerospace applications,” *Addit. Manuf. Aerosp. Ind.*, pp. 187–211.

[17] **H. Gong, K. Rafi, H. Gu, T. Starr, and B. Stucker**, 2014, “Analysis of defect generation in Ti-6Al-4V parts made using powder bed fusion additive manufacturing processes,” *Addit. Manuf.*, vol. 1, pp. 87–98.

[18] **G. Piscopo, A. Salmi, and E. Atzeni**, 2019, “On the quality of unsupported overhangs produced by laser powder bed fusion,” *Int. J. Manuf. Res.*, vol. 14, no. 2, pp. 198–216.

[19] **S. Igor**, 2019, “Aerospace applications of the SLM process of functional and functional graded metal matrix composites based on NiCr superalloys,” *Addit. Manuf. Aerosp. Ind.*, vol. 265–281.

[20] **W. Chen and Z. Li**, 2019, “Additive manufacturing of titanium aluminides,” *Addit. Manuf. Aerosp. Ind.*, pp. 235–263.

[21] **R. R. Boyer**, 1996, “An overview on the use of titanium in the aerospace industry,” *Mater. Sci. Eng. A*, vol. 213, no. 1–2, pp. 103–114.

[22] **D. F. Louw and P. G. H. Pistorius**, 2019, “The effect of scan speed and hatch distance on prior-beta grain size in laser powder bed fused Ti-6Al-4V,” *Int. J. Adv. Manuf. Technol.*, pp. 2277–2286.

[23] **N. C. Levkulich, S. L. Semiatin, J. E. Gockel, J. R. Middendorf, A. T. DeWald, and N. W. Klingbeil**, 2019, “The effect of process parameters on residual stress evolution and distortion in the laser powder bed fusion of Ti-6Al-4V,” *Addit. Manuf.*, vol. 28, no. May, pp. 475–484.

[24] **ASTM INTERNATIONAL**, 2013, “ASTM F2792-12a,” *Rapid Manuf. Assoc.*, pp. 1–3.

[25] **Q. Wang *et al.***, 2014, *Investigation of condensation reaction during phenol liquefaction of waste woody materials*, vol. 9, no. 5. 2014.

[26] **A. Salmi, F. Calignano, M. Galati, and E. Atzeni**, 2018, “An integrated design methodology for components produced by laser powder bed fusion (L-PBF) process,” *Virtual Phys. Prototyp.*, vol. 13, no. 3, pp. 191–202.

[27] **T. Kellner**, 2014, “This Electron Gun Builds Jet Engines, GE Aviation,” *General Electric*,

2014. .

[28] **F. Nabhani**, 2001, “Machining of aerospace titanium alloys,” *Robot. Comput. Integr. Manuf.*, vol. 17, no. 1–2, pp. 99–106.

[29] **M. Kamal and G. Rizza**, 2019, “Design for metal additive manufacturing for aerospace applications,” *Addit. Manuf. Aerosp. Ind.*, pp. 67–86.

[30] **J. Liu**, 2016, “Guidelines for AM part consolidation,” *Virtual Phys. Prototyp.*, vol. 11, no. 2, pp. 133–141.

[31] **S. Yang, Y. Tang, and Y. F. Zhao**, 2015, “A new part consolidation method to embrace the design freedom of additive manufacturing,” *J. Manuf. Process.*, vol. 20, pp. 444–449.

[32] **A. W. Gebisa and H. G. Lemu**, 2017, “A case study on topology optimized design for additive manufacturing,” *IOP Conf. Ser. Mater. Sci. Eng.*, vol. 276, no. 1.

[33] **K. T. Zuo, L. P. Chen, Y. Q. Zhang, and J. Yang**, 2006, “Manufacturing- and machining-based topology optimization,” *Int. J. Adv. Manuf. Technol.*, vol. 27, no. 5–6, pp. 531–536.

[34] **J. París, S. Martínez, F. Navarrina, I. Colominas, and M. Casteleiro**, 2014, “Topology optimization of structures with stress constraints: Aeronautical applications,” *IOP Conf. Ser. Mater. Sci. Eng.*, vol. 10, no. 1.

[35] **Y. Chen, J. Lu, and Y. Wei**, 2016, “Topology optimization for manufacturability based on the visibility map,” *Comput. Aided. Des. Appl.*, vol. 13, no. 1, pp. 86–94.

[36] **J. Liu and A. C. To**, 2017, “Topology optimization for hybrid additive-subtractive manufacturing,” *Struct. Multidiscip. Optim.*, vol. 55, no. 4, pp. 1281–1299.

[37] **Q. Li, W. Chen, S. Liu, and L. Tong**, 2016, “Structural topology optimization considering connectivity constraint,” *Struct. Multidiscip. Optim.*, vol. 54, no. 4, pp. 971–984.

[38] **K.-H. Chang and P.-S. Tang**, 2001, “Integration of design and manufacturing for structural shape optimization,” *Adv. Eng. Softw.*, vol. 32, no. 7, pp. 555–567.

[39] **F. Calignano**, 2014, “Design optimization of supports for overhanging structures in aluminum and titanium alloys by selective laser melting,” *Mater. Des.*, vol. 64, pp. 203–213.

[40] **Y. Tang, G. Dong, Q. Zhou, and Y. F. Zhao**, 2017, “Lattice Structure Design and Optimization With Additive Manufacturing Constraints,” *IEEE Trans. Autom. Sci. Eng.*, pp. 1–17.

[41] **A. Hussein, L. Hao, C. Yan, R. Everson, and P. Young**, 2013, “Advanced lattice support structures for metal additive manufacturing,” *J. Mater. Process. Technol.*, vol. 213, no. 7,

pp. 1019–1026.

[42] **K. Prof**, 2013, “Structural Optimization and Laser Additive Manufacturing (LAM) in lightweight design : barriers and chances,” no. April.

[43] “Altair Inspire™ 2019.” .

[44] **SolidThinking**, “PolyNURB Tutorial.”

[45] **Q. Chen *et al.***, 2019, “An inherent strain based multiscale modeling framework for simulating part-scale residual deformation for direct metal laser sintering,” *Addit. Manuf.*, vol. 28, no. December 2018, pp. 406–418.

[46] **M. Bugatti and Q. Semeraro**, 2018, “Limitations of the inherent strain method in simulating powder bed fusion processes,” *Addit. Manuf.*, vol. 23, no. June 2017, pp. 329–346.

[47] **L. Portolés, O. Jordá, L. Jordá, A. Uriondo, M. Esperon-Miguez, and S. Perinpanayagam**, 2016, “A qualification procedure to manufacture and repair aerospace parts with electron beam melting,” *J. Manuf. Syst.*, vol. 41, pp. 65–75.

[48] **S. Contents**, 2011, “e-CFR Data is current as of May 26 , 2011 Title 14 : Aeronautics and Space Browse Previous | Browse Next,” *Policy*, vol. 14, pp. 1–305.

[49] “Summary of NDE of Additive Manufacturing Efforts in NASA,” no. March 2015.

[50] **A. Manufacturing**, 2015, “16 INTERNATIONAL CONFERENCE Bronze,” no. November.

ANNEXURES

7.1 Appendix A: Image of AM technologies

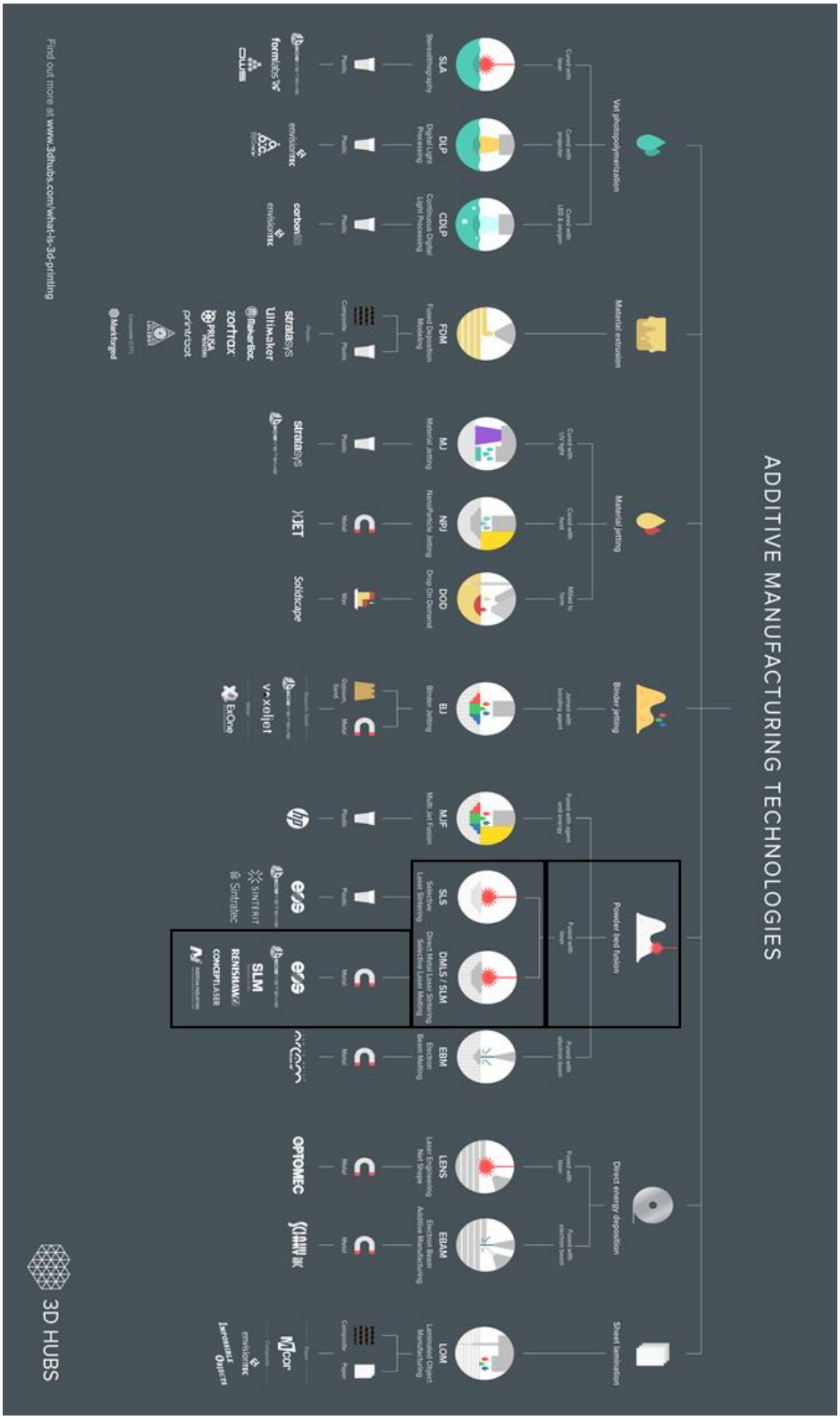

7.2 Appendix B: Altair SolidThinking Inspire Topology Optimisation Results

7.2.1 Re-evaluated Design Topology optimisation iterations

Volumetric_Bottom_bracket_Ispire_rev2 Max Stiffness Mass 20% (37)

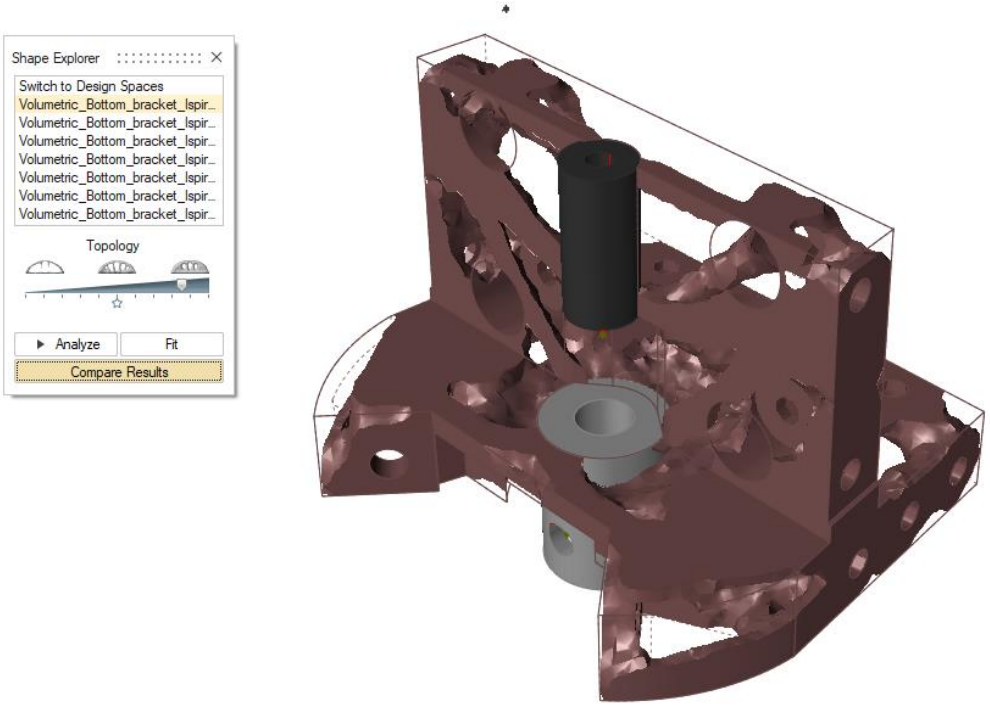

Volumetric_Bottom_bracket_Ispire_rev2 Max Stiffness Mass 20% (39)

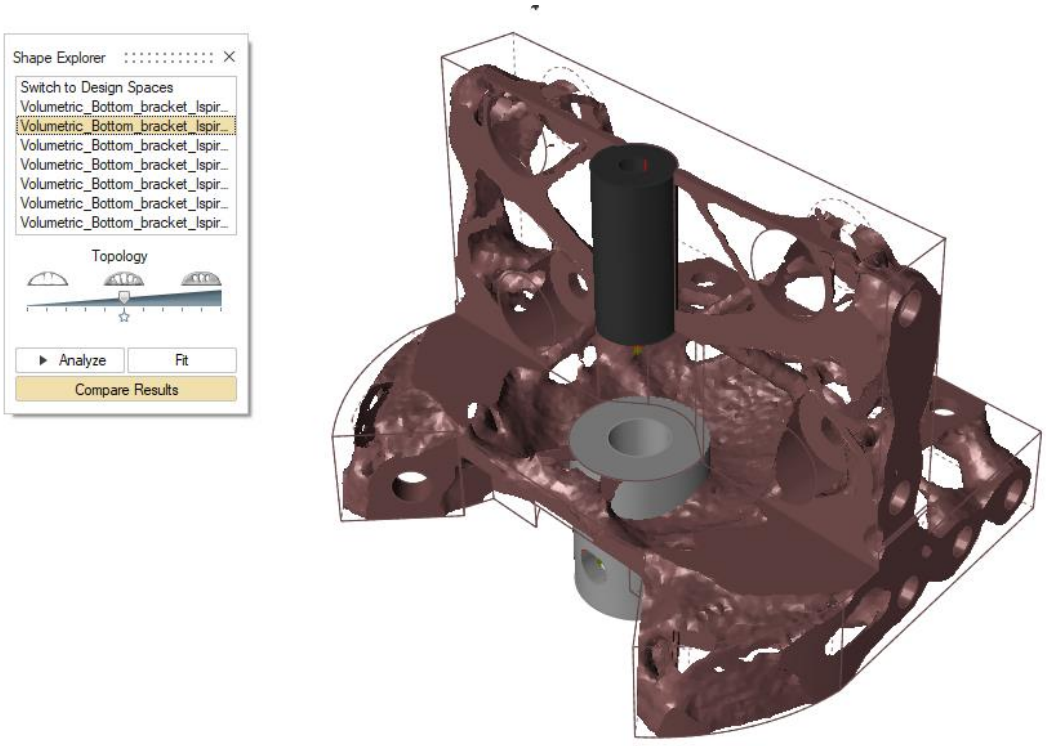

Volumetric_Bottom_bracket_Ispire_rev2 Max Stiffness Mass by Part (BODY.32 14%) (9)

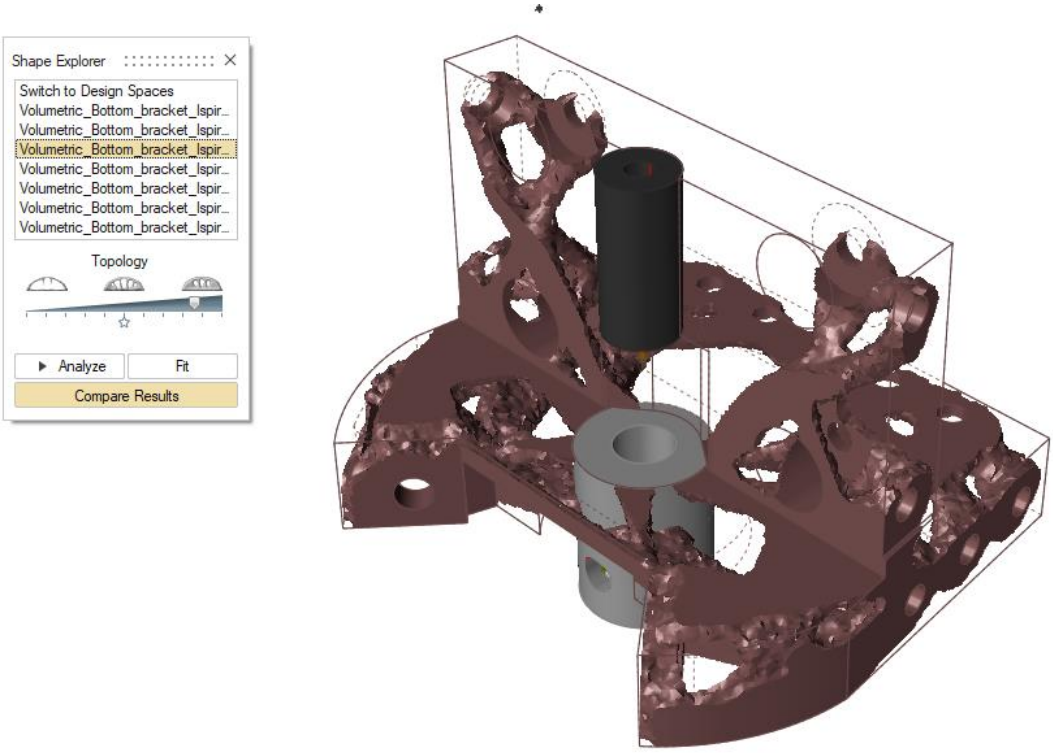

Volumetric_Bottom_bracket_Ispire_rev2 Max Stiffness Mass by Part (BODY.32 25%) (28)

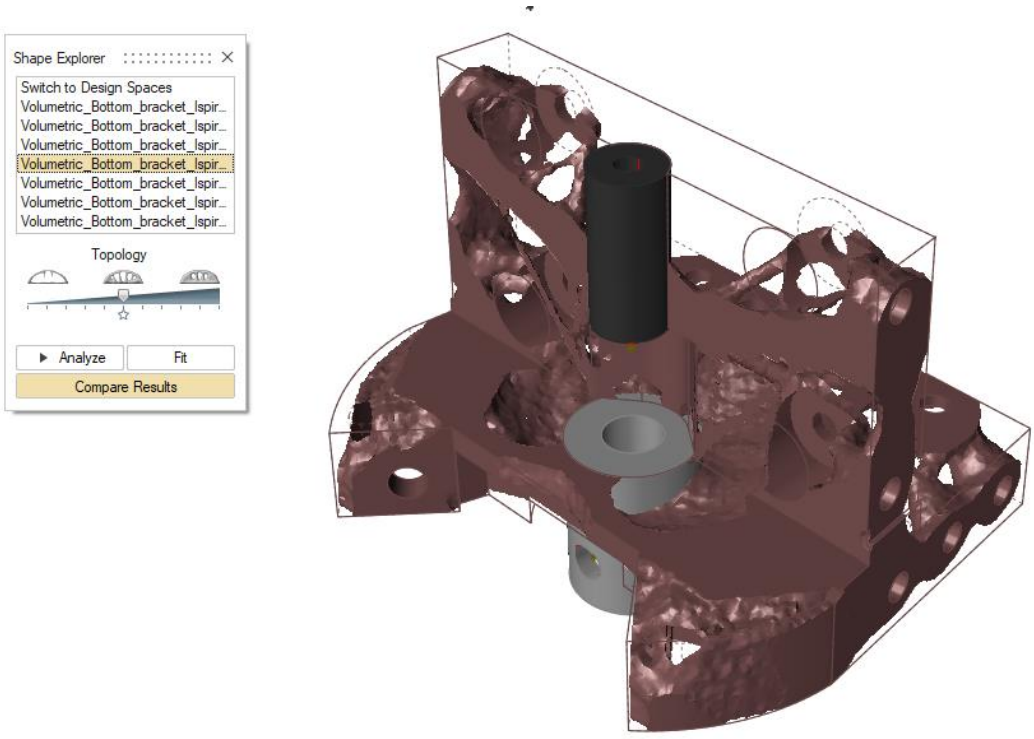

Volumetric_Bottom_bracket_Ispire_rev2 Max Stiffness Mass by Part (BODY.32 25%) (35)

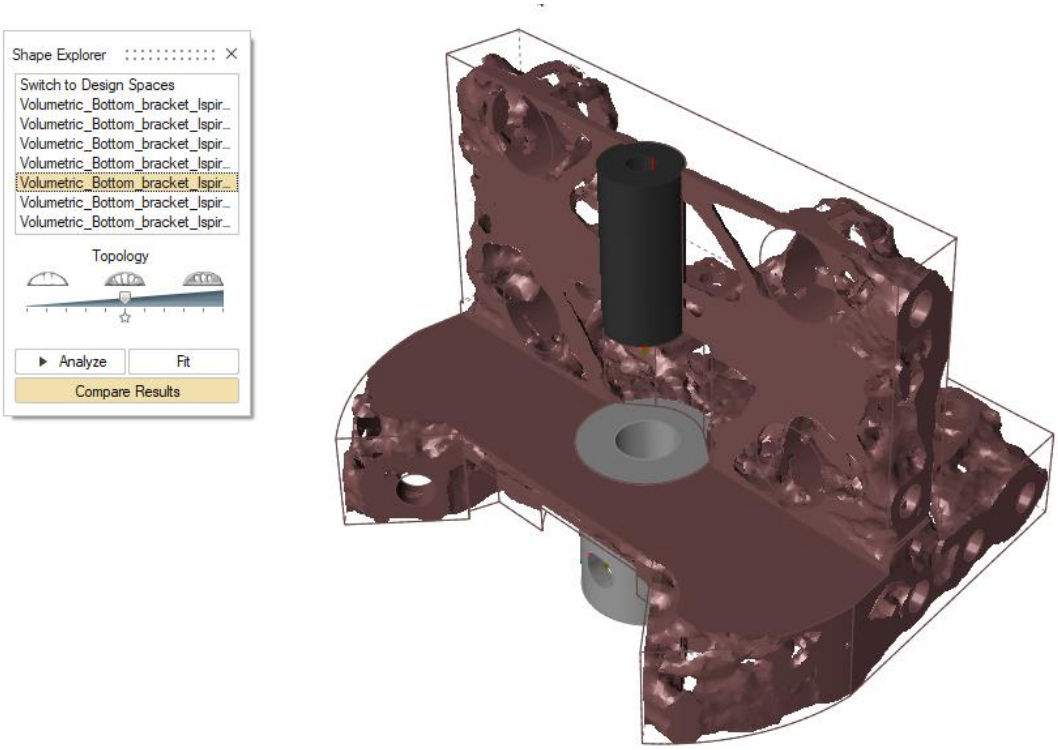

Volumetric_Bottom_bracket_Ispire_rev2 Max Stiffness Mass by Part (BODY.32 31%) (29)

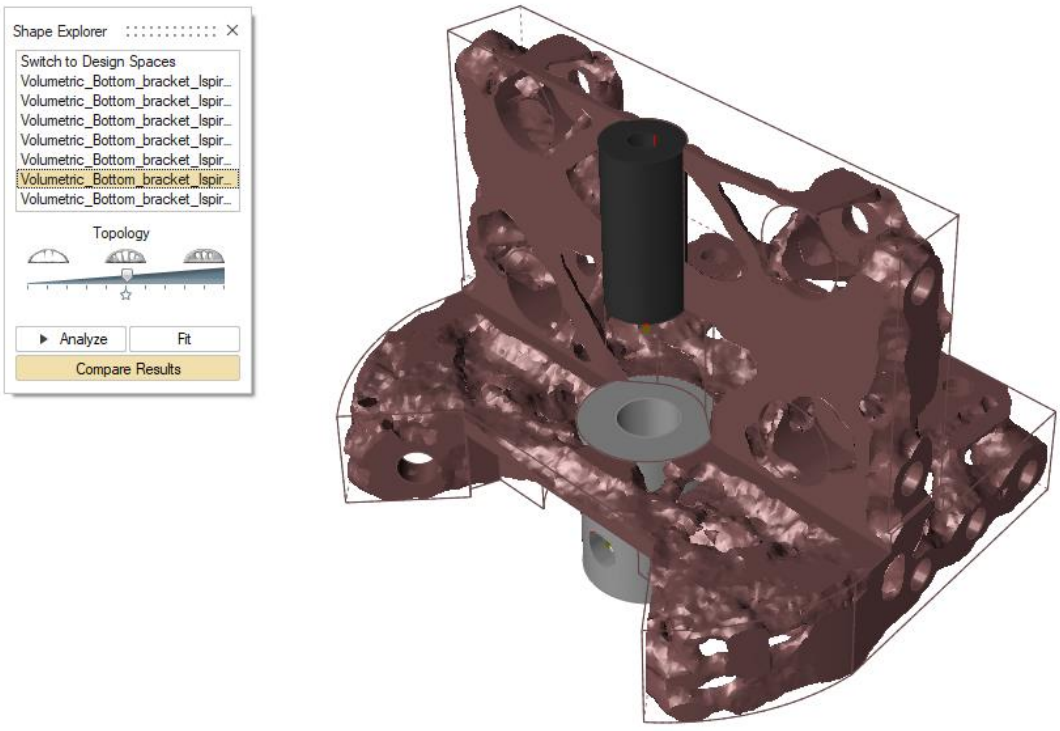

Volumetric_Bottom_bracket_Ispire_rev2 Max Stiffness Mass by Part (BODY.32 31%) (30)

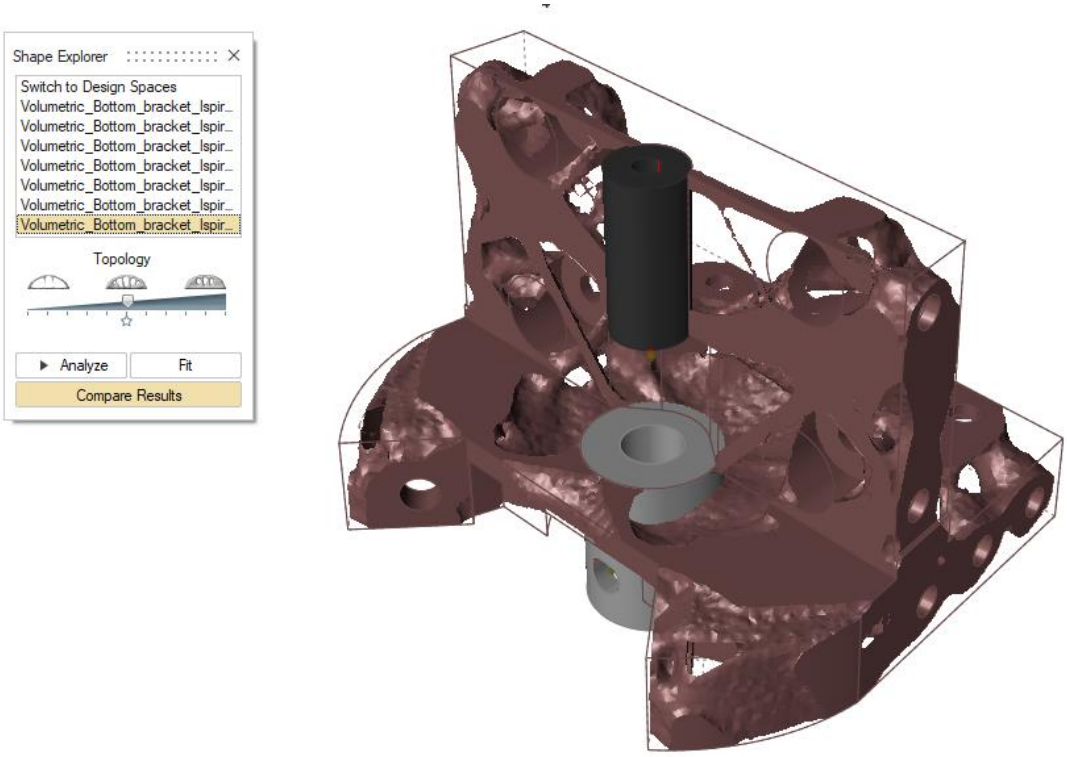

7.2.2 Initial Design Topology Optimisation iterations

Parametric_Bottom_Bracket Max Stiffness Mass 20% (6)

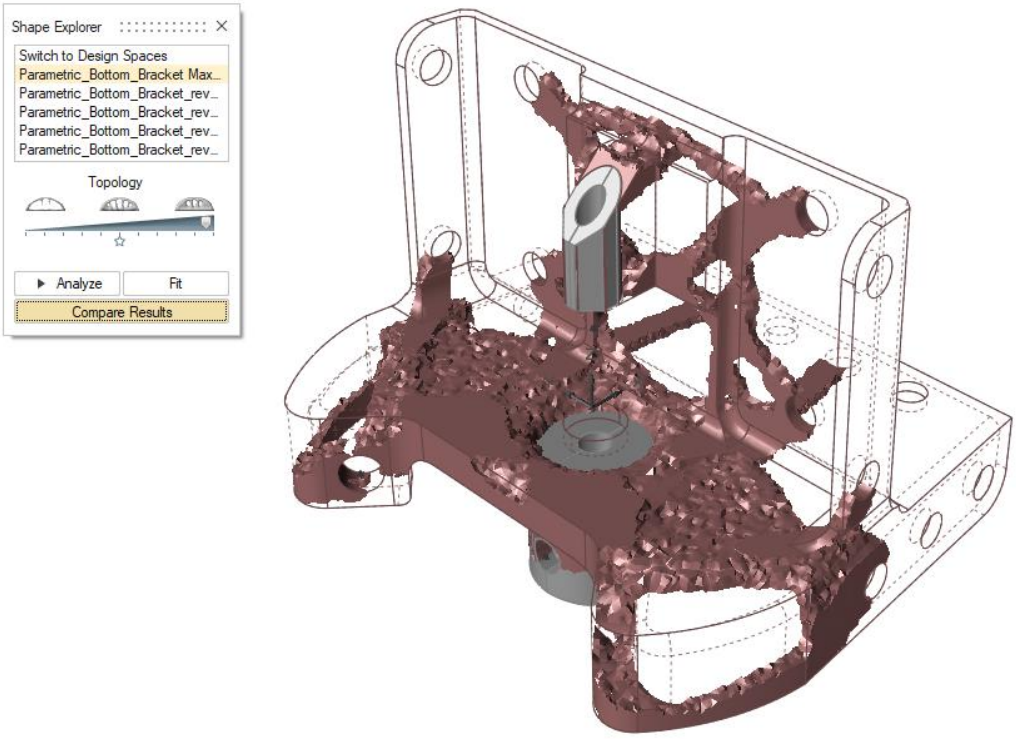

Parametric_Bottom_Bracket_rev3 Max Stiffness Mass 15% (7)

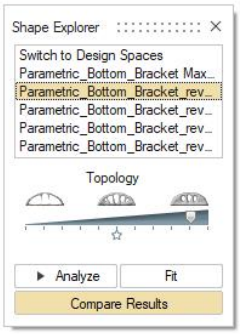

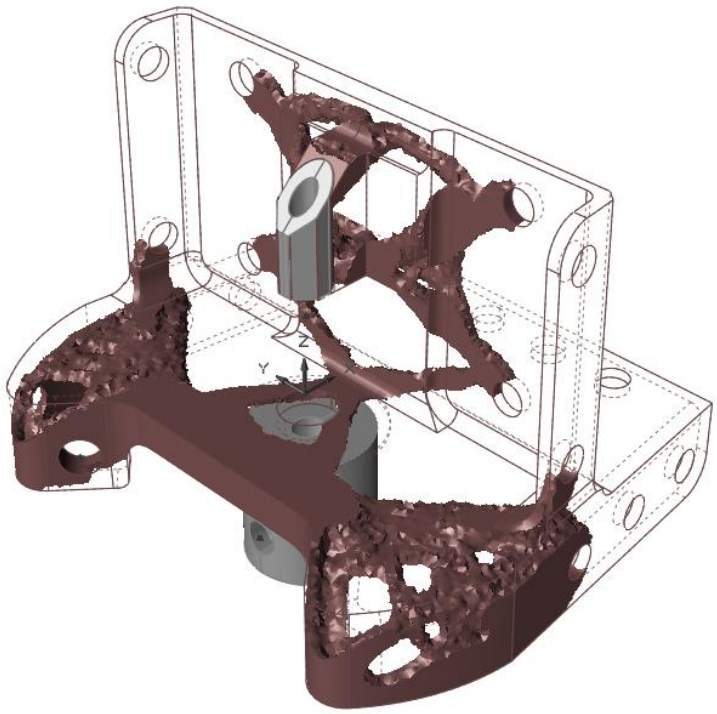

Parametric_Bottom_Bracket_rev3 Max Stiffness Mass 15% (8)

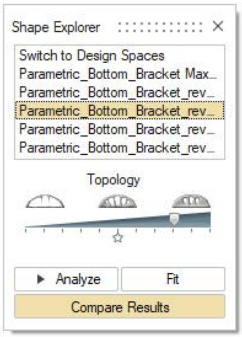

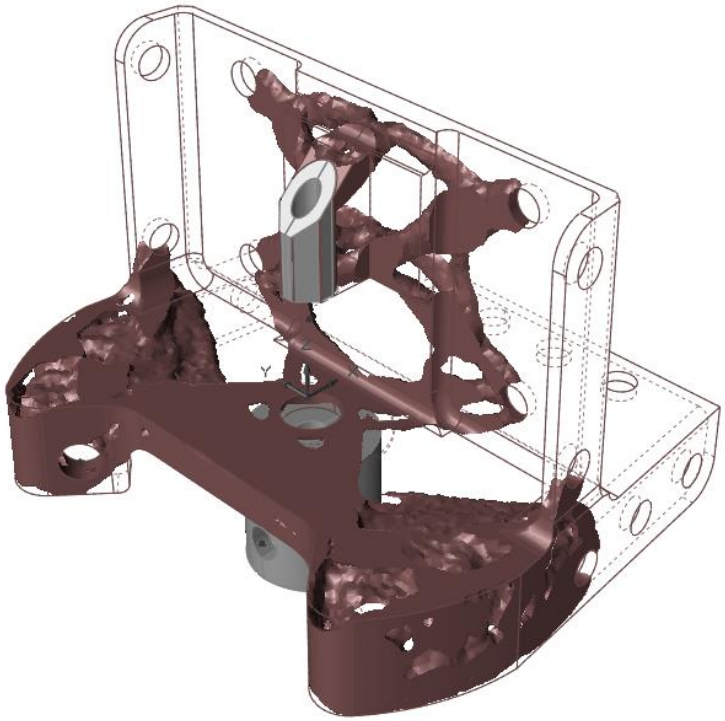

Parametric_Bottom_Bracket_rev3 Max Stiffness Mass 15% (9)

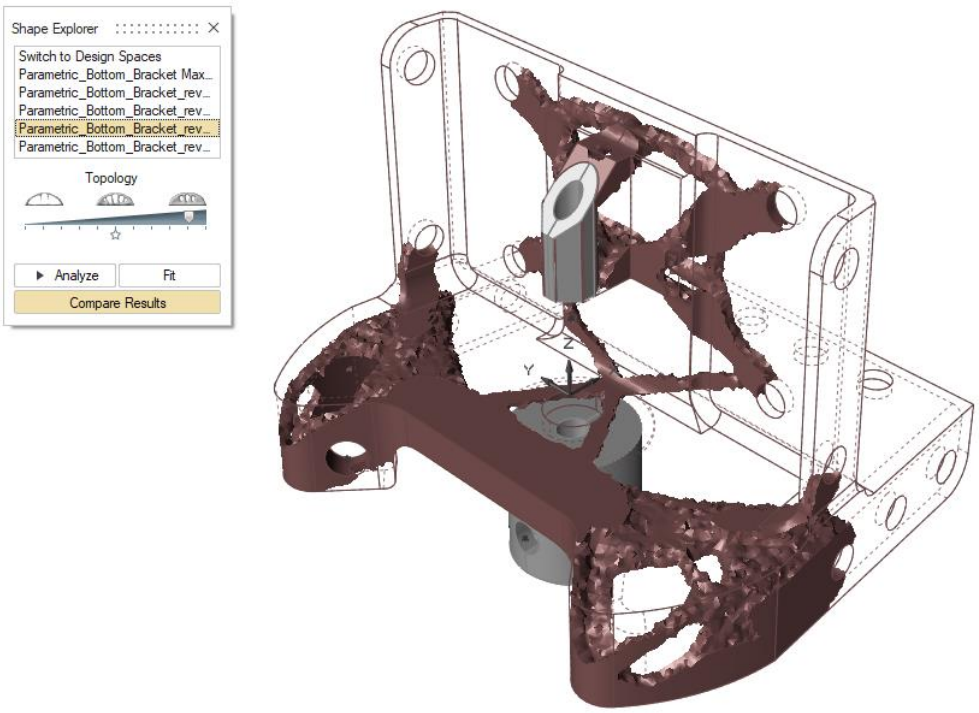

7.3 Appendix C: Manufacturability

7.3.1 Engineering Test Plan for the Manufacturability Calibrations Samples

In this Engineering Test Plan (ETP), the procedure to prepare and conduct a calibration for a specific material and machine is detailed to do accurate Simufact simulations. Simufact simulates the build process from the build itself through to support removal and finally removing the component from the build plate. The following list denoted items that profoundly influence the calibration results. Changes in the following will require calibration to be conducted again.

- Change in build strategy
- A change in powder condition in terms of virgin or blend ratio of virgin and used
- Change in material type
- Change in the state of the Machine, either a different machine or after servicing/maintenance

The Calibration is done to determine the inherent strain values. The inherent strains are produced in the building process by thermal strains, plastic strains ad phase transformation. These strains values can either be calibrated from experiments or estimated based on process parameters.

Simufact creates a calibration profile so, for the same build strategy and Build Parameters, the data can be used. If any parameters change, the calibration process will need to be rerun as the data will be inaccurate. The results presented in Chapter 5, Section 5.5.1 are from the following report:

https://figshare.com/s/a7f496a5b90de2bbf79c

7.3.2 Engineering Test Report for the Manufacturability Calibrations Samples

This document presents the results attained from the Simufact calibration testing as detailed in the ETP found in Section 7.3.1, the objective of this test was to attain the displacement values of the distortion in the Z – Direction. These values are used in Simufact to calculate the average inherent strain for the samples distributed across the build plate. The results presented in Chapter 5, Section 5.5.1 are from the following report:

https://figshare.com/s/ee116e1c1bb485943f55

7.3.3 Initial Component Assessment Results

Part Simulation of the Biomimetic Volumetric Bracket

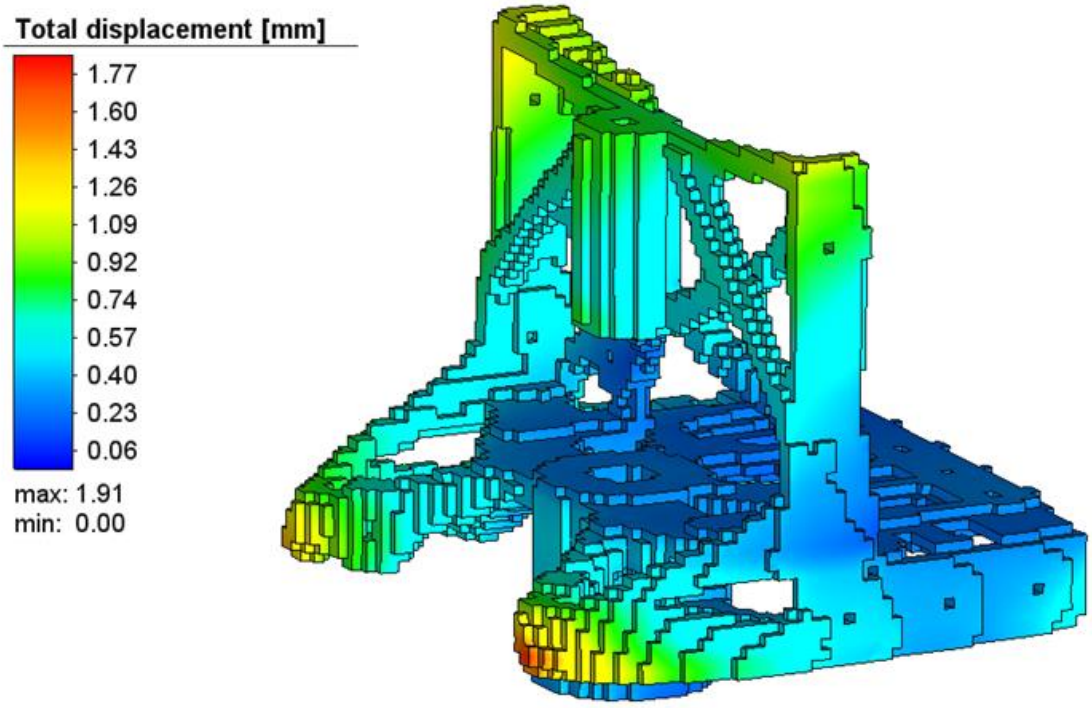

Possible areas of failure for the Biomimetic Volumetric Bracket

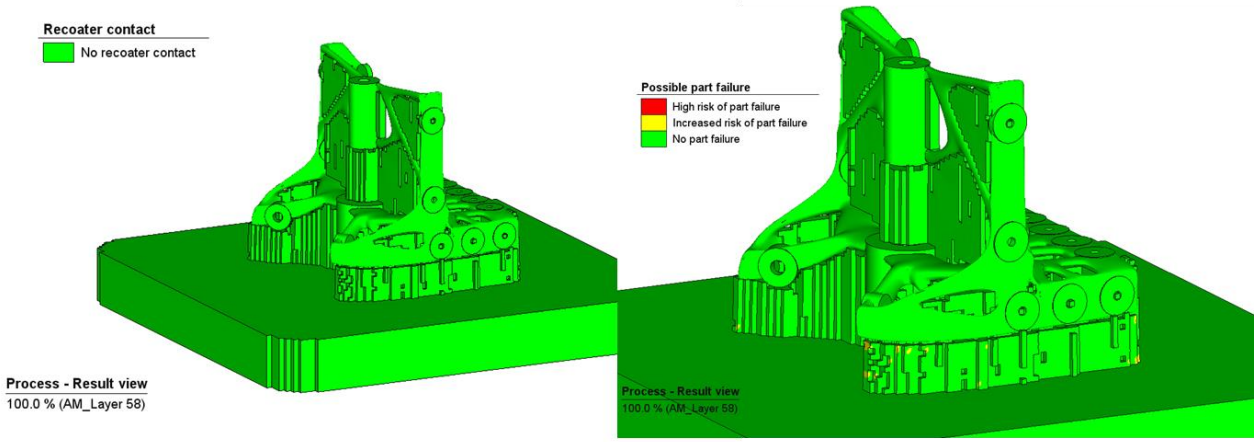

Part Simulation of the Biomimetic Current Bracket

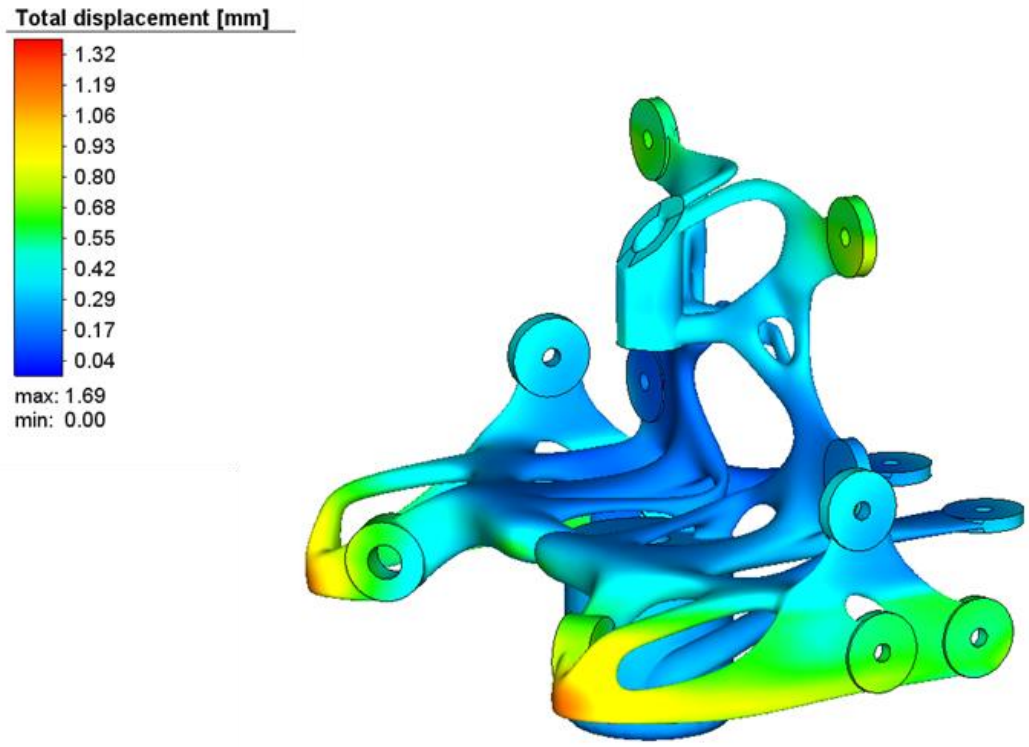

Possible areas of failure for the Biomimetic Current Bracket

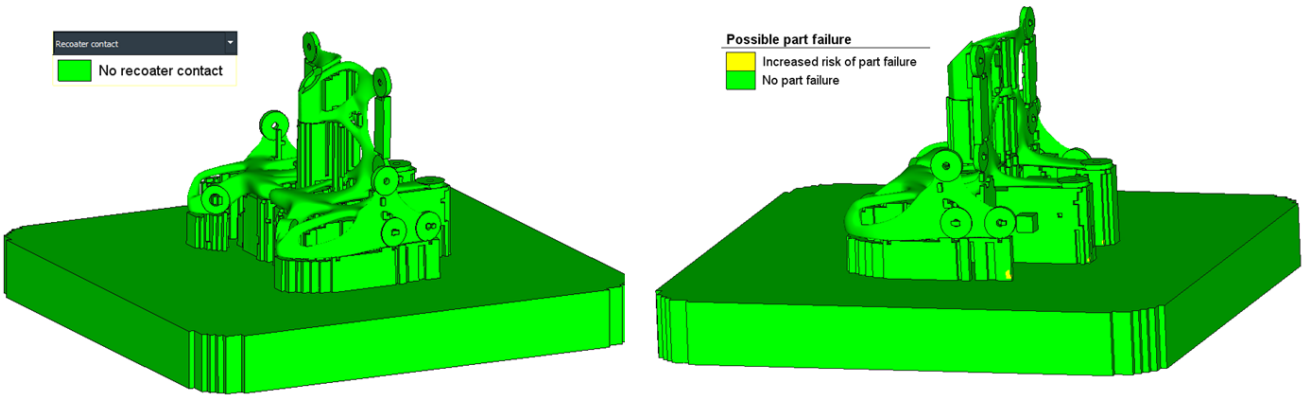

Part Simulation of the Prismatic Bracket

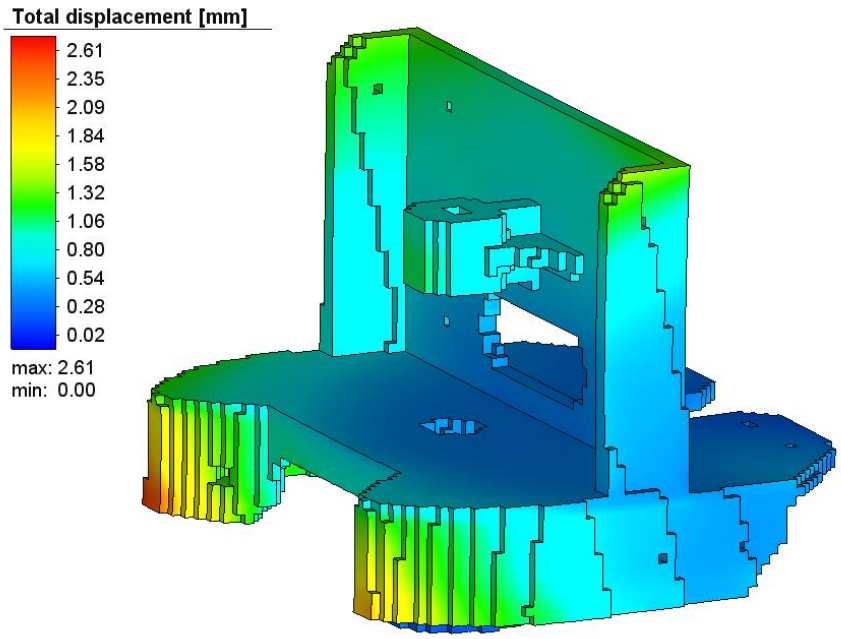

Possible areas of failure for the Prismatic Bracket

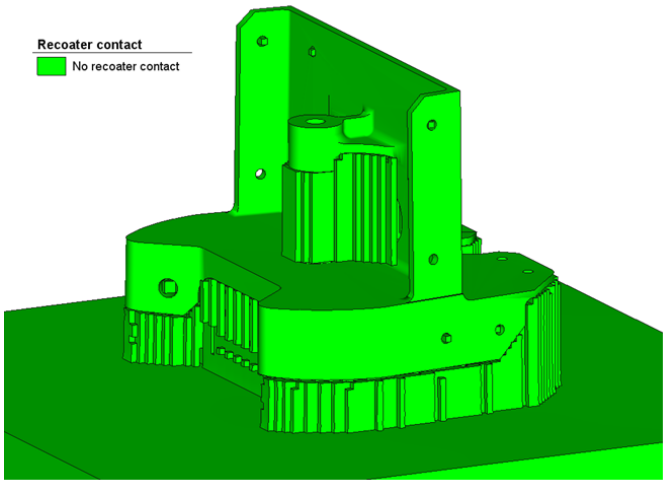

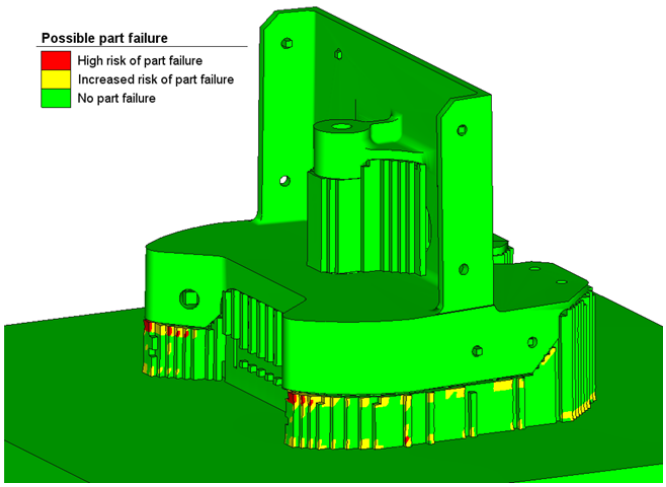

7.3.4 3D scanner report of the Volumetric Biomimetic component

AEROSUD
Aviation

20191029-03

Report Author: D. Coughlan
Date: 2019/10/30

Organization:	Aerosud
Part name:	Biomimetic_volumetric
Part #:	X0100000E001-001

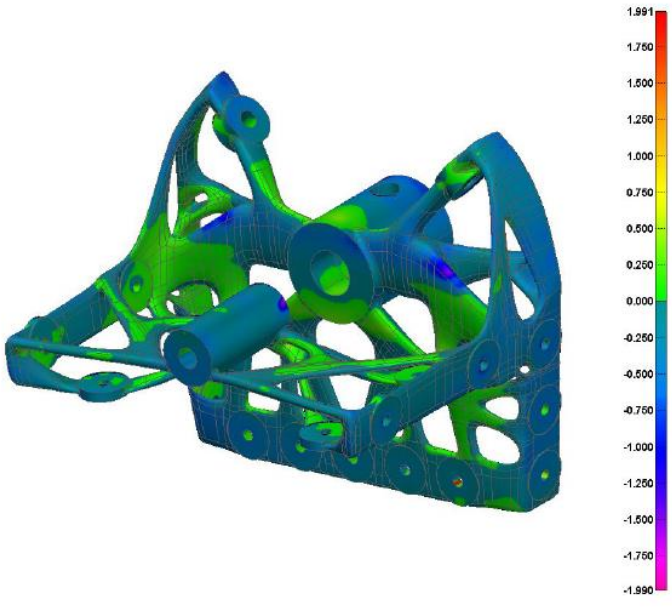

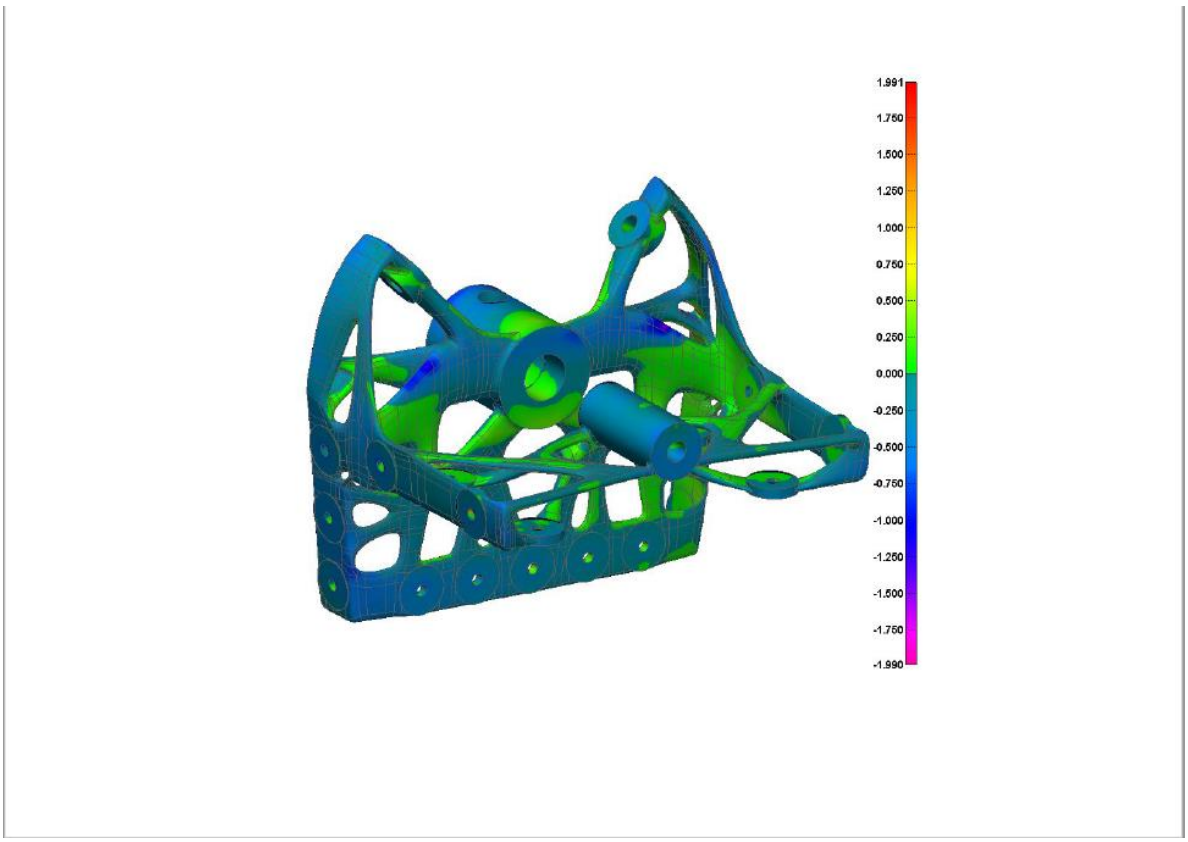
1.991
1.750
1.500
1.250
1.000
0.750
0.500
0.250
0.000
-0.250
-0.500
-0.750
-1.000
-1.250
-1.500
-1.750
-1.990

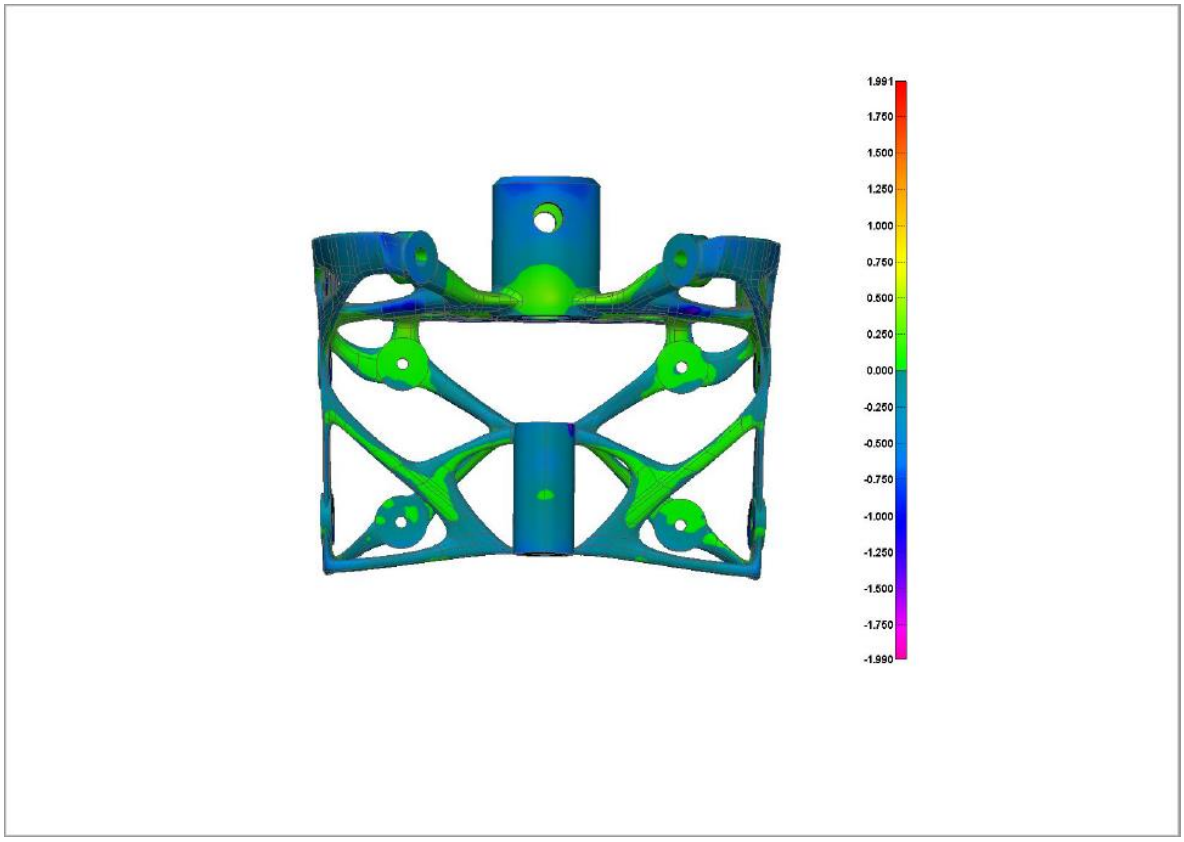
1.991
1.750
1.500
1.250
1.000
0.750
0.500
0.250
0.000
-0.250
-0.500
-0.750
-1.000
-1.250
-1.500
-1.750
-1.990

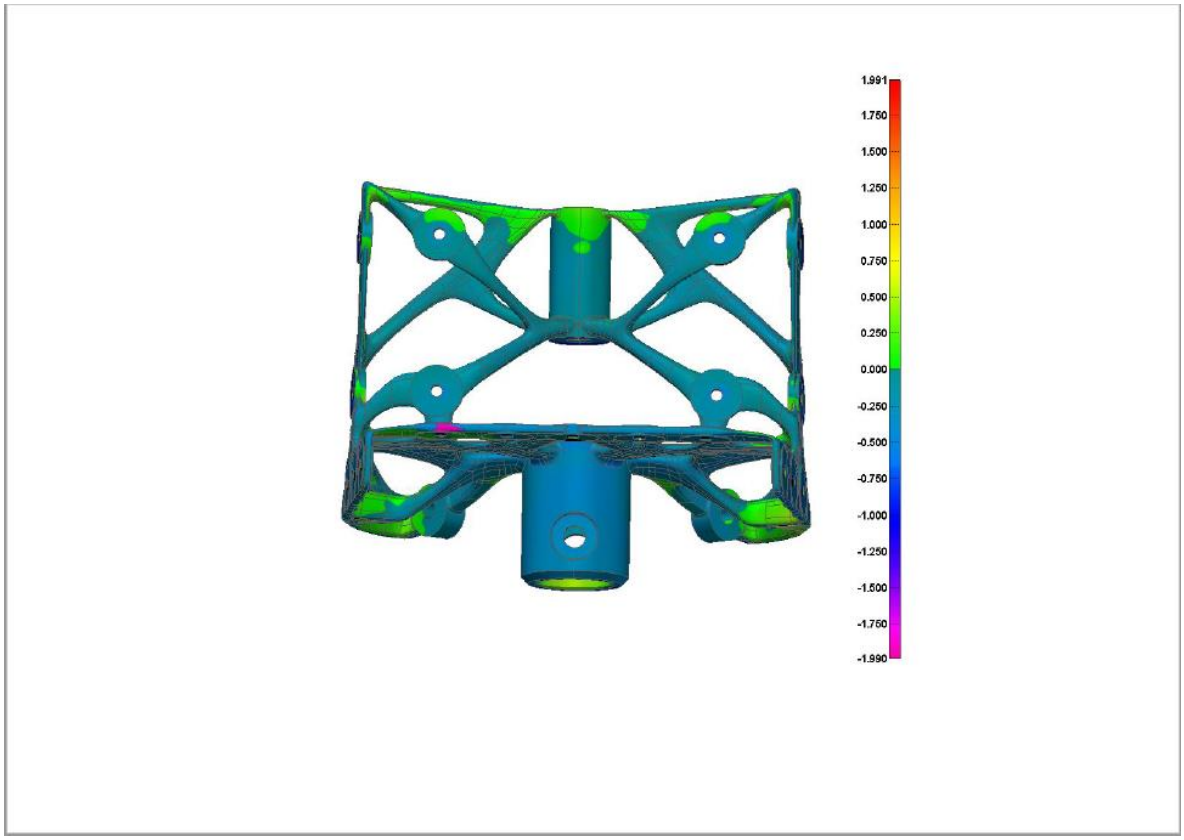
1.991
1.750
1.500
1.250
1.000
0.750
0.500
0.250
0.000
-0.250
-0.500
-0.750
-1.000
-1.250
-1.500
-1.750
-1.990

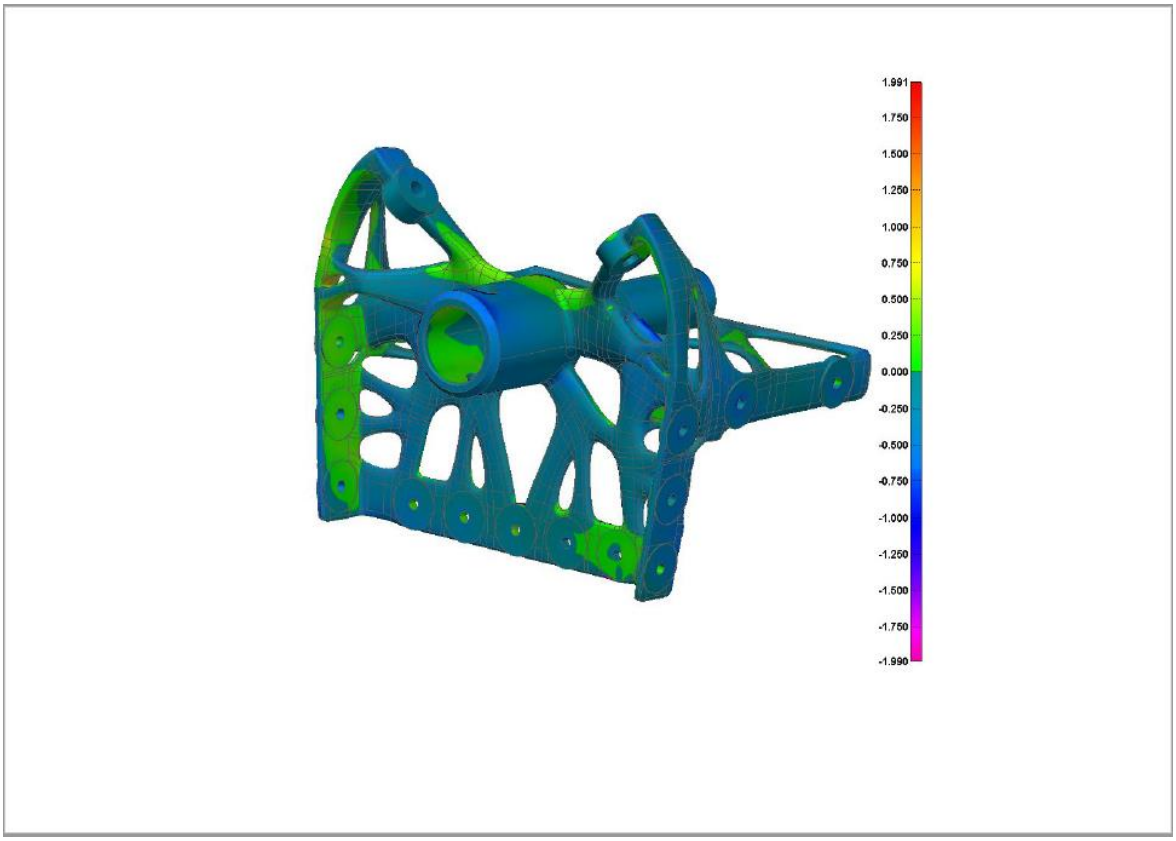
1.991
1.750
1.500
1.250
1.000
0.750
0.500
0.250
0.000
-0.250
-0.500
-0.750
-1.000
-1.250
-1.500
-1.750
-1.990

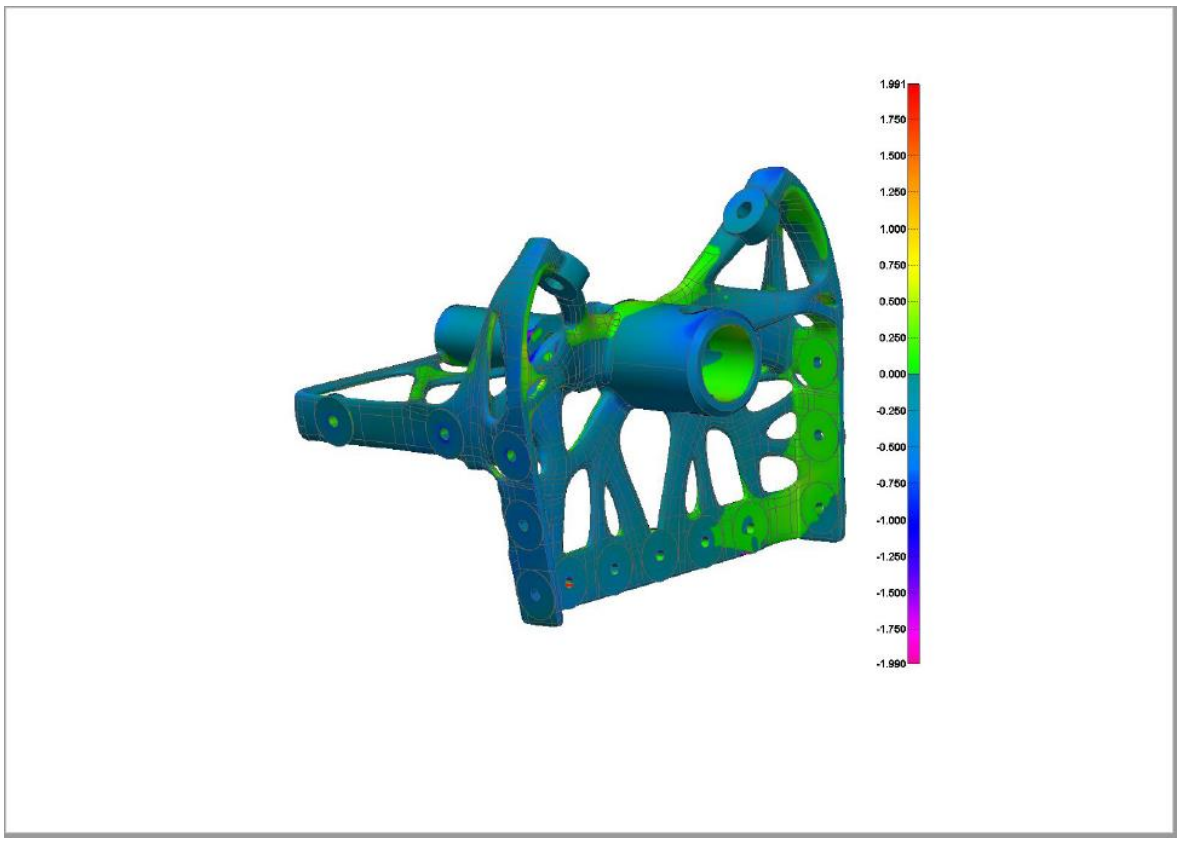
1.991
1.750
1.500
1.250
1.000
0.750
0.500
0.250
0.000
-0.250
-0.500
-0.750
-1.000
-1.250
-1.500
-1.750
-1.990

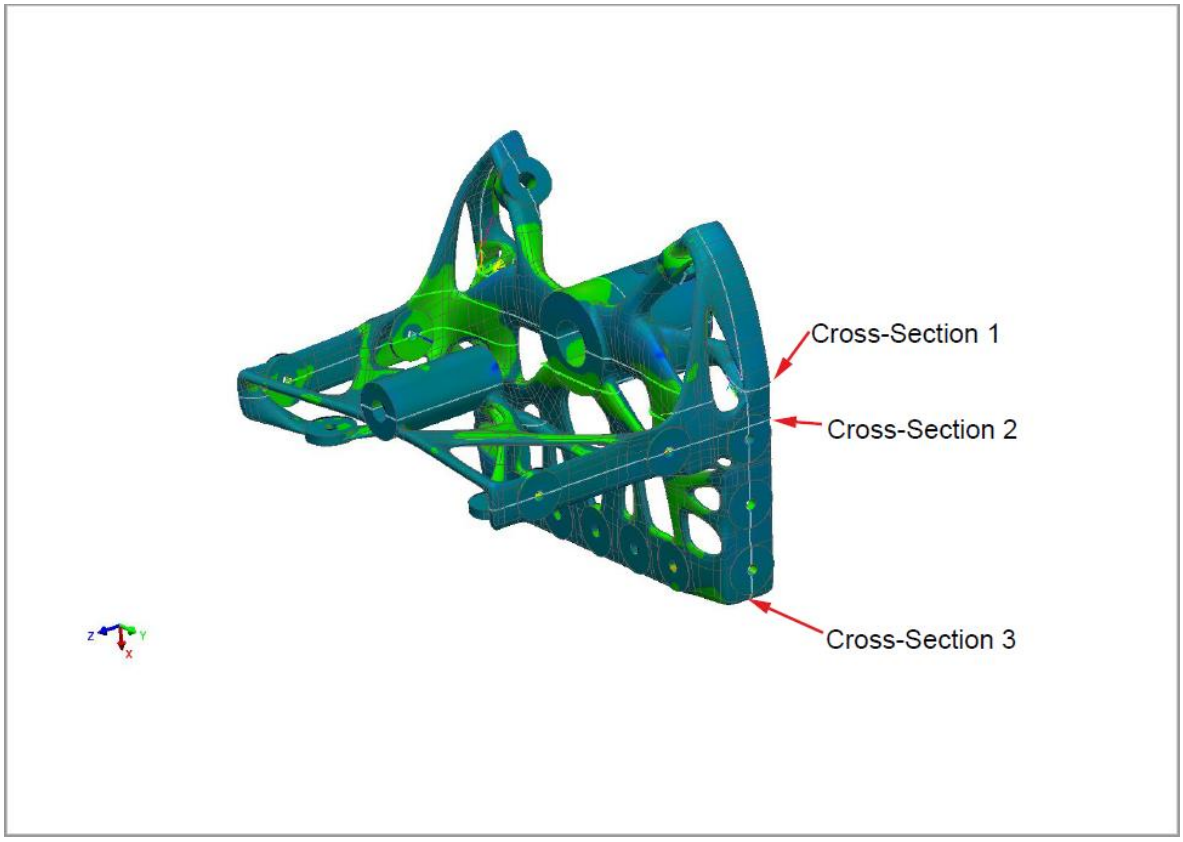
Cross-Section 1
Cross-Section 2
Cross-Section 3

Cross-Section 1

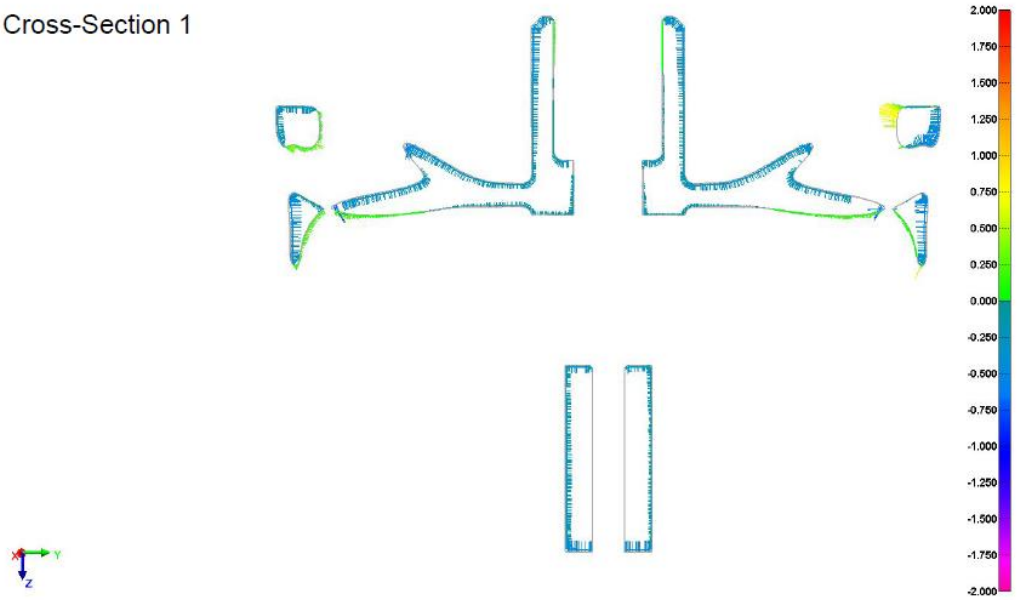

Cross-Section 2

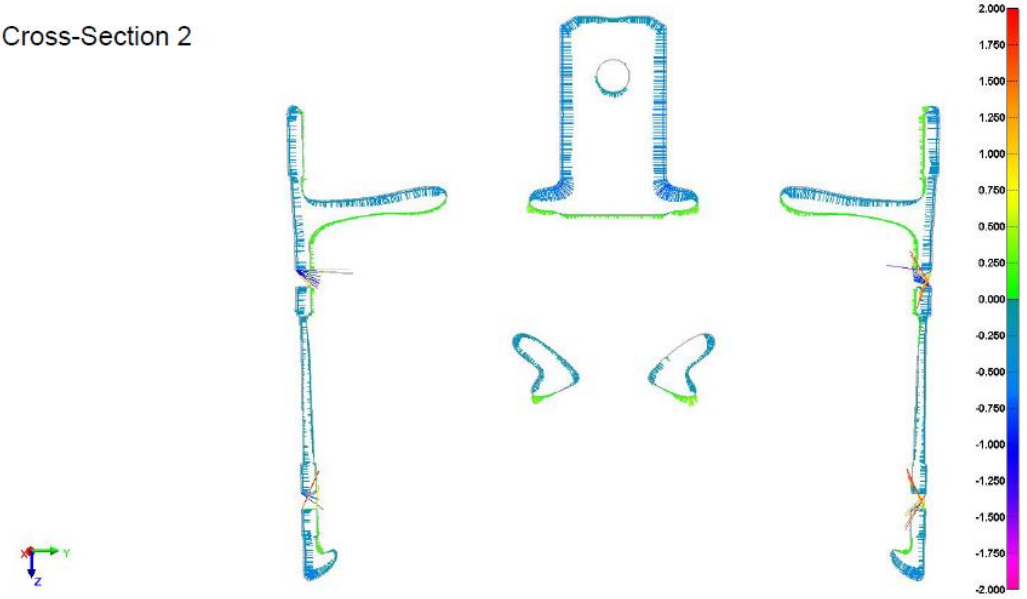

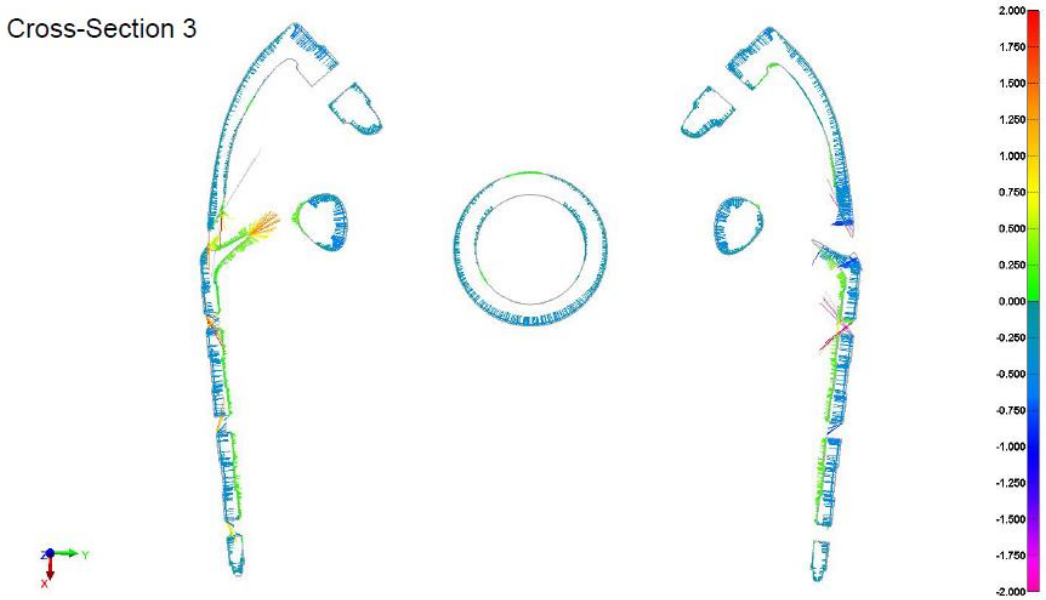
Cross-Section 3
2.000
1.750
1.500
1.250
1.000
0.750
0.500
0.250
0.000
-0.250
-0.500
-0.750
-1.000
-1.250
-1.500
-1.750
-2.000

7.3.5 Results from the Second build

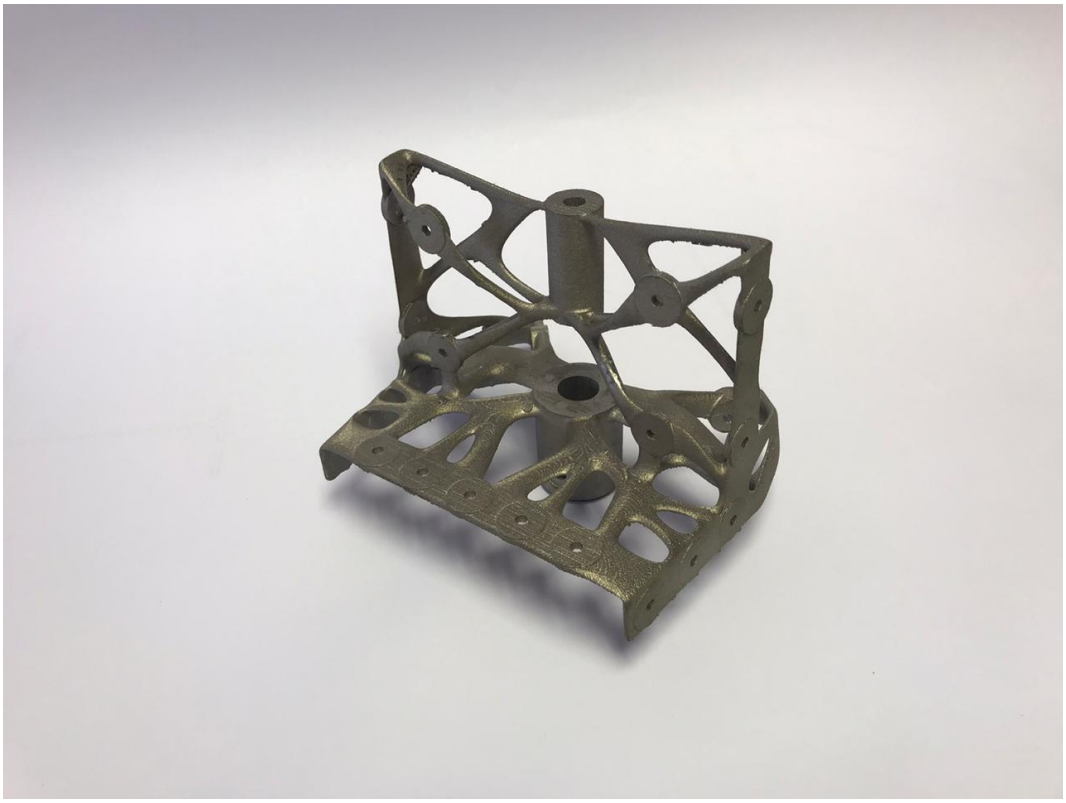

7.3.6 Detailed Drawing of the Final Geometry of the components.

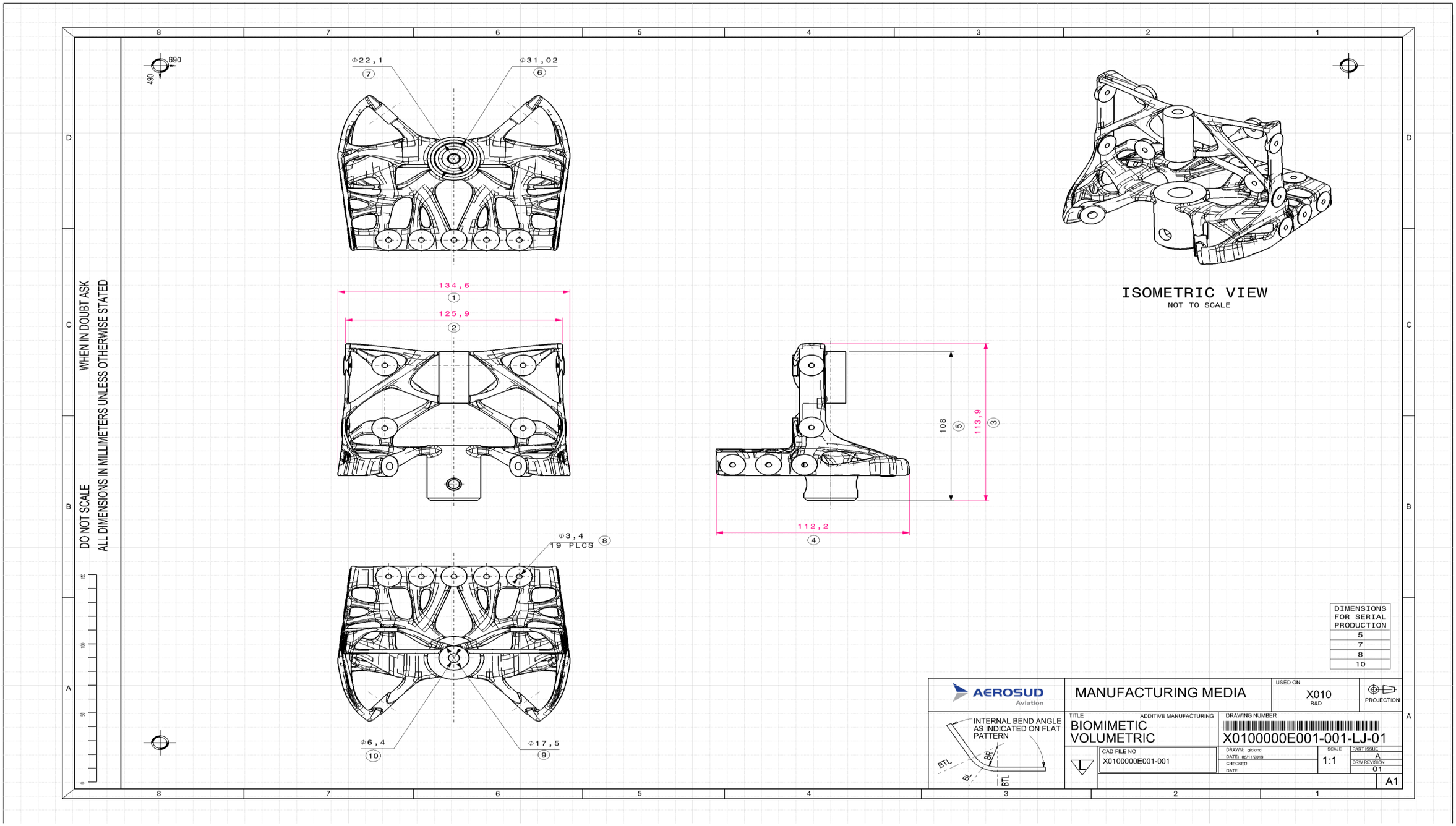

DO NOT SCALE
ALL DIMENSIONS IN MILLIMETERS UNLESS OTHERWISE STATED
WHEN IN DOUBT ASK

690
490

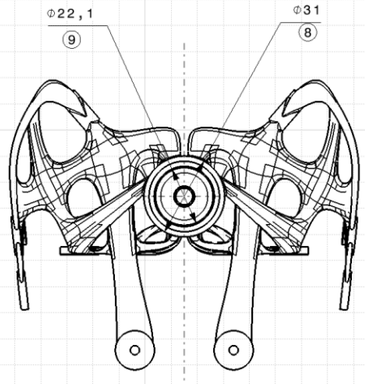

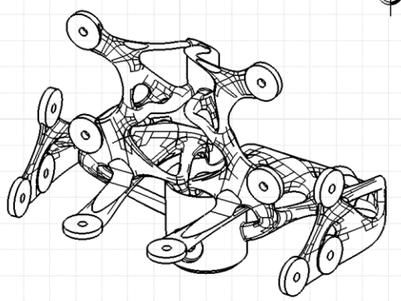

ISOMETRIC VIEW
NOT TO SCALE

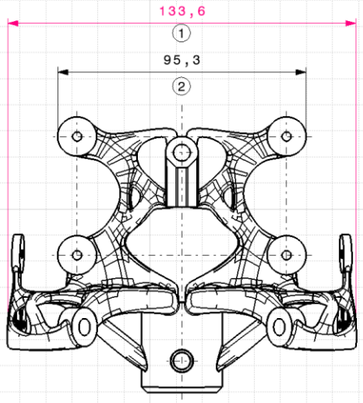

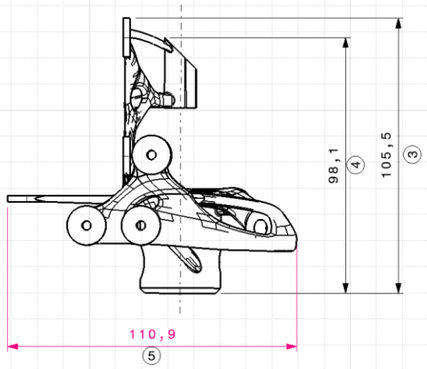

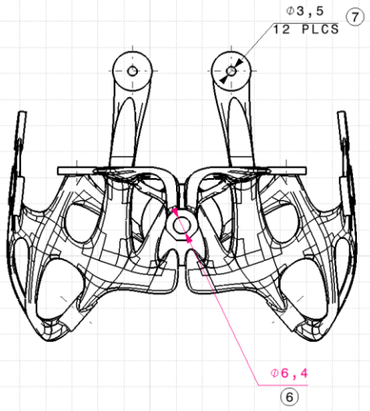

DIMENSIONS FOR SERIAL PRODUCTION
6
7
9

AEROSUD Aviation

MANUFACTURING MEDIA

USED ON: X010 R&D

PROJECTION

INTERNAL BEND ANGLE AS INDICATED ON FLAT PATTERN

TITLE: ADDITIVE MANUFACTURING
BIOMIMETIC BOTTOM BRACKET

DRAWING NUMBER: X0100000E001-002-LJ-01

CAD FILE NO: X0100000E001-002

DRAWN: gbtonc
DATE: 05/11/2019
CHECKED
DATE

SCALE: 1:1

PART ISSUE: A
DRW REVISION: 01

A1

WHEN IN DOUBT ASK
DO NOT SCALE
ALL DIMENSIONS IN MILLIMETERS UNLESS OTHERWISE STATED

690
490

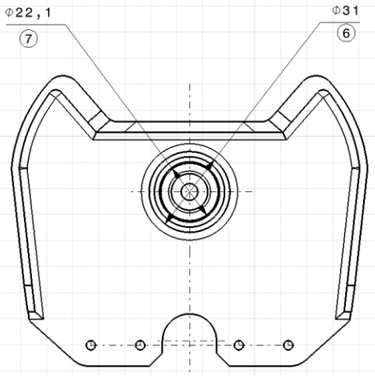

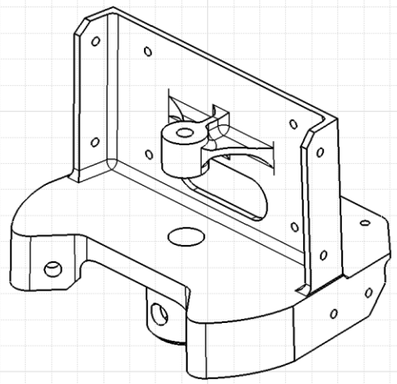

ISOMETRIC VIEW
NOT TO SCALE

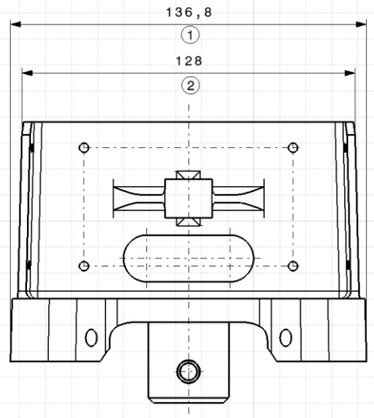

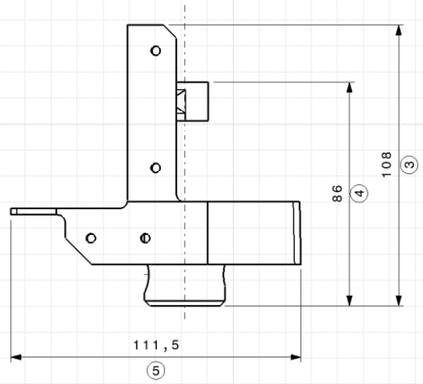

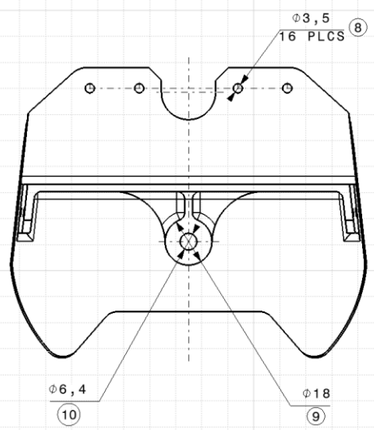

DIMENSIONS FOR SERIAL PRODUCTION
6
7
8
10

AEROSUD Aviation

MANUFACTURING MEDIA

USED ON: X010 R&D

PROJECTION

INTERNAL BEND ANGLE AS INDICATED ON FLAT PATTERN

BTL, BR, BL, BTL

TITLE: ADDITIVE MANUFACTURING
PRISAMATIC BRACKET

DRAWING NUMBER: X0100000E001-003-LJ-01

CAD FILE NO: X0100000E001-003

DRAWN: gidionc
DATE: 05/11/2019
CHECKED
DATE

SCALE: 1:1

PART ISSUE: A
DRW REVISION: 01

A1

7.4 Appendix D: Certification

7.4.1 The detailed stress report for each of the brackets

This report presents the stress analysis of the CFRTP Bottom Rudder Bracket that was manufactured using AM. The Geometry of the brackets was not conventional due to the freedom of the AM process. Thus, the shapes were complex and analysed in detail. The results presented in Chapter 5, Section 5.6.2 are from the following report:

https://figshare.com/s/42fc68a7a5baa0ddd3a5

7.4.2 Engineering test plan for the static test of the current biomimetic bottom bracket

This document presents the test procedure and methods of evaluation used to establish the strength properties of the CFRTP bottom rudder bracket. The brackets were manufactured using additive manufacturing technology called powder bed fusion with SLM as the process. The bracket was part of the CFRTP rudder assembly. The results presented in Chapter 5, Section 5.6.2 are from the following report:

https://figshare.com/s/ff7934133570b34d72dc

7.4.3 Engineering test report for static test of the CFRTP current biomimetic bottom bracket

This document describes the static test results as a means of compliance with the structural requirements of the CFRTP Rudder to test the biomimetic bottom bracket of the current design. The static test was carried out at Aerosud Aviation in accordance with the requirements of the test procedure X0100000BU002. The rudder was tested using a whiffle-tree, 1-ton load cell and digital display interface, and ENERPAC P-84 hand pump and RD-96 hydraulic actuator. The results presented in Chapter 5, Section 5.6.2 are from the following report:

https://figshare.com/s/eca5e73257538cd1e94c

7.4.4 Static test images

The images in this section depict the set-up of the test and the results.

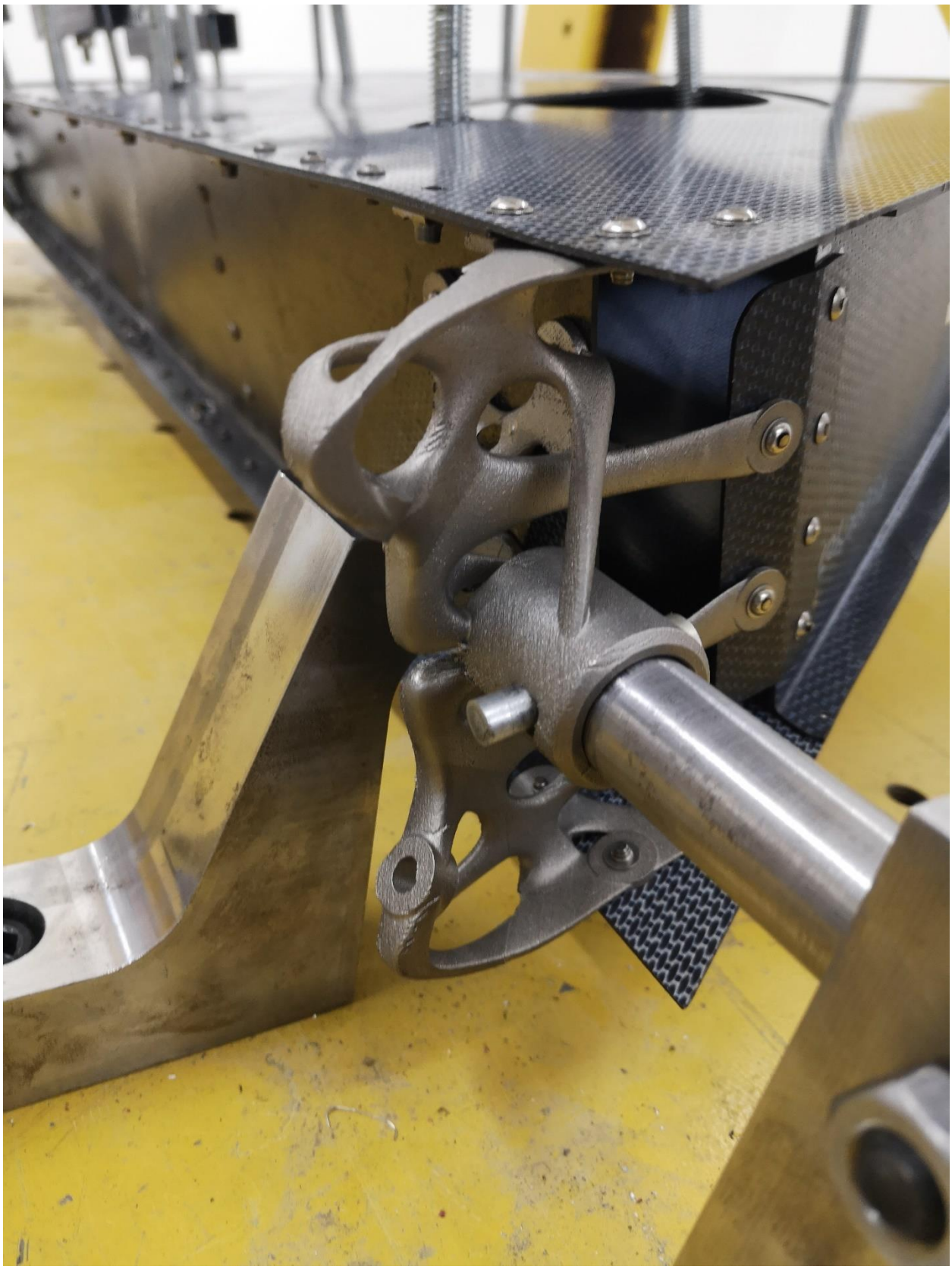

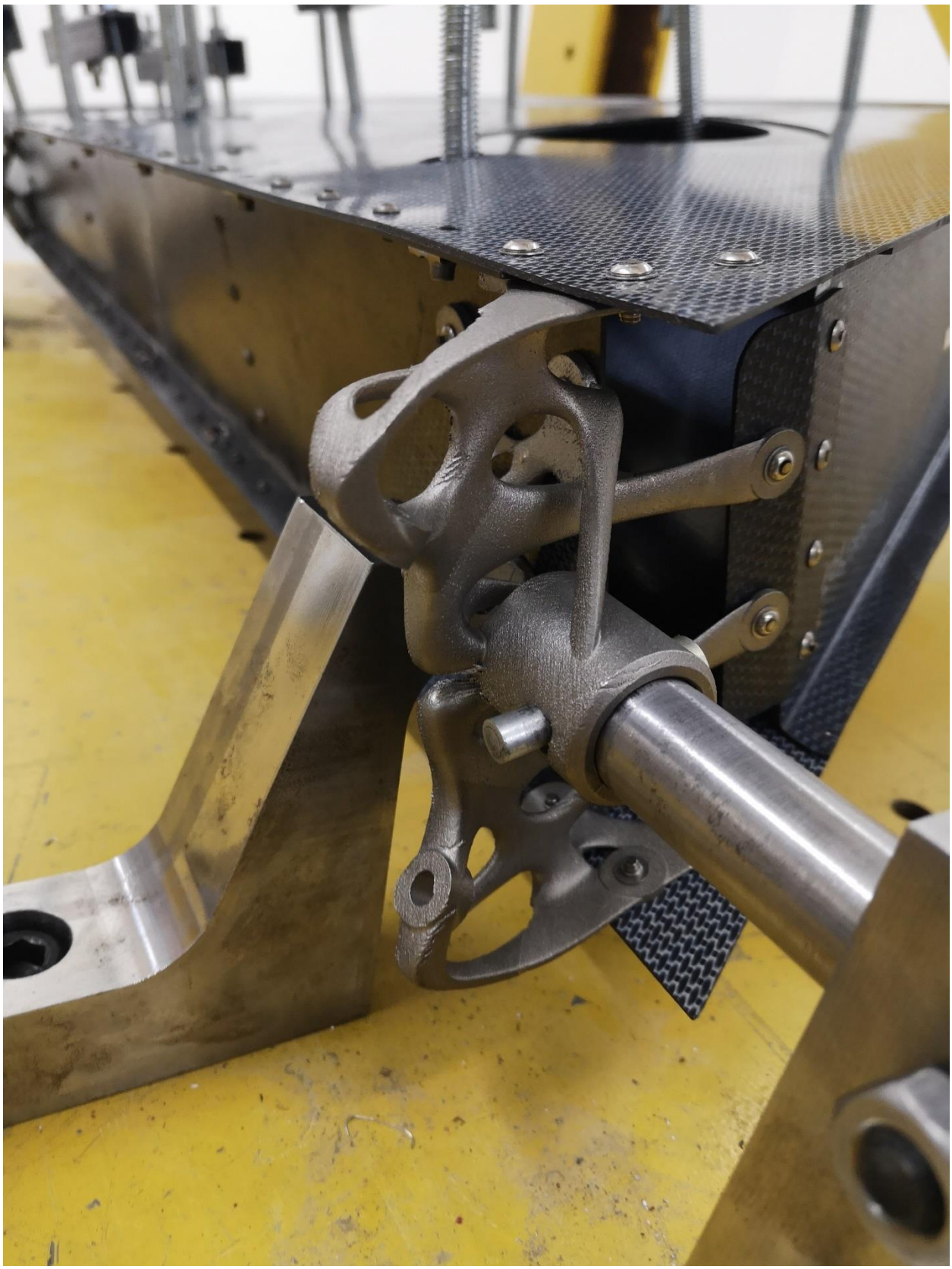

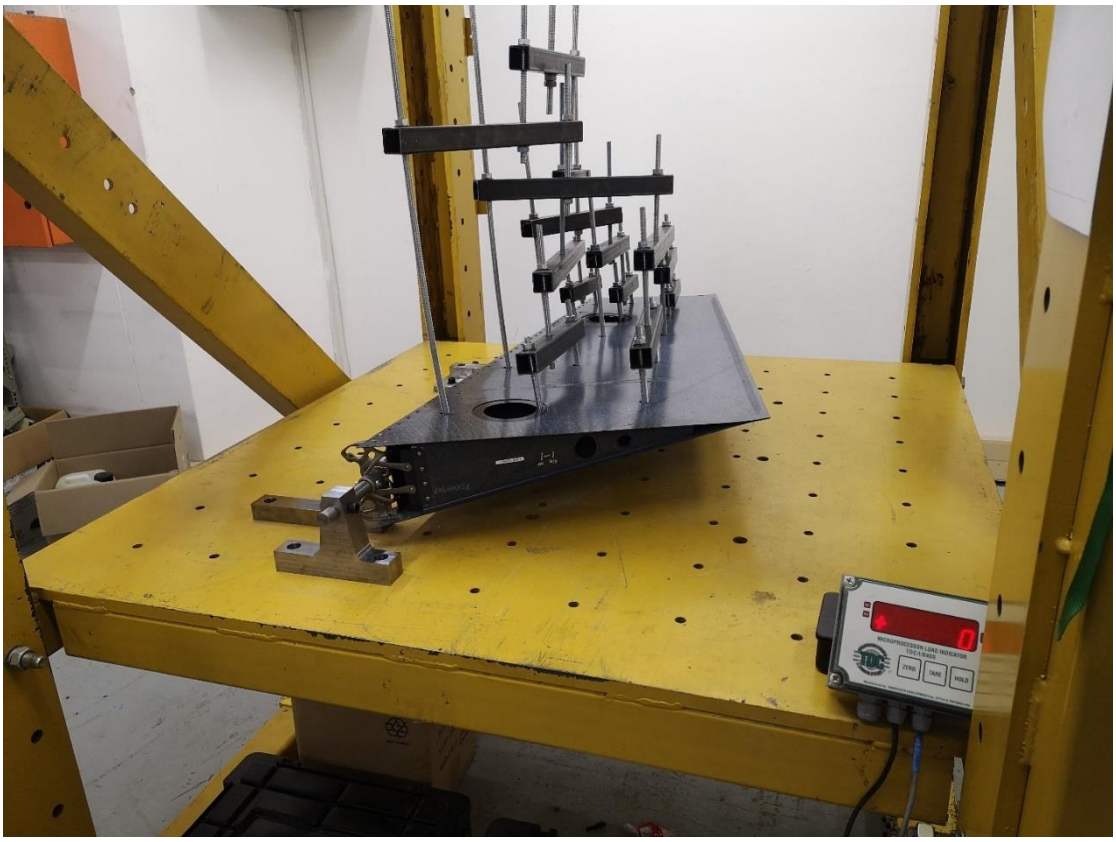

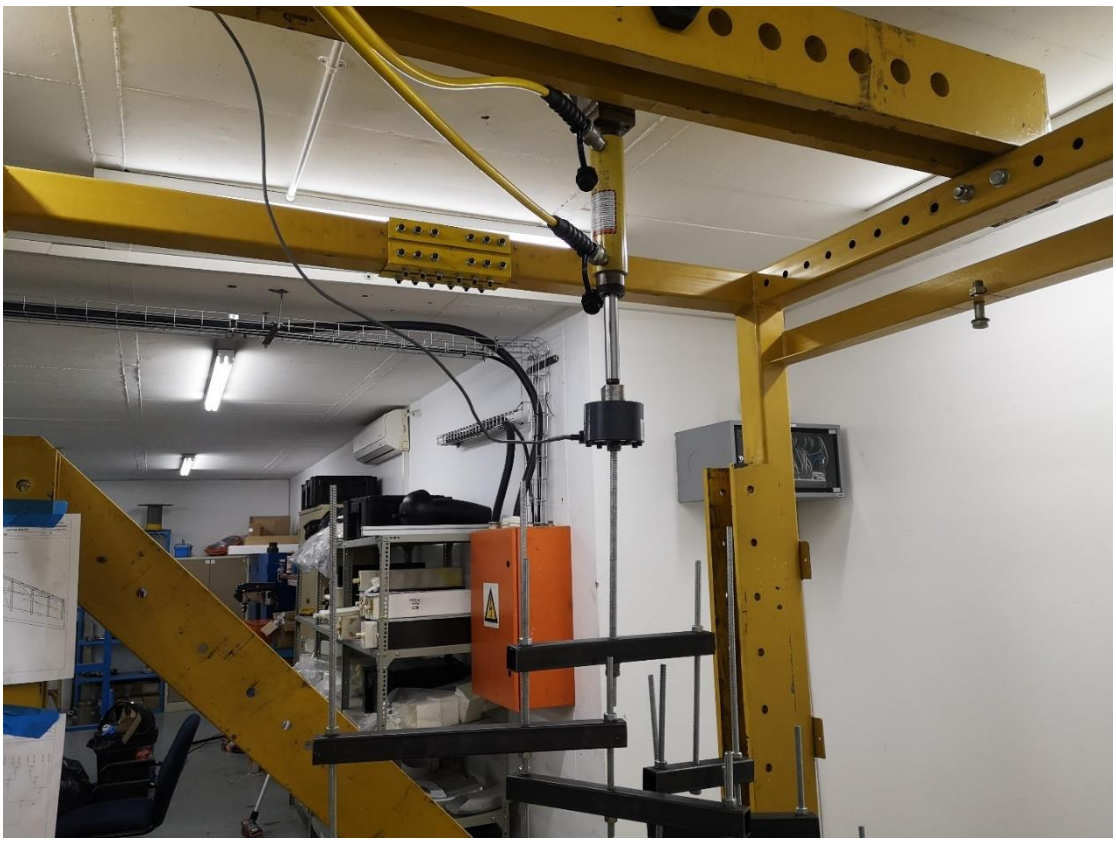

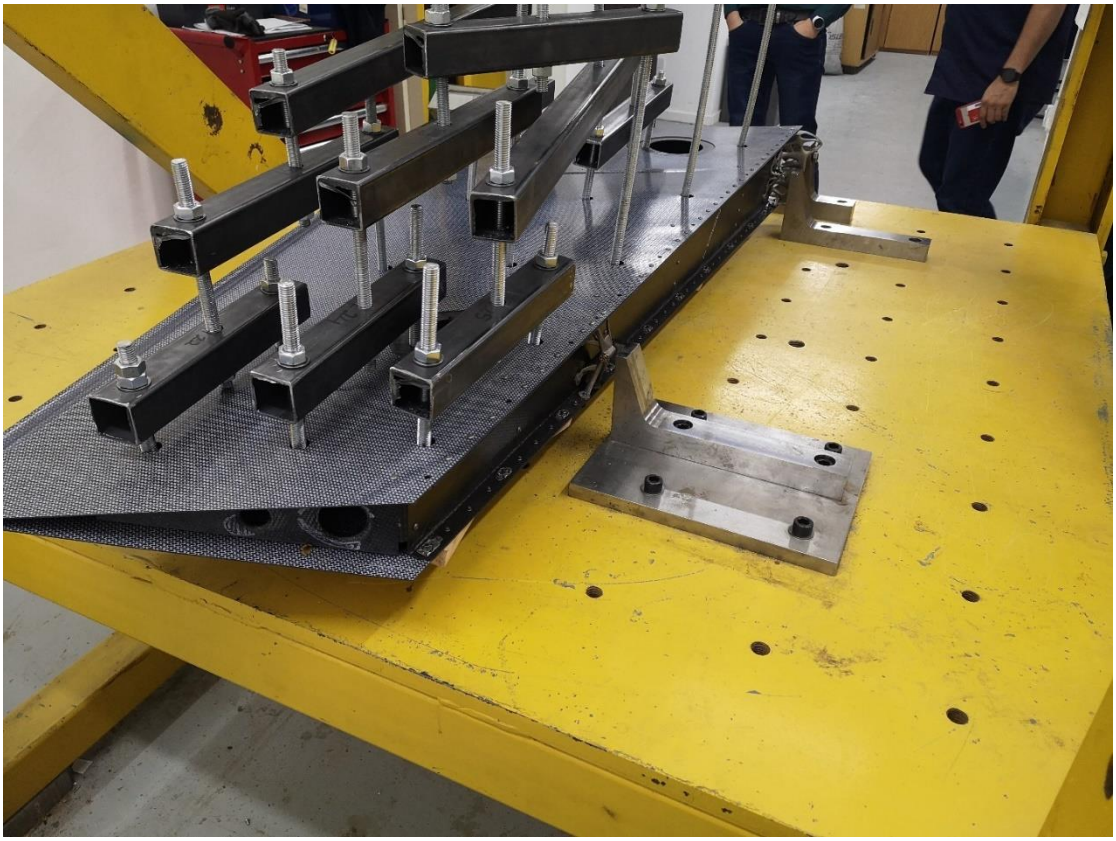

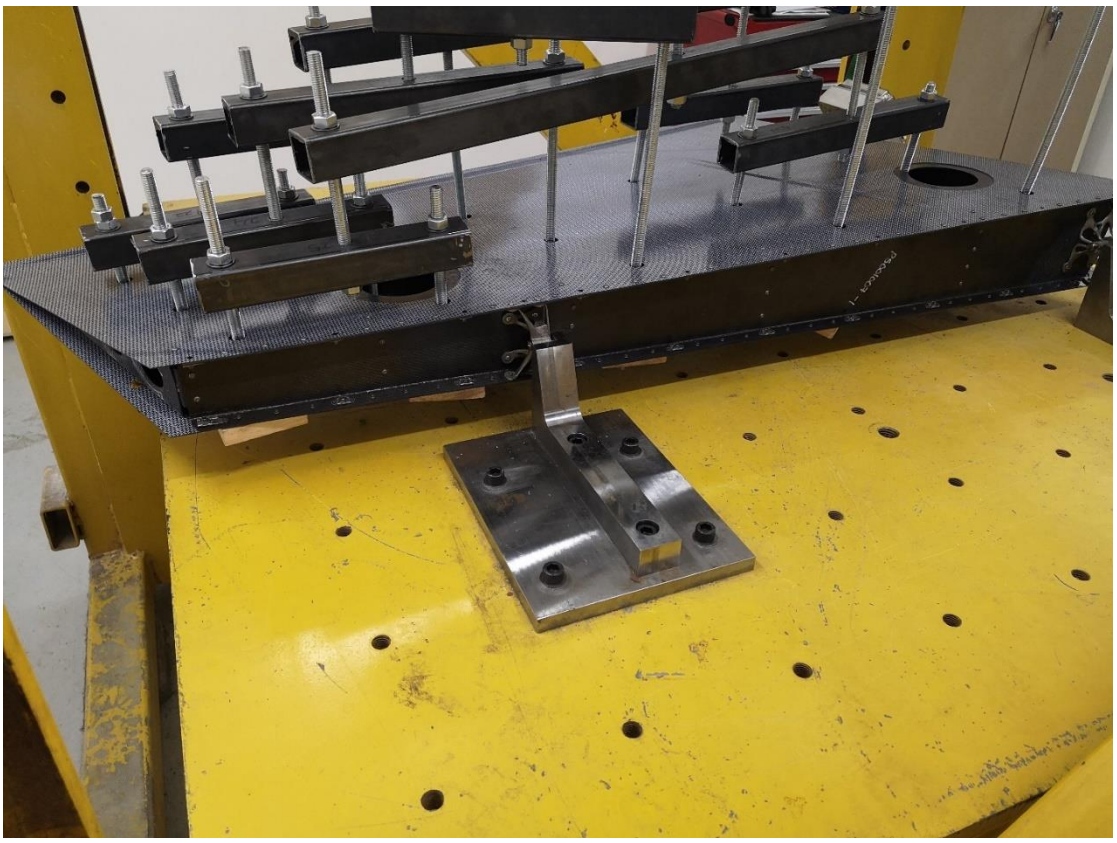

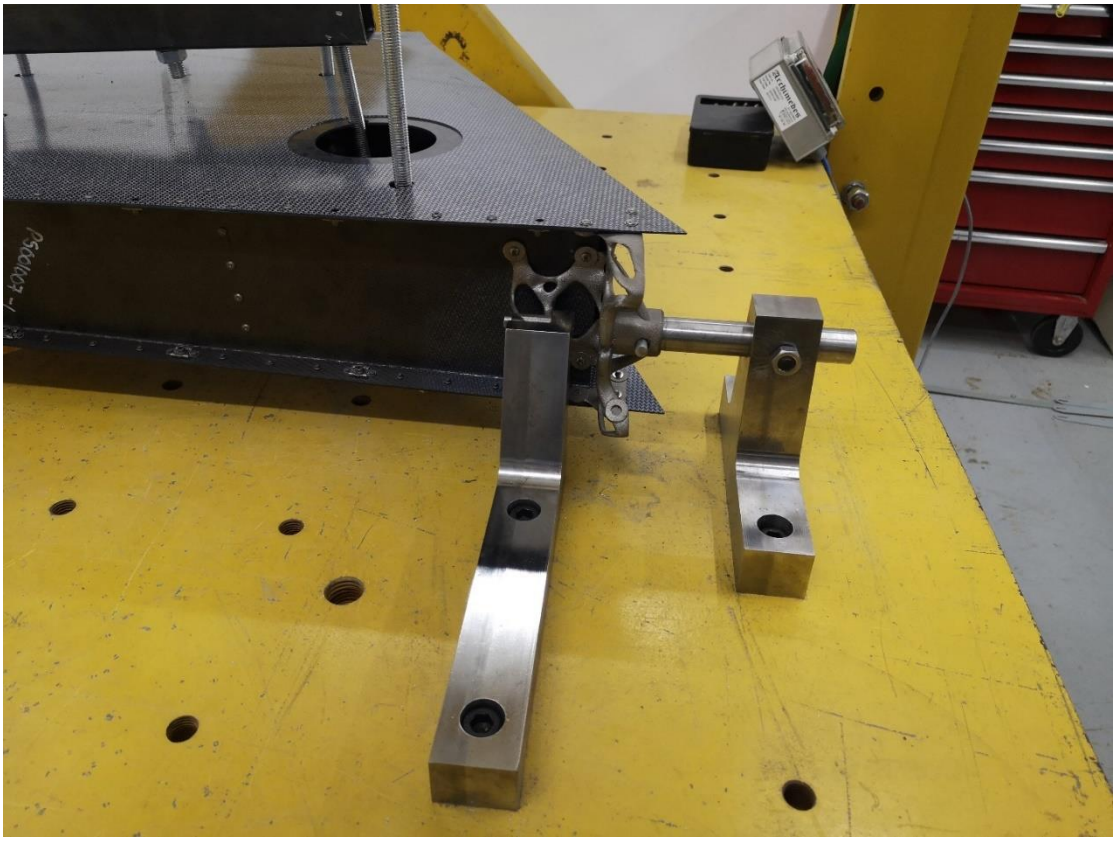

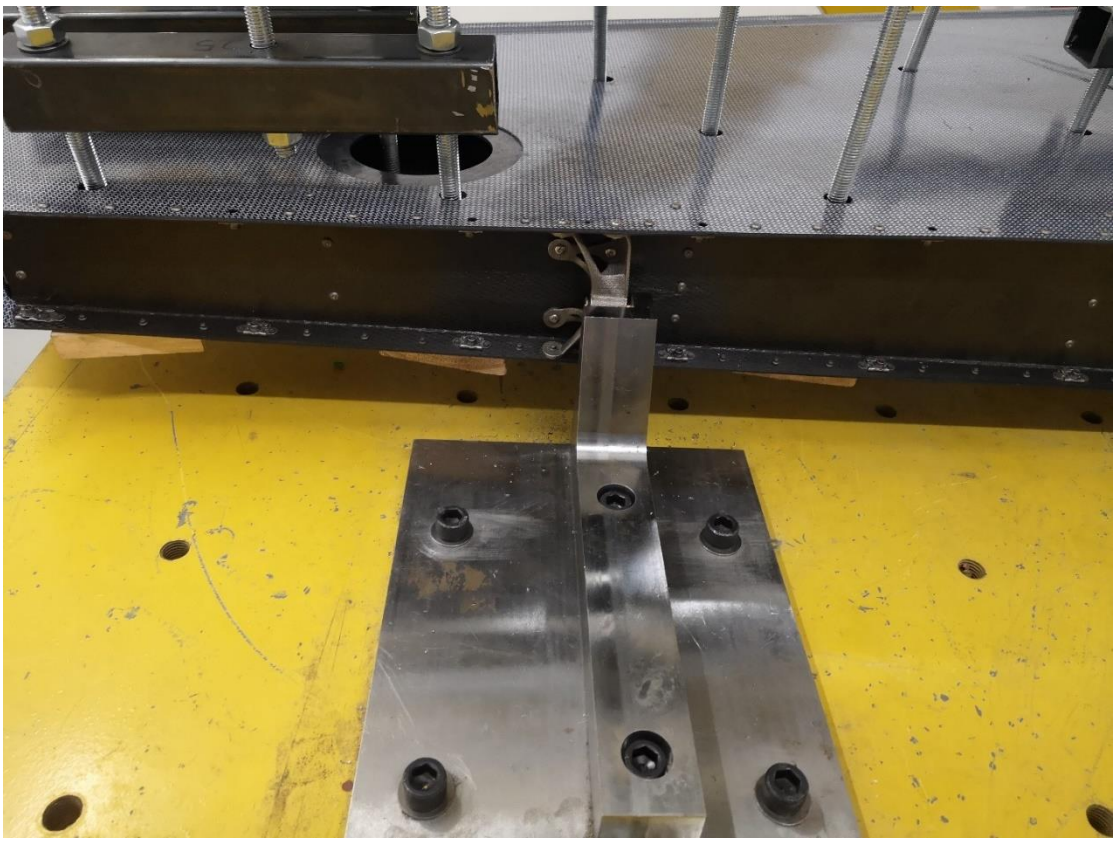

7.5 Appendix E: Process manuals

As mentioned throughout the report, the process manuals were an important part of this study to develop a generic process that could be applied to any software packages, depending on the availability to the user. The results shown in Chapter 5 were all derived from the use of the process documented in the following documents:

X0100000RA001: CPAM PROCESS REPORT – CAD

https://figshare.com/s/785e47acadf10effaa13

X0100000RA002: CPAM PROCESS REPORT – OPTIMISATION

https://figshare.com/s/1ec610cf338120bd61b7

X0100000RA003: CPAM PROCESS REPORT – INTERNAL AND EXTERNAL FEATURING

https://figshare.com/s/2e76ff9d7b2d3a5b3e33

X0100000RA004: CPAM PROCESS REPORT – MANUFACTURABILITY

https://figshare.com/s/c08687d918c53dbd30d6

X0100000RA005: CPAM PROCESS REPORT -QUALIFICATION AND CERTIFICATION

https://figshare.com/s/4ec8895fdcd982d41d31

LAST UPDATED: 25 JUNE 2021